

# Novel Pathway Design for Biopolymer Building Block Production

by

K'yal Rasean Bannister

M.S. Energy Science, Technology, and Policy, Carnegie Mellon University (2019)

B.S. Chemical Engineering, California Institute of Technology (2018)

B.S. Chemistry, Spelman College (2017)

Submitted to the Department of Chemical Engineering  
in partial fulfillment of the requirements for the degree of

Doctor of Philosophy in Chemical Engineering

at the

MASSACHUSETTS INSTITUTE OF TECHNOLOGY

May 2024

© K'yal Rasean Bannister 2024. All rights reserved.

The author hereby grants to MIT a nonexclusive, worldwide, irrevocable, royalty-free license to exercise any and all rights under copyright, including to reproduce, preserve, distribute and publicly display copies of the thesis, or release the thesis under an open-access license.

Author .....  
Department of Chemical Engineering  
April 30, 2024

Certified by .....  
Kristala L. J. Prather  
Arthur D. Little Professor of Chemical Engineering  
Department Head  
Thesis Supervisor

Accepted by .....  
Hadley D. Sikes  
Willard Henry Dow Professor of Chemical Engineering  
Graduate Officer



# Novel Pathway Design for Biopolymer Building Block Production

by

K'yal Rasean Bannister

Submitted to the Department of Chemical Engineering  
on April 30, 2024, in partial fulfillment of the  
requirements for the degree of  
Doctor of Philosophy in Chemical Engineering

## Abstract

The carbon and energy intensity associated with plastics production from petroleum, combined with the accumulation of plastics waste in the environment, necessitates the development of technologies for the production of renewably-derived, degradable alternatives. Microorganisms can be metabolically engineered to convert renewable feedstocks to plastic building blocks. This thesis aims to design and implement metabolic pathways to industrially relevant hydroxy acids (HAs) and diols with the ultimate goal of using them for sustainable plastics production.

We began by prioritizing bioaccessible HAs for bio-production. Our analysis identified 182 bioaccessible HAs. We prioritized monomers from this list based on novelty, ease of chemical polymerization, maximum theoretical yield, and potential to improve material properties in a biopolymer. 3-Hydroxyisobutyric acid (3HIB) and 3-hydroxy-2-methylbutyric acid (3H2MB) were prioritized based on their high molecular weight polymerization and ability to reduce thermal degradation when incorporated into a biopolymer.

Next, we designed a novel pathway to 3HIB and 3H2MB. This pathway involves the conversion of glucose to various branched acyl-CoAs and ultimately to 3HIB or 3H2MB. As proof of concept, we engineered *E. coli* for the production 3HIB and 3H2MB from glucose at titers as high as  $66 \pm 5$  mg/L and  $290 \pm 40$  mg/L, respectively. To our knowledge, this is the first report of 3H2MB bio-production from glucose. We optimized this pathway for 3H2MB production by deleting competing pathways and developing a byproduct recycle. Finally, we investigated mutagenesis of a pathway enzyme to expand the product range of this pathway. Future work should investigate these mutants for the production of other biopolymer building blocks.

Finally, the feasibility of biological pathways to 3-methyl-1,5-pentanediol (3MPD) was investigated. 3MPD is an attractive monomer for the production of degradable, diol-diacid copolyesters. The feasibility determining step in this pathway involves the hydroxylation of 3-methylpentanol (3MP) to 3MPD by AlkBGT from *P. putida*. Despite optimizing our system for *alkBGT* expression, strain growth, and substrate transport, no 3MP conversion to 3MPD was observed. Future work should probe other hydroxylation enzymes.

Overall, this thesis demonstrates the utility of novel pathway design to reach HAs and diols that lead to biopolymers with improved industrial application.

Thesis Supervisor: Kristala L. J. Prather

Title: Arthur D. Little Professor of Chemical Engineering

Department Head

## Acknowledgments

First and foremost, this thesis is dedicated to my parents. It is more theirs, than mine. Mama - your unconditional support for me and your belief in all of my dreams are the wings that allow me to fly at places like MIT. I remember when I first expressed my interest in doing laboratory science to you when I was 14. You proceeded to email every professor with biofuels-related research at the University of Florida until someone agreed to take me on. All these years later and I'm still in a similar research field. Dad - there is no one I look up to more than you. Your commitment to excellence in all things is something I look to emulate in all that I do. You have set an example of hard work, persistence, and diligence which have been instrumental for me to succeed in all aspects of life. To my broader family - thank you for believing in me. You all never quite understood why I stayed in school so long ;) , but you all believed that whatever goal I was striving towards, I was more than capable of getting it done.

To my science mentors along the way - thank you for opening doors to places that a little girl from rural Florida never thought she'd get to. To Ms. Emily Keeler - you introduced me to science. The science community that you cultivated in a small, underfunded high school has been unmatched in all the places that I've been since then. To Dr. Lisa Hibbard - your unique approach to pedagogy and commitment to educating young, Black women single-handedly fed my passion for chemistry as a Spelman undergrad. To Dr. Juana Mendenhall and Dr. Gayle Bentley - thank you for being wonderful mentors in the lab. You all instilled in me a dedication to rigorous science and lab organization which have been instrumental to my success as a graduate student.

To the countless friends along the way - thank you for your support. Amanda, Mya, Jaycee, Sydney, and Emily - your sisterhood has kept me afloat during this journey. You all constantly pour into me and know just the right things to say to keep me going. Thank you so much for the constant affirmation. My cup overflows.

To my MIT community - thank you for everything. Kris - you are a one-of-a-kind mentor. Your kindness, transparency, and commitment to knowing me as a scientist and person have meant so much to me. Further, your presence in places like MIT give me the courage to take up space. I would also like to thank my thesis committee - Prof. Gregory Stephanopoulos and Prof. Bradley Olsen - and the MIT-DIC Team - Prof. Desiree Plata, Dr. Atsuhisa Miyawaki, Dr. Wontae Joo, Dr. Sarah Av-Ron, Omar Tantawi, and Elijah Martin. You all created an interdisciplinary science community where knowledge and support were free flowing. To the Prather Lab - Gwen, Cynthia, Kevin, Jennifer, Mike, Yoseb, Bea, Alex, Sean, Isabella, and Jacob - you guys

are the best! I can only hope to mirror the dynamic we've created in future work communities. You all have allowed me to bring my authentic self to science. Thank you for that freedom. To my undergraduate student - Kelcey Allen - it was an absolute joy to work with you. Your flexibility and youthful passion for science inspired in me the same. I hope for all the good things for you in your own science journey.

K'yal

# Contents

<b>1</b>	<b>Introduction</b>	<b>11</b>
1.1	Metabolic engineering for sustainable plastics	12
1.2	Microbial production of hydroxy acids	14
1.2.1	Microbial production of 3-hydroxy acids	14
1.2.2	Microbial production of 2-hydroxy acids	16
1.2.3	Microbial production of $\omega$ -hydroxy acids	17
1.3	Microbial production of diols	18
1.3.1	Microbial production of C3-C4 diols	18
1.3.2	Microbial production of C5-C12 diols	20
1.4	Novel pathway design methods	21
1.5	Thesis overview	24
1.6	Thesis organization	24
<b>2</b>	<b>Identification of industrially relevant hydroxy acids for biosynthesis</b>	<b>25</b>
2.1	Introduction	26
2.2	Materials and Methods	27
2.3	Results and Discussion	28
2.4	Conclusions	30
<b>3</b>	<b>Design, implementation, and optimization of a novel, biological pathway to <math>\alpha</math>-substituted 3-hydroxy acids</b>	<b>33</b>
3.1	Introduction	34
3.2	Materials and Methods	37
3.2.1	Strain construction	37
3.2.2	Production experiments	38
3.2.3	Metabolite detection	38
3.2.4	Sodium dodecyl sulfate–polyacrylamide gel electrophoresis (SDS-PAGE)	39
3.2.5	Molecular docking	39
3.3	Results and Discussion	48
3.3.1	Designing a pathway to $\alpha$ -3HAs	48
3.3.2	Validating the production of $\alpha$ -substituted 3-hydroxy acids from branched acids	50
3.3.3	Engineering branched acid specificity from glucose	57
3.3.4	3HIB and 3H2MB production from glucose in <i>E. coli</i>	58
3.3.5	Optimizing 3H2MB production from glucose by improving precursor supply and use	61
3.3.6	Developing a novel isobutyrate recycle system	63
3.3.7	PhaJ for the production of other 3HAs	65
3.4	Conclusions	69

<b>4</b>	<b>Design and feasibility analysis of pathways to 3-methyl-1,5-pentanediol</b>	<b>70</b>
4.1	Introduction . . . . .	71
4.2	Materials and Methods . . . . .	73
4.2.1	Strain construction . . . . .	73
4.2.2	Production experiments . . . . .	74
4.2.3	Permeabilized cell studies . . . . .	75
4.2.4	Fatty acid methyl ester derivitization . . . . .	75
4.2.5	Metabolite detection . . . . .	75
4.3	Results and Discussion . . . . .	78
4.3.1	Designing biological pathways to 3-methyl-1,5-pentanediol . . . . .	78
4.3.2	Determining the feasibility of the 3-methylpentanol-mediated pathway to 3-methyl-1,5-pentanediol . . . . .	83
4.4	Conclusions . . . . .	87
<b>5</b>	<b>Conclusions, future directions, and outlook</b>	<b>88</b>
5.1	Summary of thesis work . . . . .	88
5.1.1	Prioritizing industrially relevant hydroxy acids for bio-production . . . . .	89
5.1.2	Engineering <i>E. coli</i> for the production of $\alpha$ -substituted 3-hydroxy acids . . . . .	89
5.1.3	Design and feasibility analysis of pathways to 3-methyl-1,5-pentanediol . . . . .	90
5.2	Future directions . . . . .	90
5.2.1	Continued optimization of the 3-hydroxy-2-methylbutyric acid pathway . . . . .	90
5.2.2	Bio-producing other hydroxy acids . . . . .	91
5.2.3	Troubleshooting the 3-methyl-1,5-pentanediol pathway . . . . .	93
5.3	Outlook . . . . .	93
	<b>References</b>	<b>95</b>

# List of Figures

1.1	Representative examples of bio-based polyesters . . . . .	13
1.2	Hydroxy acid structural diversity in the microbial metabolome . . . . .	14
1.3	Current biological routes to 3-hydroxy acids . . . . .	15
1.4	2-ketoacid based pathways to 2HAs . . . . .	17
1.5	Pathways to $\omega$ -hydroxy acids . . . . .	19
1.6	Metabolic pathways for the bio-production of various diols. . . . .	22
2.1	Poly(3-hydroxybutyrate) thermal degradation mechanism . . . . .	26
2.2	Process for prioritizing industrially relevant hydroxy acids . . . . .	28
2.3	Maximum theoretical yield vs polymerizability score for biologically accessible hydroxy acids	29
2.4	Final list of industrially relevant hydroxy acids . . . . .	32
3.1	Previously reported biological routes to 3-hydroxyisobutyric acid and 3-hydroxy-2-methylbutyric acid . . . . .	36
3.2	Biological route to 3-hydroxyisobutyric acid and 3-hydroxy-2-methylbutyric route glucose .	49
3.3	SDS-PAGE analysis of module 2 enzymes from <i>Pseudomonas taiwanensis</i> VLB120 . . . . .	50
3.4	Enoic acids to 3-hydroxy acids production experiment . . . . .	51
3.5	Tiglic Acid to 3H2MB Shake Flask Production Experiment . . . . .	52
3.6	Examining the growth advantage of strains expressing the truncated module 2 pathway . . .	53
3.7	Electron transfer in acyl-CoA dehydrogenases and acyl-CoA oxidases . . . . .	54
3.8	3-Hydroxyisobutyric acid and 3-hydroxy-2-methylbutyric acid production from branched acid	55
3.9	Dynamic production run data for selected module 2 strains . . . . .	56
3.10	Isobutyrate and 2-methylbutyrate production from glucose . . . . .	57
3.11	3-hydroxyisobutyric acid production from glucose in recombinant <i>E. coli</i> . . . . .	59
3.12	3-hydroxy-2-methylbutyric acid production from glucose in recombinant <i>E. coli</i> . . . . .	60
3.13	Effects of activation enzyme choice on 3-hydroxy-2-methylbutyric acid production . . . . .	61
3.14	Improving 2-methylbutyric acid production by deleting competing pathways . . . . .	62
3.15	Isobutyrate recycle system . . . . .	63
3.16	Conversion of isobutyrate to butyrate by cells with an isobutyryl-CoA mutase . . . . .	64
3.17	Testing the isobutyrate acid recycle in 2-methylbutyrate production strains . . . . .	65
3.18	Examining enoyl-CoA hydratase mutant activity on crotonate . . . . .	66
3.19	Examining enoyl-CoA hydratase mutant activity on 2-pentenoic acid . . . . .	67
3.20	Docking octenoyl-CoA into the active site of PhaJ using AutoDock Vina . . . . .	68
3.21	Docking 2-methyl-2-pentenoyl-CoA into the active site of PhaJ using AutoDock Vina . . . . .	68
4.1	Previously developed routes to 3-methyl-1,5-pentanediol . . . . .	72
4.2	Compounds structurally similar to 3-methyl-1,3-pentanediol in the microbial metabolome . .	78
4.3	Proposed metabolic pathway from 2-keto-4-methylhexanoate to 3-methyl-1,5-pentanediol . .	81
4.4	Proposed metabolic pathway from mevalonate to 3-methyl-1,5-pentanediol . . . . .	82



4.5	Assay design for determining the efficacy of AlkBGT for 3-methyl-1,5-pentanediol production	83
4.6	Examining plasmid design to reduce growth burden from overexpressing <i>alkBGT</i>	84
4.7	Measures to reduce growth burden associated with <i>alkBGT</i> overexpression	85
4.8	3-methylpentanol hydroxylation study in permeabilized cells	86
4.9	3-methylpentanol hydroxylation study in strains with FadL or AlkL	87
5.1	Potential pathways to straight chain 2-hydroxy acids	92

# List of Tables

2.1	Polymerizability score definition . . . . .	27
2.2	Additional hydroxy acids with connection to the microbial metabolome . . . . .	31
3.1	Previous reports of 3HIB and 3H2MB bio-production . . . . .	34
3.2	List of background strains used . . . . .	37
3.3	List of plasmid backbones used . . . . .	38
3.4	Gene block sequences for 3HIB and 3H2MB production strains . . . . .	40
3.5	3HIB and 3H2MB plasmid construct descriptions . . . . .	42
3.6	List of 3HIB and 3H2MB production strains . . . . .	46
4.1	Gene block sequences for 3MPD production . . . . .	73
4.2	3MPD plasmid construct descriptions . . . . .	76
4.3	List of 3MPD production strains . . . . .	76
4.4	Comparison of the 3-methyl-1,5-pentanediol pathways . . . . .	80
5.1	CYP153As for inclusion in the 3-methyl-1,5-pentanediol pathway . . . . .	93

# Chapter 1

## Introduction

### Abstract

The carbon and energy intensity associated with plastics production from petroleum feedstocks, combined with the accumulation of plastics waste in the environment, necessitates the development of technologies for the production of renewably-derived, degradable alternatives. Metabolic engineering for biopolymer production represents a sustainable alternative to conventional plastics use. Many microorganisms naturally possess pathways for polyester synthesis and degradation. Polyesters are a diverse class of plastics and their monomer structure can be tuned to realize a breadth of material properties useful for industrial application. However, this diversity remains untapped since conventional pathways for biopolymer building block production yield limited structural diversity. Further, microorganisms have been harnessed for the commercial production of a few polyesters with material properties that limit their application. This chapter reviews metabolic pathways for the production of polyester building blocks with specific emphasis on the product diversity achievable by these pathways. Next, we introduce novel pathway design as an integral tool for reaching new biopolymer building blocks.

**This section contains text and figures adapted from:**

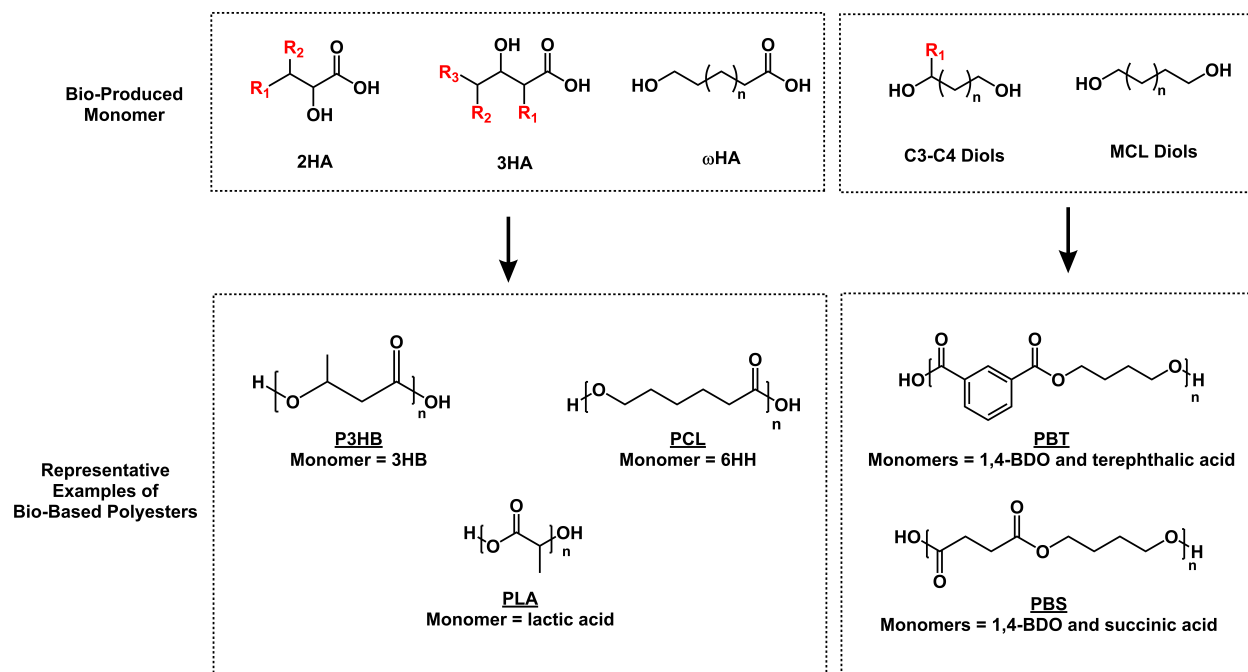
Bannister, K.R., Prather, K.L.J. Engineering polyester monomer diversity through novel pathway design. *Curr. Opin. Biotechnol.*, **79** (2023) 102852.

## 1.1 Metabolic engineering for sustainable plastics

Plastics are ubiquitous in everyday life, filling material niches in diverse industries. Their utility and low cost make them an essential part of technological innovations that generate innumerable societal benefits related to health, safety, energy savings, and material conservation.<sup>1</sup> Despite the myriad of benefits associated with it, global plastics use is responsible for a host of environmental issues. Current estimates put yearly world plastics production at 460 million tonnes (MMT).<sup>2</sup> This production begins with the conversion of petroleum to plastics precursors through steam cracking — the largest energy consumer in the chemical industry. It ends with losses to the environment as 253 MMT of mismanaged or land filled plastic waste/yr<sup>2</sup> and 104 MMT CO<sub>2</sub>-equivalent greenhouse gas emissions/yr.<sup>3</sup> Plastics' landfill-by-design life cycle and the documented, negative impacts of greenhouse gases (GHGs) on our global ecosystem motivate the exploration of recombinant microorganisms as chassis for sustainable plastics production.

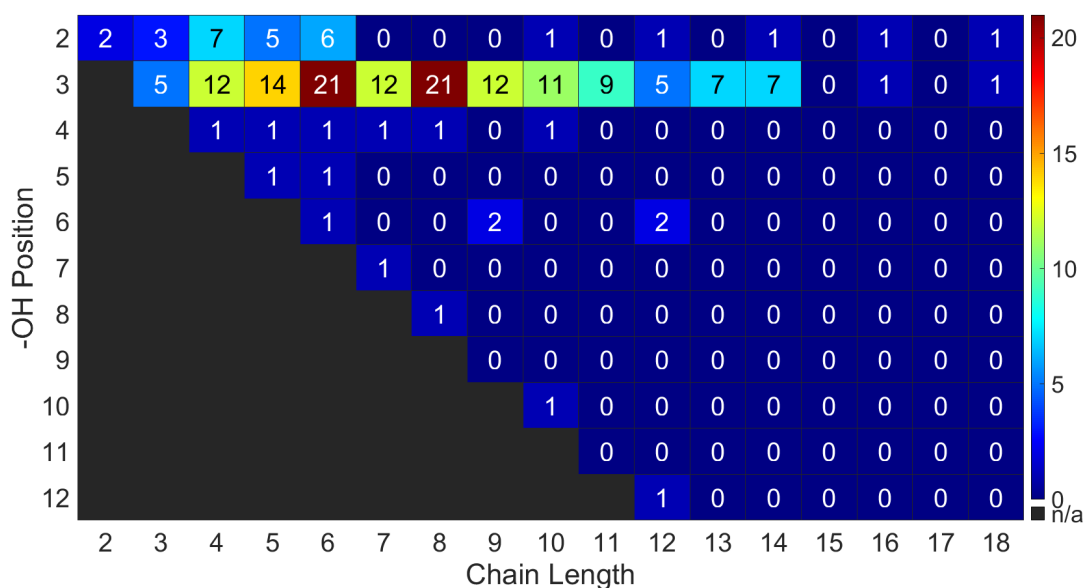
The metabolisms of microorganisms represent an ideal background for the synthesis of sustainable plastics because they have been honed by millions of years of evolution to efficiently produce an array of chemicals from renewable materials. Microbial chemical production obviates the need for the harsh conditions, exotic catalysts, and expensive separation schemes that typify traditional chemical production because metabolic pathways operate at physiological conditions to produce stereospecific products.<sup>4</sup> Metabolic engineering — manipulating metabolic pathways to harness them for the production of target compounds — remains the most powerful tool for engineers to traverse chemical space to convert metabolites to a target compound.<sup>5</sup>

Many microorganisms possess natural metabolic pathways for polyester synthesis and degradation. Polyesters are a diverse class of plastics typified by ester linkages between diols and diacids (e.g. polybutylene succinate) or between hydroxy acids (i.e. polyhydroxyalkanoates) (Figure 1.1). This research focuses on hydroxy acids (HAs) and diols as promising bio-based plastics monomers based on their industrial significance to our project sponsor. Polyester composition and monomer structure can be adjusted for selection of industrially relevant material properties. Polyhydroxyalkanoates (PHAs) stand out as biopolymers because they are natural, degradable polyesters produced by bacteria and archaea as redox equivalent sinks during nutrient limitation.<sup>6</sup> More than 150 HAs with connection to the microbial metabolome have been cataloged across several genera.<sup>7–9</sup> If unlocked, this structural diversity promises a lexicon of sustainable plastics to augment and even supplant the material niches that petroleum-derived plastics currently fill.



**Figure 1.1.** Bioproducted HA and diols classes and representative examples of bio-based polyesters

Despite their potential as plastics alternatives, commercial biopolymer production remains stunted by limited monomer diversity (Figure 1.2) and high production costs. Limited monomer diversity is due to the narrow substrate specificity of enzymes involved in biological HA production. Two of the most commercially successful biopolymers by production volume are polylactic acid (PLA) and poly(3-hydroxybutyrate) (P3HB).<sup>10,11</sup> PLA exhibits limited ocean biodegradation and brittleness,<sup>10</sup> while P3HB is thermally unstable.<sup>12</sup> These non-ideal properties are exacerbated by high production costs. PHA production costs are estimated to be 15x that of polypropylene, with 30% of that cost attributed to PHA extraction.<sup>6</sup> Since PHAs are large, hydrophobic inclusion bodies, unsustainable solvent extraction techniques that reduce yield are required for separation. To circumvent PHA extraction from whole-cell cultures, a hybrid approach has been employed in PLA production that involves microbial lactic acid synthesis followed by chemical polymerization to PLA.<sup>13</sup> Additionally, chemical polymerization allows for the precise control of PHA composition, since natural PHAs are random combinations of cytoplasmic HAs. Advances in industrial biopolymer production will rely on increasing monomer diversity through novel pathway design and using hybrid synthesis schemes.



**Figure 1.2.** This heatmap represents the number of HAs at varying hydroxyl group position and chain length found as substituents of PHAs. Heatmap compiled using data from Steinbüchel and Valentin,<sup>7</sup> Agnew and Pflieger,<sup>8</sup> Choi et al.,<sup>9</sup> and Bannister and Prather<sup>14</sup>

## 1.2 Microbial production of hydroxy acids

### 1.2.1 Microbial production of 3-hydroxy acids

Natural PHAs are primarily composed of 3-hydroxy acids (3HAs). Two primary routes for 3HA production are (1) fatty acid biosynthesis or (2)  $\beta$ -oxidation reversal (rBOX) (Figure 1.3). In the fatty acid biosynthesis pathway, fatty acid metabolism intermediates are converted to 3HAs. The product diversity of this pathway is limited by the substrate specificity of fatty acid biosynthesis enzymes which generally prefer straight-chain substrates with backbones at least four carbons long. The rBOX pathway produces C3-C6 (R)-3HAs in a three-step reaction that involves the condensation of acyl-CoAs by a thiolase, followed by a reduction of the condensation product to yield 3HAs. Thiolases catalyze the ordered condensation of priming and extending acyl-CoAs and determine the structural diversity of the rBOX pathway. Thiolase preference for acetyl-CoA as both priming and extending units limits this pathway to straight chain 3HAs. The rBOX pathway stands out from the fatty acid biosynthesis pathway because it does not require ATP or NADPH.<sup>15</sup>

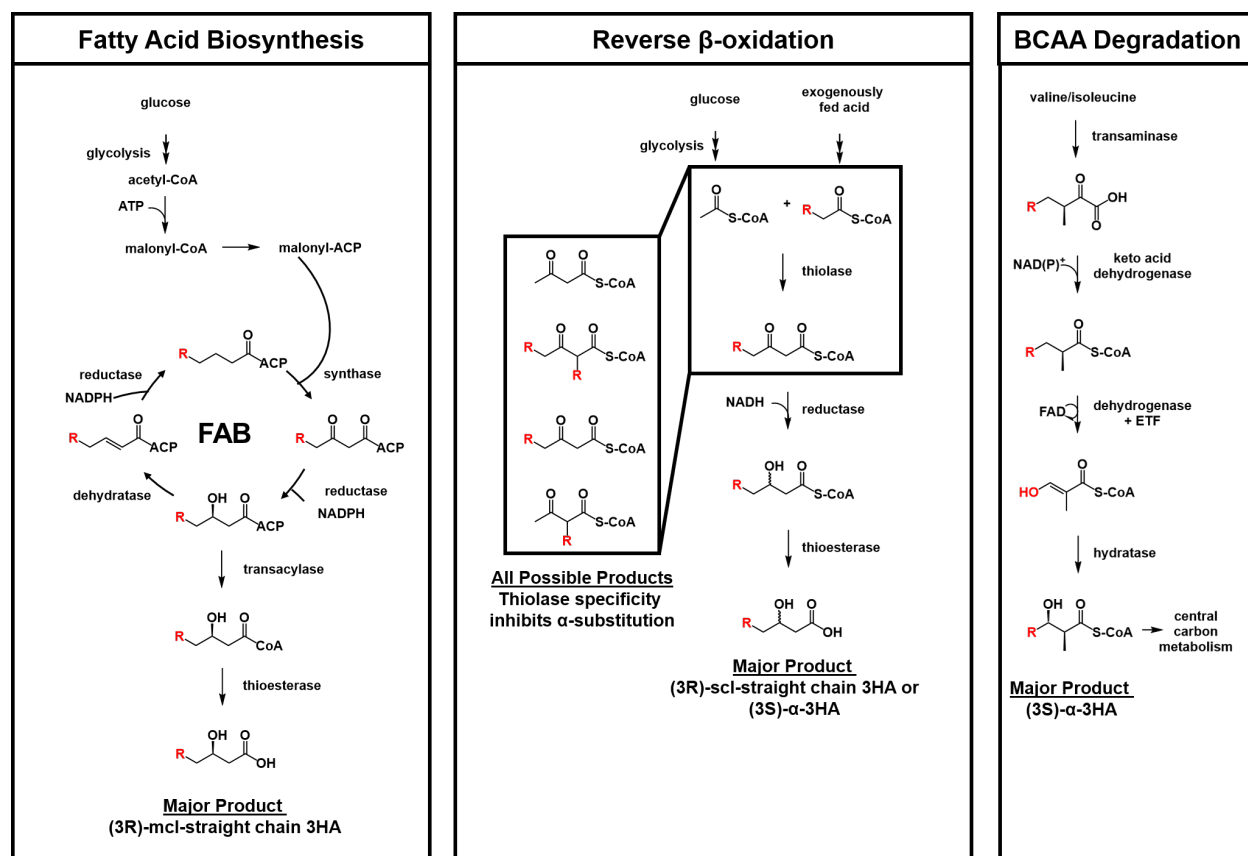


Figure 1.3. 3HA Production Routes

The literature is rife with examples of the use of metabolic engineering to produce 3HAs in recombinant microorganisms. The Prather lab previously developed an rBOX pathway that converts activated organic acids to 3HAs.<sup>16,17</sup> Although this pathway was successful at producing 3-hydroxy- $\gamma$ -butyrolactone - a key precursor for many pharmaceuticals - it failed to specifically produce branched and medium-chain-length (mcl) 3HAs. Others have demonstrated that branched and mcl 3HAs can be used as comonomers with 3-hydroxybutyrate (3HB) to improve PHA material properties.<sup>18</sup>

The condensation of butyryl-CoA and acetyl-CoA to form 3-hydroxyhexanoic acid or 3-hydroxy-2-ethylbutyric acid showed that mutations to increase priming or extending binding site size allows for specific production of branched or mcl 3HAs.<sup>19,20</sup> However, low yields from this pathway suggest the need for additional thiolase engineering. Another group characterized the branched-chain-specific thiolase Acat3 (*Ascaris suum*) and used it for the synthesis of PHA containing 3-hydroxy-2-methylbutyric acid (3H2MB).<sup>21</sup> Subsequent analysis of 3H2MB-containing PHA revealed its improved ductility and biodegradability relative to commercially available biopolymers.<sup>22</sup> This highlights the power of HA structure to transform material prop-

erties.

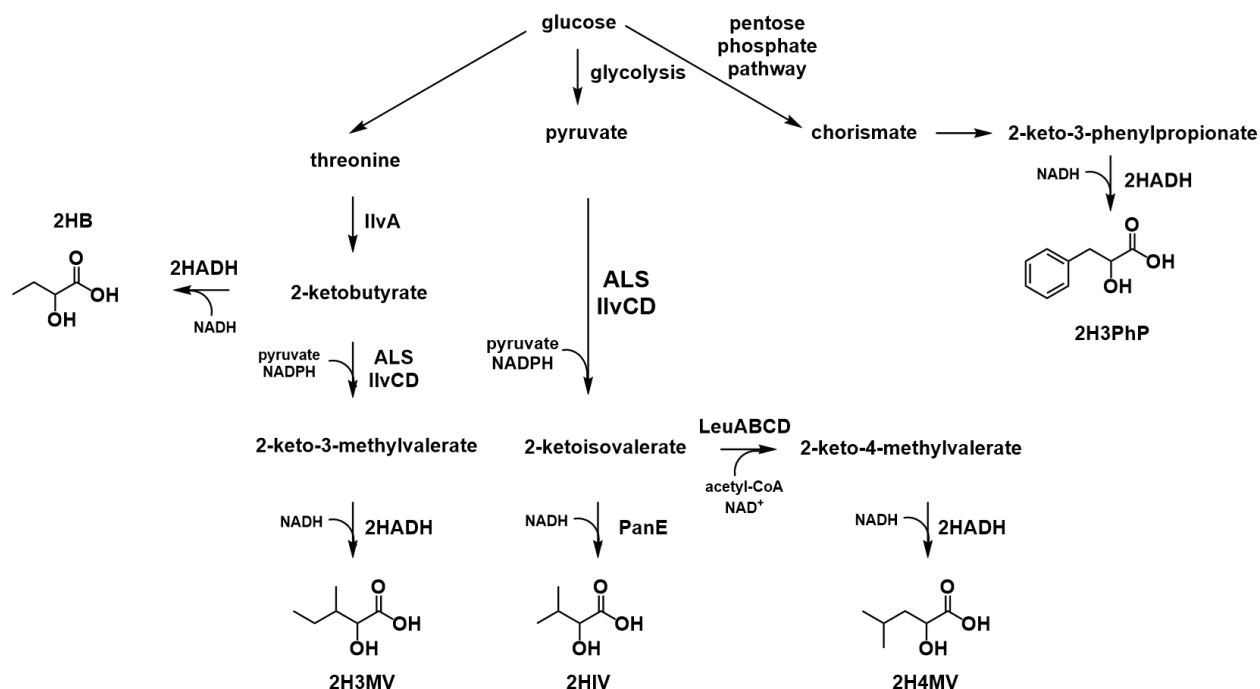
Natural pathways to branched compounds serve as good starting points for thiolase-independent pathways to HAs. Branched-chain amino acid (BCAA) degradation pathways were used for the production of 3-hydroxyisobutyric acid (3HIB)<sup>23</sup> and 3-hydroxy-3-methylbutyric acid(3H3MB).<sup>24</sup> High yields realized by these pathways support the usefulness of BCAA-based pathways for the production of branched 3HAs. Polyketide synthases are another natural source of branching. One group investigated the lipomycin polyketide synthase (PKS) and its ability to condense methylmalonyl-CoA and butyryl-CoA for 3HA production. This system produced 3HAs with branching patterns not achievable through other pathways, including some di- and tri-branched monomers.<sup>25,26</sup> Achieving bio-production of 3HAs at high titer and yield is integral for industrial usage. Routes to 3HAs that do not rely on traditional thiolases streamline this process since they exploit enzymes working in their native context to circumvent enzyme engineering.

### 1.2.2 Microbial production of 2-hydroxy acids

Polyesters containing 2-hydroxy acids (2HAs) received considerable attention in recent years because of the commercial success of 2HA-containing materials like PLA and polyglycolic acid (PGA). PLA's rigidity and opacity give it wide utility in biomedical applications. Polyesters containing glycolic acid exhibit excellent gas barrier properties, giving them application in dissolvable sutures and packaging material.<sup>27</sup> This success sets the stage for the development of microbial cell factories to produce other 2HAs.

Various 2HAs are accessible from 2-ketoacids in amino acid biosynthesis and C1 carbon metabolism (Figure 1.4). 2-Ketoacid pathways involve the overexpression of amino acid biosynthesis genes to produce a 2-keto acid followed by reduction to the corresponding 2HA using a 2HA dehydrogenase. This pathway has been used to produce 2-hydroxy-3-methylvaleric acid, 2-hydroxy-4-methylvaleric acid, and 2-hydroxy-3-phenylpropionic acid from threonine, leucine, and phenylalanine biosynthesis intermediates, respectively.<sup>28</sup> Another group produced 2-hydroxyisovaleric acid at 73% theoretical yield by overexpressing valine biosynthesis genes and using a C5-specific 2HA dehydrogenase —PanE (*Lactococcus lactis*).<sup>29</sup> Another route involves the conversion of C1 substrates to 2HAs via a novel 2-hydroxyacyl-CoA lyase (HACL). Chou et al. employed this HACL mediated route to condense aldehydes and formyl-CoA. They demonstrated the production of 2-hydroxydecanoic acid, 2-hydroxybutyric acid, 2-hydroxyisobutyric acid, and glycerate via this pathway.<sup>30</sup>





**Figure 1.4.** 2-ketoacid based routes to 2HAs. Abbreviations used in this figure include: ALS (acetolactate synthase), IlvA (threonine deaminase) IlvC (ketol-acid reductoisomerase from *E. coli*), IlvD (dihydroxy-acid dehydratase from *E. coli*), LeuA (2-isopropylmalate synthase from *E. coli*), LeuB (3-isopropylmalate dehydrogenase from *E. coli*), LeuCD (3-isopropylmalate dehydratase from *E. coli*), PanE (2-hydroxyacid dehydrogenase from *Lactococcus lactis*), 2HADH (2-hydroxyacid dehydrogenase), 2HB (2-hydroxybutyric acid), 2H3MV (2-hydroxy-3-methylvaleric acid), 2HIV (2-hydroxyisovaleric acid), 2H4MV (2-hydroxy-4-methylvaleric acid), and 2H3PhP (2-hydroxy-3-phenpropionic acid)

### 1.2.3 Microbial production of $\omega$ -hydroxy acids

$\omega$ -Hydroxy acids ( $\omega$ HAs) are HAs with hydroxylation past C3. These monomers stand out for the production of industrially relevant biopolymers because they have been shown to improve thermal stability when incorporated as comonomers with 3HB.<sup>31</sup> Commercially produced PHAs with  $\omega$ HA monomers include poly(4-hydroxybutyrate) (P4HB) and poly(3-hydroxybutyrate-co-4-hydroxybutyrate).<sup>11</sup> In particular, P4HB is highly elastomeric and the only PHA with FDA approval for medical applications.<sup>32</sup> 4-hydroxybutyric acid (4HB) is produced from an unrelated carbon source via a pathway involving the oxidation of the citric acid cycle (TCA) intermediate - succinate semialdehyde.<sup>33,34</sup>

Other  $\omega$ -HAs with demonstrated biological routes include 5-hydroxyvaleric acid (5HV),<sup>35,36</sup> 6-hydroxyhexanoic acid,<sup>37–41</sup> 7-hydroxyheptanoic acid,<sup>40</sup> 8-hydroxyoctanoic acid,<sup>42–45</sup> 10-hydroxydecanoic acid,<sup>42,44,45</sup> and 12-hydroxydodecanoic acid.<sup>42,44,45</sup> High yield, metabolic routes for these compounds take two forms: (1) oxidative conversion of semialdehydes from central carbon metabolism for the production of C4 and

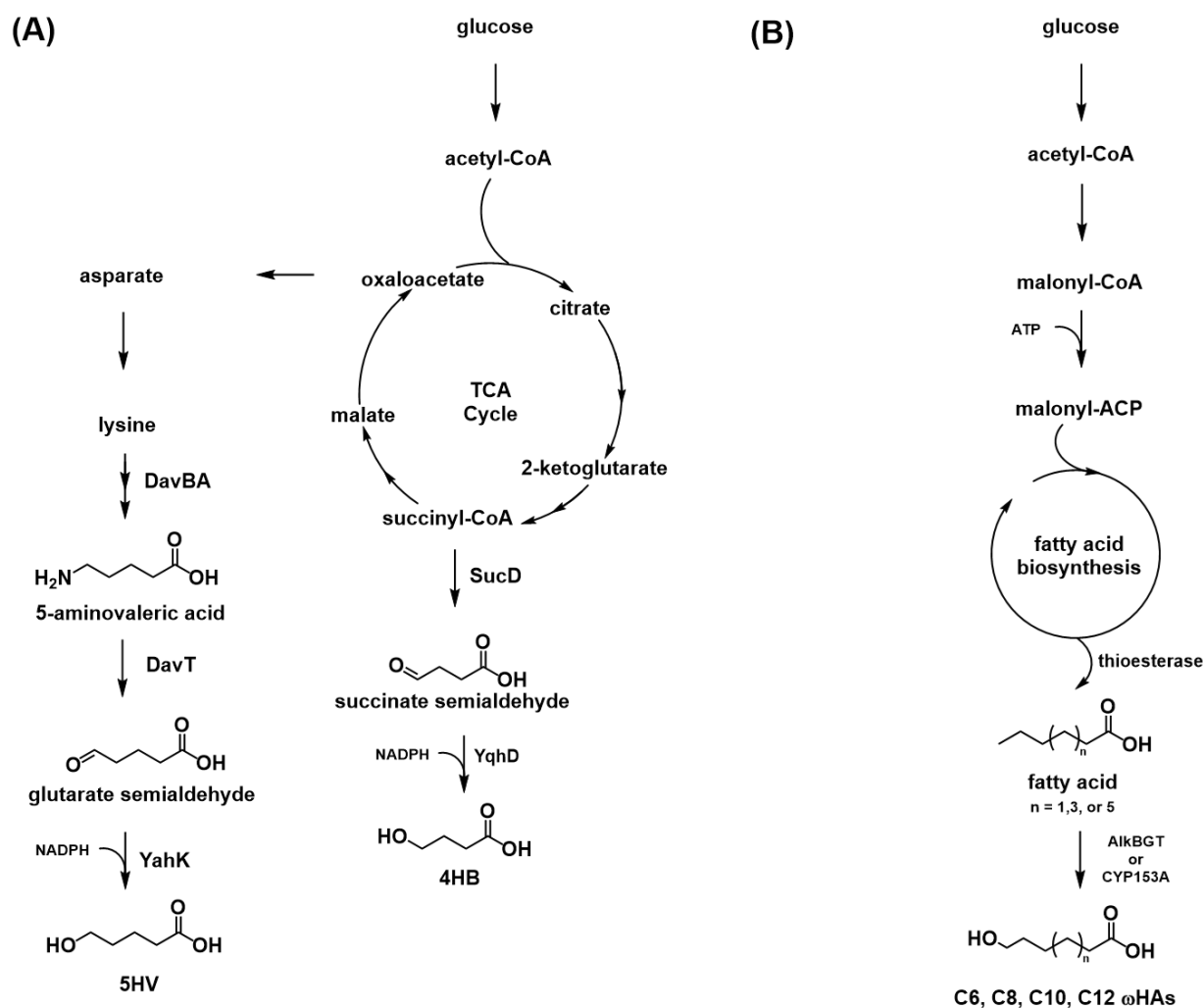
C5  $\omega$ HAs or (2)  $\omega$ -hydroxylation of fatty acids for the production of C6-C12  $\omega$ -HAs. Wang et al.,<sup>46</sup> Sohn et al.,<sup>36</sup> and Cen et al.<sup>35</sup> demonstrated the effectiveness of co-opting lysine degradation intermediates for the production of 5HV in *E. coli* and *Corynebacterium glutamicum*. 6-hydroxyhexanoic acid has been produced at low yield via an rBOX pathway involving the condensation of succinyl-CoA and acetyl-CoA. However, yields were <1% indicating the need for thiolase engineering. 6-hydroxyhexanoic acid stands out as a promising monomer because it can be polymerized to produce polycaprolactone - a commercially successful polymer typically produced from the petroleum derived monomer  $\epsilon$ -caprolactone. He et al. and Yoo et al. produced C8, C10, and C12  $\omega$ HAs via a pathways involving  $\omega$ -hydroxylation of fatty acids or fatty acid methyl esters by the alkane-1-monoxygenase system – AlkBGT - from *Pseudomonas putida* Gp1.<sup>42</sup> AlkBGT exhibits broad action on C5-C12 compounds.<sup>47</sup> CYP153As – a type of cytochrome P450 - can also perform  $\omega$ -hydroxylation and various groups have engineered CYP153s for the production of 8-hydroxyoctanoic acid.<sup>48-50</sup>  $\omega$ -Hydroxylation of fatty acids represents a promising platform for the biosynthesis of diverse  $\omega$ -HAs. Continued prospecting for monooxygenases and CYP153As capable of acting efficiently on branched and C5-C7 fatty acids is integral to further increasing the structural diversity of bio-producible  $\omega$ -HAs.

## 1.3 Microbial production of diols

### 1.3.1 Microbial production of C3-C4 diols

Microorganisms do not naturally produce the copolyester formed from diols and diacids, but they have been exploited for the production of both monomeric units (Figure 1.6). Recent literature outlines key advances in the microbial production of diacids.<sup>51</sup> The bio-production of C3–C4 diols such as 1,3-propanediol (1,3-PDO), 1,4-butanediol (1,4-BDO), and 1,3-butanediol (1,3-BDO) has been studied extensively. For example, the bio-production of 1,3-PDO via the Covation Biomaterials route has replaced its traditional synthesis from petroleum feedstocks. 1,3-PDO is condensed with terephthalic acid to produce polytrimethylene terephthalate, a polyester used to make bio-based carpet fibers. The need to supply expensive vitamin B<sub>12</sub> in this pathway opened the door for glycerol-independent pathways to 1,3-PDO. Attempts have been made to reduce the vitamin-B<sub>12</sub> dependency of this pathway in *Klebsiella pneumoniae*, but extensive strain engineering was required at the expense of cell fitness.<sup>52</sup>

Several glycerol-independent 1,3-PDO pathways have been constructed, including ones from malate,<sup>53</sup> homoserine,<sup>54,55</sup> aspartate,<sup>46</sup> malonyl-CoA,<sup>56</sup> and threonine.<sup>57</sup> The malonyl-CoA pathway produced the



**Figure 1.5.** Routes across various organisms and substrates have been established for the biosynthesis of  $\omega$ HAs. (a) Routes to 4HB and 5HV based on the oxidation of succinate semialdehyde and glutarate semialdehyde, respectively (b) Routes to C6, C8, C10, and C12  $\omega$ HAs which rely on hydroxylation of fatty acids. The following abbreviations were used: AlkB (alkane-1-monooxygenase from *Pseudomonas putida* GPo1), AlkT (rubredoxin from *Pseudomonas putida* GPo1), AlkR (rubredoxin reductase from *Pseudomonas putida* GPo1), DavA (5-aminovalamidase from *P. putida*), DavB (lysine monooxidase from *Pseudomonas putida*), DavT (5-aminovalerate transaminase from *Pseudomonas putida*), TCA (the citric acid cycle), YahK (aldehyde dehydrogenase from *E. coli*), YqhD (aldehyde dehydrogenase from *E. coli*)

highest 1,3-PDO yields of the glycerol-independent pathways, most likely due to its reliance on the well-established 3-hydroxypropionic acid pathway. Other new routes for 1,3-PDO production involve aldolases and have the added benefits of being orthogonal to native metabolism and utilizing 100% of substrate carbon for 1,3-PDO formation.<sup>58,59</sup> Taken together, new routes for 1,3-PDO synthesis exhibit similar theoretical yields as the glycerol route. Improving yields from these pathways will rely on engineering pathway enzymes for increased activity on pathway substrates. However, the ability to initiate synthesis from a myriad of substrates suggests that the glycerol-independent pathways may ultimately be most useful in combination, thereby enabling high-yield conversion of complex feedstocks to 1,3-PDO.

New pathways for butanediol synthesis expand feedstock range and exploit well-described pathways to reach new compounds. 1,3-BDO has been bio-produced using rBOX<sup>35,60–62</sup> and aldolase-based pathways.<sup>63</sup> Of note is the exploitation of thiolase preference for 3HB production for high-yield 1,3-BDO biosynthesis in *E. coli*<sup>57</sup> and *Cupriavidus necator*.<sup>60</sup> 1,4-BDO is used to produce polybutylene terephthalate (PBT) which has similar applications to polyethylene terephthalate (PET).<sup>3</sup> The current standard for 1,4-BDO bio-production is the Genomatica-patented route that involves the reduction of succinyl-CoA. Newly developed pathways for 1,4-BDO include a glutamate catabolism pathway,<sup>46</sup> a pathway involving norvaline oxidation,<sup>57</sup> and pathways from erythritol<sup>64</sup> and xylose.<sup>65</sup> Challenges to the industrial implementation of these new pathways include the cost associated with vitamin-B<sub>12</sub> supplementation in the xylose and erythritol pathways and product specificity issues in the norvaline pathway because it employs a promiscuous amino acid hydroxylase. The glutamate catabolism pathway represents an opportunity for high titer 1,4-BDO bio-production since it relies on glutamate — the most intracellularly abundant amino acid.

### 1.3.2 Microbial production of C5-C12 diols

While C3–C4 diol synthesis is well-studied, reports for C5–C12 and branched diols are rare. Some linear C5–C12 diols are industrially interesting because their polyesters exhibit properties comparable to PBT and can serve as a safer alternative to it. Further, polyesters containing branched diols are more amorphous and hydrolytically stable than analogous linear polyesters that make them useful for coatings.<sup>66</sup> C5–C12 diol production begins from the hydroxylation of alkane,<sup>67</sup> free fatty acid,<sup>45</sup> or fatty acid methyl ester feedstocks.<sup>44</sup> These pathways employ diverse monooxygenases and continued monooxygenase discovery will aid in the bio-production of new diols from this pathway.

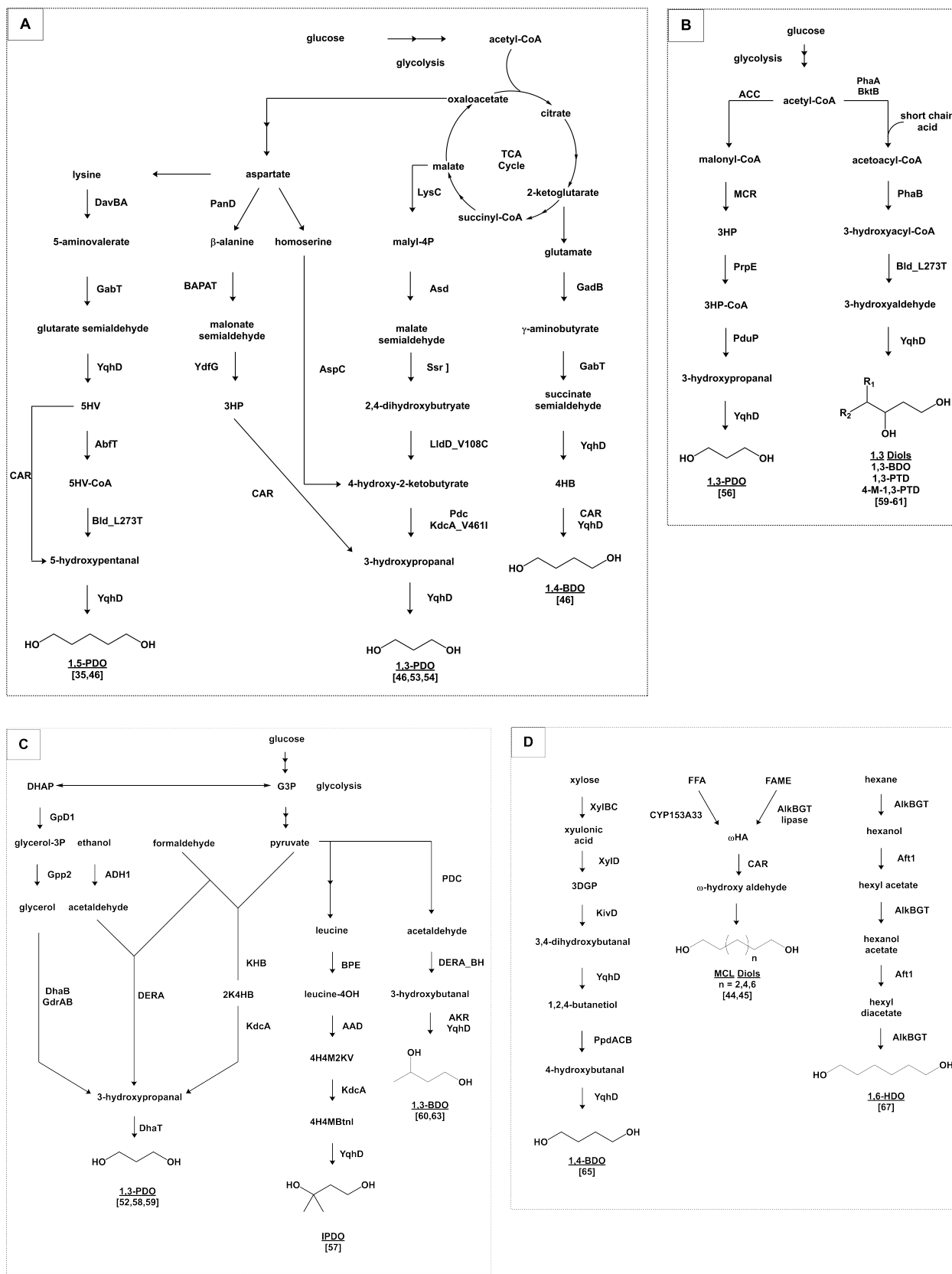
Amino acid pathways serve as a valuable reservoir of pathways to odd-chain and branched diols. 1,5-

pentanediol is bio-produced from CoA<sup>46</sup> and non-CoA<sup>35</sup> dependent pathways where lysine is catabolized to 5HV followed by reduction. The CoA-dependent pathway produced nearly 10x as much 1,5-pentanediol as the CoA-independent pathway, despite its additional energy requirements. This is most likely due to imbalances between 5HV production and reduction to 1,5-pentanediol. The pathway from Liu et al.<sup>57</sup> allows for the bio-production of branched diols from related amino acids through the promiscuity of amino acid hydroxylases. Unlike other amino acid pathways that are entirely reductive, this pathway includes two oxidative steps that reduce cofactor requirements. Amino acid hydroxylases can add hydroxyl groups at many carbon positions allowing for synthesis of diols not previously bio-produced. The diol diversity offered by this pathway opens the door to the bio-production of novel polyesters with unprecedented material properties. However, a major challenge for industrial implementation of this pathway from an unrelated carbon source is product specificity, since the hydroxylases used in this pathway can hydroxylate many amino acids efficiently. The current landscape of microbial HA and diol production highlights both the success of metabolic engineering to produce a variety of natural polyester building blocks and failure to develop high-yield pathways for non-natural ones. Increasing biopolymer building block diversity will rely on novel pathway design.

## 1.4 Novel pathway design methods

Novel pathway design can be leveraged to bio-produce new polyester building blocks and to reimagine bio-production of conventional ones. It allows for the production of new monomers to widen the space of material properties currently realized by bio-produced polyesters. Additionally, it allows for the redesign of traditional pathways for attributes such as carbon economy, number of pathway steps, and cofactor utilization, which affect how efficiently energy is transduced from the substrate for target compound formation.

Novel pathway design strategies include: (1) fine-tuning native pathways by gene deletion or overexpression and enzyme engineering, (2) combining hybrid pathways from individual organisms into a single organism, or (3) *de novo* design where non-natural biosynthetic schemes are proposed as enzymatic reactions that interconvert functional groups.<sup>68</sup> Strategy 1 is commonly used for the production of PHAs from non-chassis organisms. Strategy 2 is used for the production of PHAs in *E. coli* by combining central carbon metabolism with PHA biosynthetic routes from microorganisms like *Pseudomonas putida* or *Cupriavidus necator*. Since the chemicals produced by native metabolic pathways occupy a small place in chemical space, design strategies 1 and 2 produce limited biopolymer building block diversity.



**Figure 1.6.** Metabolic pathways for the bio-production of various diols. Caption continued on next page.

**Figure 1.6.** Routes across various organisms and substrates have been established for the biosynthesis of diols. (a) Routes to diols with TCA cycle compounds as precursor from central metabolic pathways. (b) Routes to diols with acetyl-CoA as precursor from central metabolic pathways. (c) Routes to diols with glycolysis compounds as precursors. (d) Routes to diols from alternative carbon sources. The following additional enzyme abbreviations were used: AbfT (CoA transferase from *Clostridium aminobutyricum*), CAR (carboxylic acid reductase from *Mycobacterium marinum*), BldL273T (butyraldehyde dehydrogenase from *Clostridium saccharoperbutylacetonicum*), AspC (aspartate transaminase from *E. coli*), Ssr (mutant malate semialdehyde reductase from *Metallosphaera sedula*), Asd (mutant malate semialdehyde dehydrogenase), LysC (mutant aspartate kinase from *E. coli*), LldDV108C (lactate dehydrogenase from *E. coli*), KdcA (ketoacid decarboxylase from *Lactococcus lactis*), Pdc (pyruvate decarboxylase from *Zymomonas mobilis*), MCR (malonyl-CoA reductase from *Chloroflexus aurantiacus*), PrpE (3-hydroxypropionyl-CoA synthetase from *M. sedula*), PduP (aldehyde dehydrogenase from *Salmonella typhimurium*), DERA (deoxyribose-5-phosphate aldolase from *Thermotoga maritima*), KHB (2-keto-4-hydroxybutyrate aldolase from *E. coli*), DhaT (aldehyde dehydrogenase from *Klebsiella pneumoniae*), BPE (amino acid hydroxylase from *Bordetella petrii*), AAD (amino acid deaminase from *Pseudomonas vulgaris*), DERABH (deoxy-5-phosphate aldolase from *Bacillus halodurans*), AKR (aldo/ ketoreductase from *Pseudomonas aeruginosa*), CYP153A33 (cytochrome P450 monooxygenase from *Marinobacter aquaeolei*), Atf1 (alcohol acetyltransferase from *Saccharomyces cerevisiae*), GpD1 (glycerol-3-phosphate dehydrogenase from *Saccharomyces cerevisiae*), Gpp2 (glycerol-3-phosphate phosphatase from *Saccharomyces cerevisiae*), DhaB (glycerol dehydratase from *Klebsiella pneumoniae*), GdrAB (glycerol dehydratase activator), PhaA (thiolase from *Cupriavidus necator*), XylBC (xylose dehydrogenase from *Caulobacter crescentus*), XylD (xyulonic acid dehydratase from *C. crescentus*), PpdACB (engineered diol dehydratase from *Klebsiella oxytoca*). Additional compound abbreviations used in this figure include: 3-hydroxypropionic acid (3HP), malyl-4-phosphate (malyl-4P), dihydroxyacetone phosphate (DHAP), glyceraldehyde-3-phosphate (G3P), glycerol-3P (glycerol-3-phosphate), 4-hydroxy-4-methyl-2-ketovaleric acid (4H4M2KV), 4-hydroxy-4-methylbutanal (4H4MBtnl), 2-keto-4-hydroxybutyrate (2K4HB), 3-deoxy-glyceropentulosnic acid (3DGP).

*De novo* design offers a route to fully harness the synthetic capabilities of metabolic pathways because it removes the constraint of starting at known pathways. *De novo* design is bolstered by *in silico* tools that identify enzymes and cascading reactions to convert metabolites to a target chemical.<sup>69</sup> One tool - RetroPath<sup>70</sup> - was used to identify retro-biosynthetic pathways to compounds as diverse as pinocembrin and mandelic acid in recombinant *E. coli*.<sup>71</sup> These pathways can be prioritized for implementation via flux balance analysis, thermodynamic favorability, cofactor usage, and number of non-native steps among other criteria. *De novo* design represents marked improvements over traditional strategies in terms of target chemical diversity, but it has shortcomings. Specifically, *de novo* design produces many pathways for which feasibility analysis doesn't always reduce to a tractable number. Further, this technique often requires years of enzyme engineering to ultimately produce pathways only capable of making one compound. Manual *de novo* design like that described by Vila-Santa et al.<sup>72</sup> - while laborious - can be used to design a small number of feasible pathways.

Combined, recent advances in novel pathway design for HAs and diols illustrate four large themes: (1) redesigning natural pathways to reduce energy and supplementation requirements, (2) using natural pathways for branched compounds as inspiration for non-natural, branched HAs and diols, (3) the usefulness of enzyme discovery for unlocking new pathways to HAs and diols, and (4) designing new pathways from different

substrates. An examination of these pathways reveals their complexity and interconnectedness, but also hints at the HAs and diols yet to be produced. Clearly, novel pathway design is integral for producing biopolymer building blocks that lead to plastics with increased industrial utility.

## 1.5 Thesis overview

This thesis aims to design, implement, and optimize novel metabolic pathways for the production of biopolymer building blocks. Specific goals include:

- (1) The prioritization of industrially relevant HAs to construct biological pathways towards
- (2) The design, construction, and optimization of a biological pathway for the prioritized HAs
- (3) Design, analysis, and possible implementation of a biological pathway to 3-methyl-1,5-pentanediol

We began by prioritizing building blocks for biosynthesis based on novelty, maximum theoretical yield, ease of chemical polymerization, and potential material property improvements conferred by the monomer once incorporated into a biopolymer. Next, we design and implement a novel pathway from a renewable feedstock to the prioritized monomers - 3HIB and 3H2MB - in *E. coli*. As proof-of-concept we optimize our novel pathway by deleting competing pathways, de-bottlenecking key pathway steps via enzyme selection, and the development of a unique by-product recycle. Lastly, we design pathways to 3-methyl-1,5-pentanediol - a monomer of significant interest to our industrial sponsor - and determine the feasibility of each pathway. This work illustrates the utility of novel pathway design for the bio-production of novel HAs and diols which lead to biopolymers with industrially relevant properties.

## 1.6 Thesis organization

This thesis is divided into five chapters. Chapter 1 reviews metabolic pathways for biopolymer building block production. Chapter 2 describes the process used to identify and prioritize industrially relevant HAs for biological synthesis. In chapter 3, we discuss the design and implementation of a novel metabolic pathway to two industrially relevant building blocks - 3HIB and 3H2MB. We further optimized this pathway for 3H2MB production. In chapter 4, we turn our attention to designing and determining the feasibility of novel pathways to 3-methyl-1,5-pentanediol - a monomer of significant interest to our industrial sponsor, DIC. Finally, chapter 5 summarizes chapters 1-4 and discusses the implications of this work.



## Chapter 2

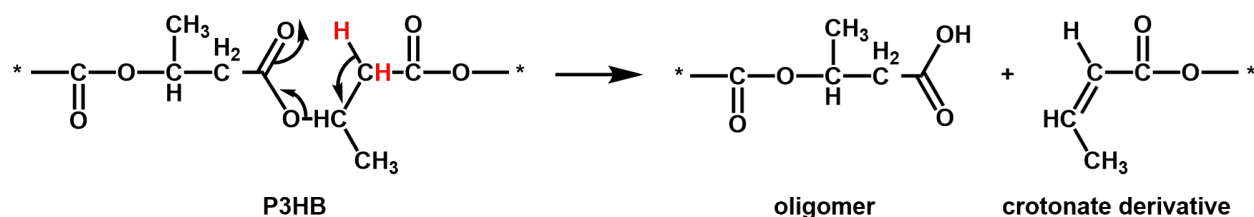
# Identification of industrially relevant hydroxy acids for biosynthesis

## Abstract

Biopolymer industrial application is currently limited due to their unfavorable material properties. Most prototypically, P3HB is susceptible to thermal degradation via a mechanism facilitated by its thermally-labile  $\alpha$ -hydrogens. HA structural properties shown to improve thermal stability include  $\alpha$ -substitution and  $\omega$ -hydroxylation. In hopes of producing biopolymers with broader industrial application, we prioritized bioaccessible HAs for bio-production. Our analysis identified 182 potentially bioaccessible HAs - including 31 bioaccessible HAs which have not been cataloged by others. We prioritized monomers from this list based on novelty, ease of chemical polymerization, maximum theoretical yield, and potential to confer thermal stability properties in the context of biopolymers. This analysis yielded a list of 17 2HAs,  $\alpha$ -substituted 3HAs and  $\omega$ HAs with the potential to produce biopolymers with novel properties. 3HIB and 3H2MB were ultimately prioritized for bio-production based evidence of their high molecular weight polymerization and ability to reduce thermal degradation when incorporated into a biopolymer.

## 2.1 Introduction

Designing, synthesizing, and characterizing new polyesters with the favorable properties of natural PHAs and improved material properties relative to currently available biopolymers is essential for wider industrial application. P3HB - a homopolymer of 3HB - is the most well-studied and widely available PHA. P3HB exhibits a narrow thermal processing window. Specifically, it degrades near its melting temperature via a  $\beta$ -elimination mechanism that relies on thermally labile  $\alpha$ -hydrogens to produce crotonate and oligomers (Figure 2.1).<sup>12</sup> Operationally, this means that when P3HB is melted to mold it for final application, it also begins to degrade. This degradation behavior is in stark contrast to petroleum derived plastics like PET and polypropylene which exhibit wide thermal processing windows allowing them to be melt-processed over a wide temperature range without yield reductions.<sup>73</sup> Based on this, we focused on prioritizing HAs for bio-production which might confer improved thermal stability when incorporated into a biopolymer.



**Figure 2.1.** Poly(3-hydroxybutyrate) thermal degradation mechanism. P3HB degrades primarily via a  $\beta$ -elimination mechanism to produce crotonate and oligomers. Thermally labile hydrogens are indicated by red text

Previous studies showed that PHAs composed of  $\alpha$ -substituted monomers exhibit improved thermal properties relative to their unsubstituted counterparts.<sup>18,22,74,75</sup> For example, PHAs composed of  $\alpha$ - $\alpha$ -dimethylated HAs were shown to exhibit enhanced thermal stability, ductility, and toughness compared to P3HB.<sup>75</sup> Further, copolymerization of 3HB with  $\omega$ HAs like 4HB<sup>31</sup> or 5HV<sup>76</sup> substantially increases the polymer processing window by reducing melting temperature while maintaining degradation temperature. These studies show that  $\alpha$ -substitution and  $\omega$ -functionalization are integral monomer characteristics to tune when designing novel PHAs with desirable thermal properties. Herein, a systematic process is described for prioritization of industrially relevant HAs for bio-production. In short, HAs with connection to the microbial metabolome were prioritized for bio-production based on novelty, ease of chemical polymerization, maximum theoretical yield, and expected thermal stability enhancements conferred by the HA when incorporated into a biopolymer.

## 2.2 Materials and Methods

HAs with connection to the microbial metabolome were identified by mining the literature, KEGG,<sup>77</sup> and MetaCyc.<sup>78</sup> This list of monomers was initially culled to eliminate HAs with heteroatoms, cyclization, and 4-hydroxy acids. Next, the maximum theoretical yield based on an energy balance ( $Y_E$ ) and polymerizability score<sup>A</sup> were determined for each HA.  $Y_E$  was calculated based on the metric defined by Dugar and Stephanopoulos.<sup>79</sup>

$$Y_E = \frac{\gamma_S}{\gamma_P} \quad (2.1)$$

$\gamma_S$  and  $\gamma_P$  are the degree of reduction of the substrate and product, respectively (Eq. 2.1). Degree of reduction is the sum of the valence states of each atom in a given compound. The polymerizability score is a heuristic metric developed by Prof. Bradley Olsen's lab (MIT, Department of Chemical Engineering) that ranges from 0-5, with increasing scores representing monomers expected to be easier to polymerize (Table 2.1).

**Table 2.1.** Polymerizability score definition

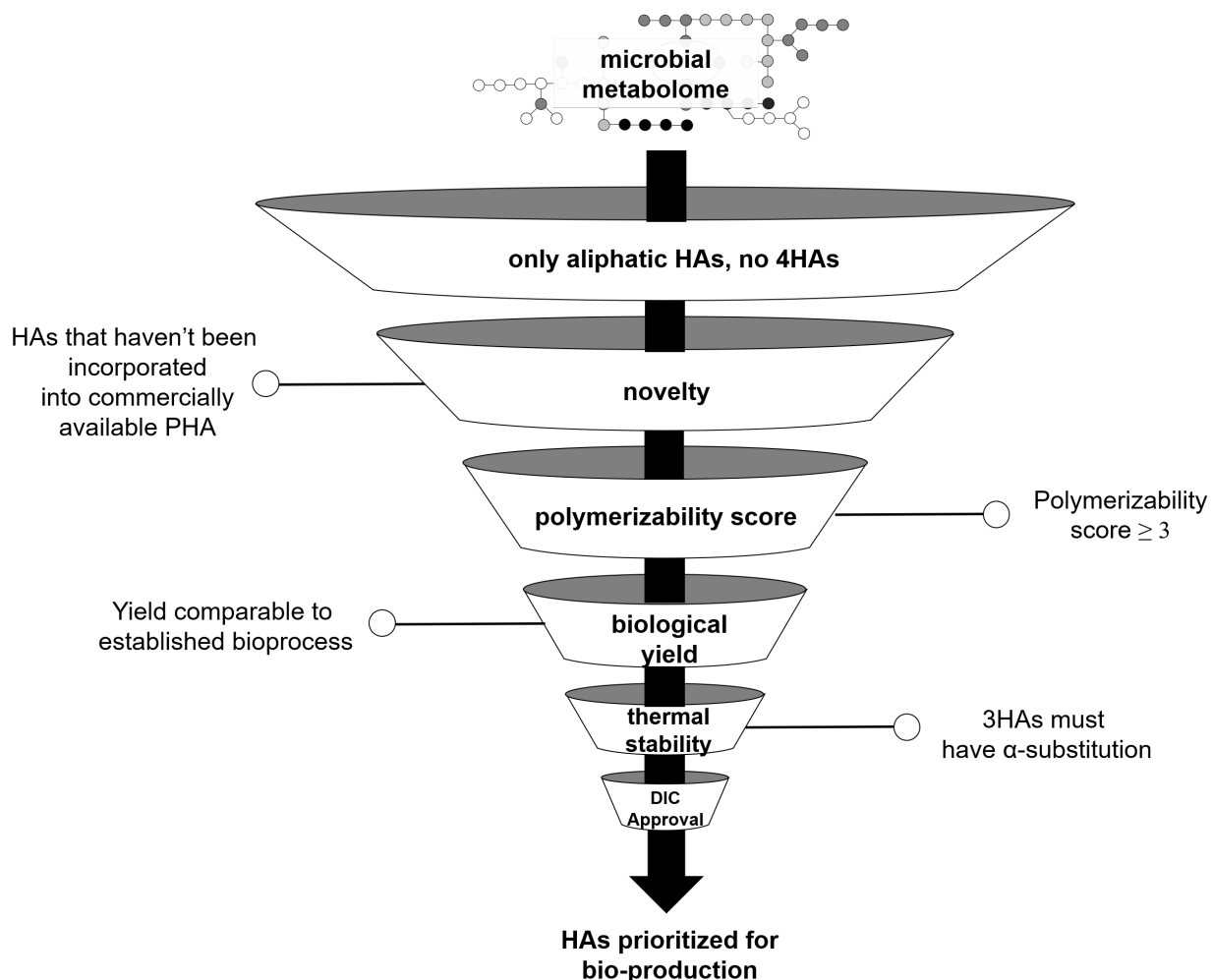
Score	Description
5	There are known routes to polymerize the monomer to high molar mass in the form it is naturally produced
4	There are known routes to polymerize the monomer to high molar mass with minor derivitization (i.e. lactic acid)
3	There are known routes to polymerize the monomer to high molar mass with significant derivitization
2	There may be routes to polymerize the monomer to high molar mass in its original form
1	There may be routes to polymerize the monomer to high molar mass in a derivitized form
0	The monomer most likely cannot be polymerized

Monomers with polymerizability scores  $< 3$  or  $Y_E < 0.51$  g/g glucose were removed from the list.  $Y_E = 0.51$  represents the maximum theoretical yield for biological production of ethanol from glucose - a well-established bioprocess. As a final sieve, we removed 3HAs from this list without  $\alpha$ -substitution. From this list of high-yield, easy-to-polymerize monomers, our industrial sponsor selected HAs for biosynthesis based on internal experiments to confirm ease of chemical polymerization and biodegradation of biopolymers composed of these HAs (Figure 2.2).

<sup>A</sup>Polymerizability score for each monomer was kindly determined by Dr. Wontae Joo - a former postdoctoral associate in the Olsen lab

## 2.3 Results and Discussion

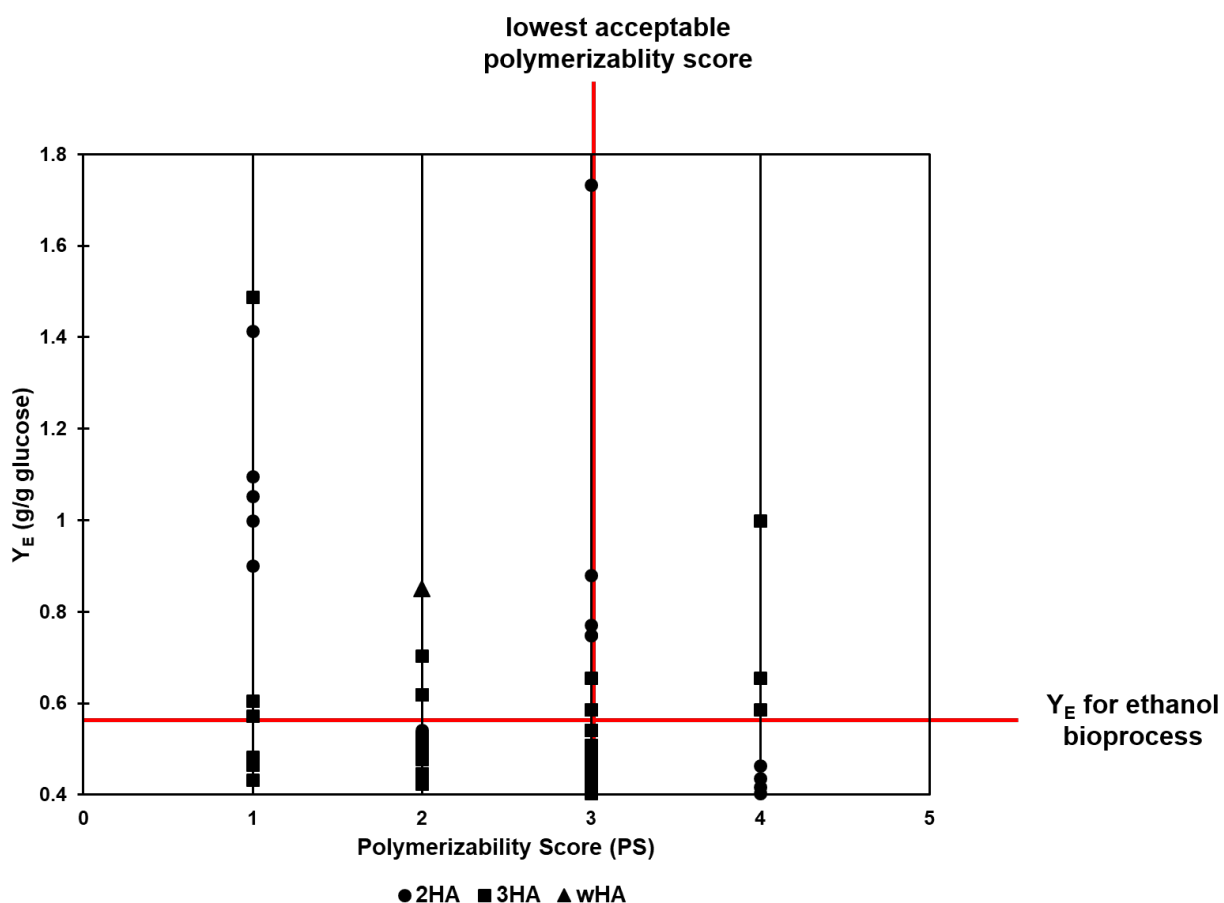
A list of candidate monomers for novel, industrially relevant PHAs was identified by cataloging HAs with connection to the microbial metabolome. Previously, Steinbüchel and Valentin,<sup>7</sup> Agnew and Pflieger<sup>8</sup> and Choi et al.<sup>9</sup> collectively identified 151 such monomers. This list was supplemented with HAs produced as intermediates in biological pathways identified by mining the MetaCyc<sup>78</sup> and KEGG<sup>77</sup> databases. Finally, monomers not previously described in reviews by others were identified from the literature to produce a list of 182 HAs. The monomers not previously described by others are detailed in Table 2.2. Most of these HAs are 2HAs,  $\alpha$ -substituted 3HAs ( $\alpha$ -3HAs), and *mcl*  $\omega$ HAs. These newly cataloged HAs and an evaluation of the biological pathways that produce them are available in our recent review.<sup>14</sup>



**Figure 2.2.** Process for prioritizing industrially relevant hydroxy acids

This initial list was culled to exclude HAs with heteroatoms and 4-hydroxyacids (4HAs). 4HAs are

known to favor the formation of lactones over the polymer which greatly reduces yield during chemical polymerization.<sup>32</sup> Next, the monomer list was assessed for novelty to remove HAs like 3HB and lactic acid which have commercial routes for the production of their biopolymers. Polymerizability scores and theoretical yields ( $Y_E$ ) were assigned to the remaining 111 HAs to identify high yield, easy to polymerize monomers (Figure 2.3). Monomers with polymerizability score < 3 and/or yields less than the maximum theoretical yield of ethanol bioproduction (i.e. an established bioprocess) were removed from the list. As a final sieve, 3HAs without  $\alpha$ -substitution were eliminated from the list to select for monomers which lead to biopolymers with improved thermal stability.



**Figure 2.3.** Maximum theoretical yield vs polymerizability score for biologically accessible hydroxy acids

The current monomer list includes 17 high yield, easily polymerizable 2HAs,  $\alpha$ -3HAs, and  $\omega$ HAs (Figure 2.4). The 2HAs included on this list are accessible via 2-ketoacid intermediates of amino acid biosynthesis pathways.  $\alpha$ -3HAs stand out in this list because their polyesters exhibit improved thermal stability and ductility compared to P3HB.<sup>18,22,74,75</sup> These  $\alpha$ -3HAs were bio-produced primarily via a lipomycin PKS capable of

condensing methylmalonyl-CoA with a variety of acyl-CoAs.<sup>26</sup> The  $\omega$ HAs included on the final monomer list were mcl and have been shown to expand the polymer processing window when incorporated as comonomers with 3HAs.<sup>31,76</sup> From this shorter list, 3HIB (IUPAC name: (2S)-3-hydroxy-2-methylpropanoic acid ) and (2S,3R)-3H2MB (IUPAC Name: 3-hydroxy-2-methylbutyric acid) were prioritized for biological synthesis based on internal experiments by our industrial sponsor to confirm their high molecular weight chemical polymerization and improved degradation properties relative to other monomers from the list.

## 2.4 Conclusions

Identifying HAs which lead to biopolymers with improved properties is essential for their industrial application. Our analysis identified 182 potentially bioaccessible HAs - including 31 bioaccessible HAs which have not been cataloged by others (Table 2.2). We prioritized monomers from this list based on novelty, ease of chemical polymerization, maximum theoretical yield, and potential to confer thermal stability properties in the context of biopolymers. 3HIB and 3H2MB were ultimately prioritized from our final monomer list based on evidence of their high molecular weight polymerization and ability to reduce thermal degradation when incorporated into a biopolymer.

**Table 2.2.** Additional hydroxy acids with connection to the microbial metabolome

IUPAC Name	$Y_E$ (g/g glucose)	Polymerizability Score	Reference
3-hydroxy-2-oxopropanoic acid	1.73	3	MetaCyc
3-hydroxy-2-methylpropanoic acid	0.77	3	[80]
2,3-dihydroxypropanoic acid	1.41	1	[81]
2-hydroxypentanoic acid	0.66	4	[30]
2,4-dihydroxybutanoic acid	1	1	[82]
(2E,4Z)-2-hydroxyhexa-2,4-dienoic acid	0.66	1	KEGG
3-hydroxy-3-methyl-2-oxobutanoic acid	0.88	3	KEGG
(2S)-2-hydroxy-2-methyl-3-oxobutanoic acid	0.88	3	KEGG
2-ethyl-3-hydroxybutanoic acid	0.59	3	[20]
6-hydroxyhexanoic acid	0.59	3	[37–39, 41, 83]
2-hydroxy-3-methylpentanoic acid	0.59	4	[84]
2-hydroxyhexanoic acid	0.59	4	Prather Lab
5-hydroxy-2,4-dioxopentanoic acid	1.21	3	KEGG
(R)-3-hydroxy-3-methyl-2-oxopentanoic acid	0.75	3	KEGG
(2S)-2-ethyl-2-hydroxy-3-oxobutanoic acid	0.75	3	KEGG
3-hydroxy-2-methylhexanoic acid	0.54	3	[26]
3-hydroxy-2,4-dimethylpentanoic acid	0.54	3	[26]
7-hydroxyheptanoic acid	0.54	2	[40]
(2R)-2-hydroxypentanedioic acid	1.01	1	KEGG
3-hydroxy-2,5-dimethylhexanoic acid	0.51	3	[26]
3-hydroxy-2,4-dimethylhexanoic acid	0.51	3	[26]
2-(1-hydroxyethyl)hexanoic acid	0.51	3	[20]
8-hydroxyoctanoic acid	0.51	3	[42, 44, 45]
2-hydroxyhexanedioic acid	0.9	1	KEGG
2-hydroxydecanoic acid	0.46	4	[85]
10-hydroxydecanoic acid	0.7	3	[42, 44, 45]
2-hydroxydodecanoic acid	0.44	4	[85]
12-hydroxydodecanoic acid	0.44	3	[42, 44, 45]
2-hydroxytetradecanoic acid	0.41	4	[85]
2-hydroxyhexadecanoic acid	0.4	4	[85]
(2R)-2-hydroxyoctadecanoic acid	0.39	4	KEGG

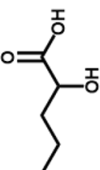
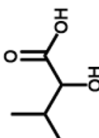
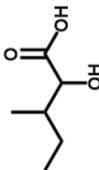
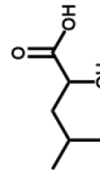
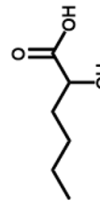
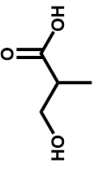
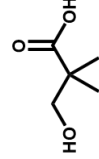
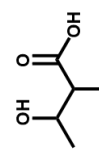
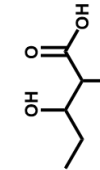
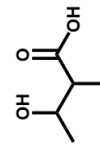



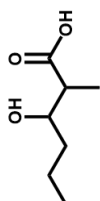
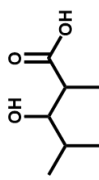
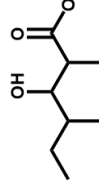
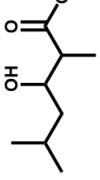
2HAS	3HAS	ωHAS
<p> 2-hydroxypentanoic acid <math>Y_E = 0.66</math> ; <math>PS = 4</math></p> <p> 2-hydroxy-3-methylbutanoic acid <math>Y_E = 0.66</math> ; <math>PS = 4</math></p> <p> 2-hydroxy-3-methylpentanoic acid <math>Y_E = 0.66</math> ; <math>PS = 4</math></p> <p> 2-hydroxy-4-methylpentanoic acid <math>Y_E = 0.59</math> ; <math>PS = 4</math></p> <p> 2-hydroxyhexanoic acid <math>Y_E = 0.66</math> ; <math>PS = 4</math></p>	<p> 3-hydroxy-2-methylpropanoic acid <math>Y_E = 0.77</math> ; <math>PS = 3</math></p> <p> 3-hydroxy-2,2-dimethylpropanoic acid <math>Y_E = 0.66</math> ; <math>PS = 3</math></p> <p> 3-hydroxy-2-methylbutanoic acid <math>Y_E = 0.66</math> ; <math>PS = 3</math></p> <p> 3-hydroxy-2-methylpentanoic acid <math>Y_E = 0.59</math> ; <math>PS = 3</math></p> <p> 2-ethyl-3-hydroxybutanoic acid <math>Y_E = 0.66</math> ; <math>PS = 3</math></p>	<p> 5-hydroxypentanoic acid <math>Y_E = 0.66</math> ; <math>PS = 4</math></p> <p> 5-hydroxyhexanoic acid <math>Y_E = 0.59</math> ; <math>PS = 4</math></p> <p> 6-hydroxyhexanoic acid <math>Y_E = 0.59</math> ; <math>PS = 3</math></p>
	<p> 3-hydroxy-2-methylhexanoic acid <math>Y_E = 0.54</math> ; <math>PS = 3</math></p> <p> 3-hydroxy-2,4-dimethylpentanoic acid <math>Y_E = 0.54</math> ; <math>PS = 3</math></p> <p> 3-hydroxy-2,4-dimethylhexanoic acid <math>Y_E = 0.51</math> ; <math>PS = 3</math></p> <p> 3-hydroxy-2,5-dimethylhexanoic acid <math>Y_E = 0.51</math> ; <math>PS = 3</math></p>	

Figure 2.4. Final list of industrially relevant hydroxy acids



## Chapter 3

# Design, implementation, and optimization of a novel, biological pathway to $\alpha$ -substituted 3-hydroxy acids

### Abstract

PHAs are renewably-derived, microbial polyesters composed of HAs. Demand for sustainable plastic alternatives, combined with the unfavorable thermal properties exhibited by some PHAs, motivates the discovery of novel ones. The rBOX pathway – the canonical pathway for HA production – is unable to produce  $\alpha$ -substituted HAs which lead to thermostable PHAs because it utilizes thiolases with narrow substrate specificity. Here, we present a thiolase-independent pathway to two  $\alpha$ -substituted HAs – 3HIB and 3H2MB. This pathway involves the conversion of glucose to various branched acyl-CoAs and ultimately to 3HIB or 3H2MB. As proof of concept, we engineered *E. coli* for the specific production 3HIB and 3H2MB at titers as high as  $66 \pm 5$  mg/L and  $290 \pm 40$  mg/L, respectively. To our knowledge, this is the first report of 3H2MB synthesis from glucose. We optimized our pathway for 3H2MB production by deleting genes that encode for competing pathways and via a novel, byproduct recycle. Finally, we investigated mutagenesis of a major pathway gene as a way to expand the product range of this pathway to other branched HAs. This work illustrates the utility of novel pathway design for the production of HAs leading to PHAs with industrially relevant properties.

**This section contains work adapted from**

Bannister, K.R., Prather, K.L.J.  $\alpha$ -Substituted 3-hydroxy acid production from glucose in *Escherichia coli*. *In preparation*

### 3.1 Introduction

3HIB and 3H2MB represent advantaged monomers for sustainable plastics production. They were prioritized for bio-production based on ease of chemical polymerization and their ability to prevent thermal degradation in the context of a biopolymer (Chapter 2). Prioritization of these monomers was further supported by internal experiments from our industrial sponsor confirming their high molecular weight chemical polymerization and the biodegradability of the corresponding biopolymers.

Several routes exist for the chemical synthesis of 3HAs like 3HIB and 3H2MB: (1) reacting epoxides with hydrogen cyanide followed by hydrolysis, (2) Kolbe nitrile synthesis where hypochlorous acid is added to an olefin, followed by hydrolysis of the resulting hydroxynitrile, (3) a Reformatsky reaction with an  $\alpha$ -halocarboxylic acid ester and a ketone over a zinc catalyst, (4) hydrolysis of  $\beta$ -lactones, (5) alkaline hydration of enoic acids, or (6) catalytic hydrogenation of  $\beta$ -ketoacids.<sup>86</sup> Many of these synthetic schemes are complicated - requiring multiple workup steps, several petroleum-derived reactants, and catalysts. Further, these schemes often yield racemic mixtures. Thus, a biological route to 3HIB and 3H2MB is preferred because it can be engineered to initiate product synthesis from a renewable feedstock and produce enantiopure product.

**Table 3.1.** Previous reports of 3HIB and 3H2MB bio-production

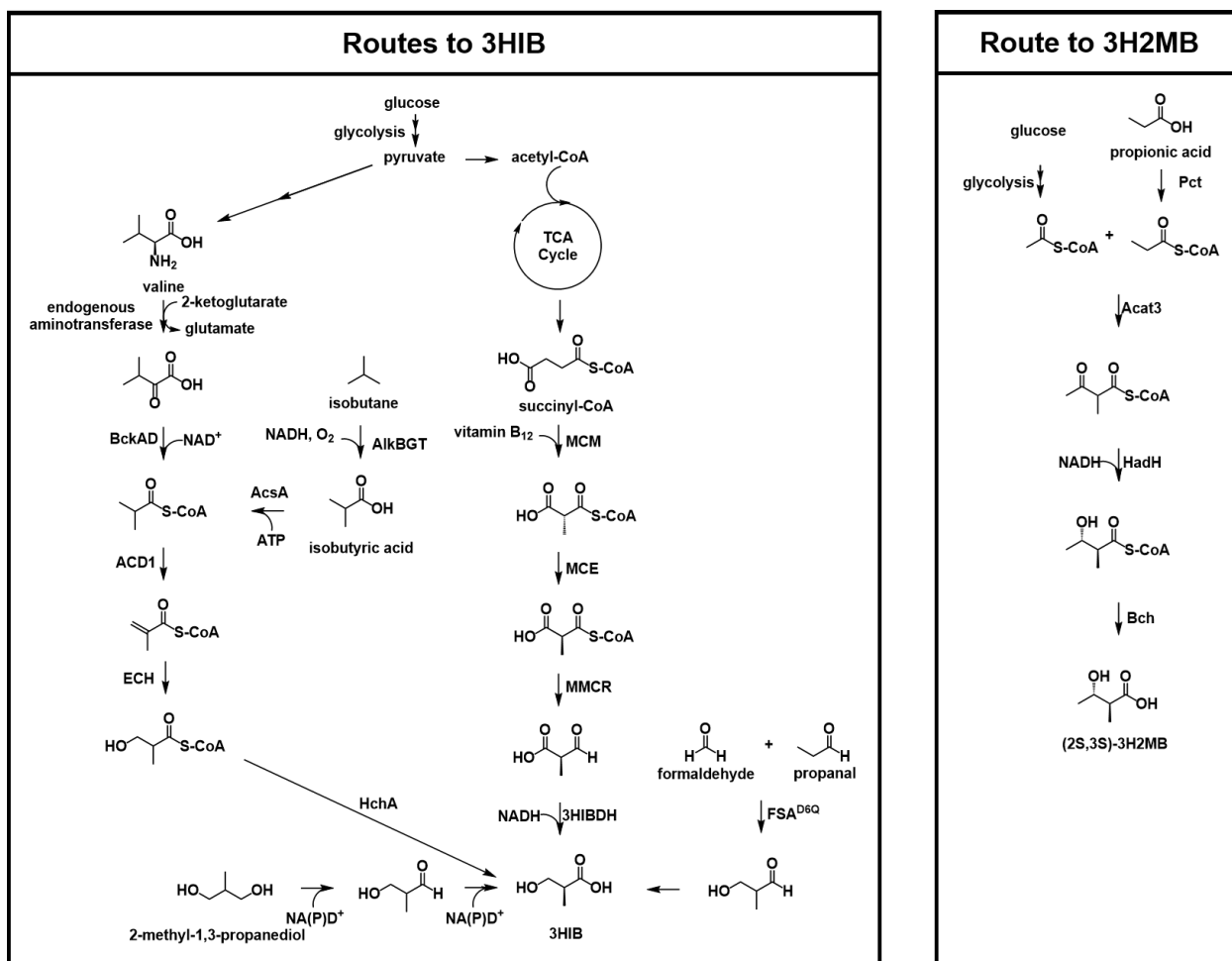
Monomer	Pathway	Substrate	Titer (g/L)	Organism	Reference
3HIB	BCAA degradation	glucose	0.63	<i>Pseudomonas taiwanensis</i>	[23]
3HIB	diol oxidation	2-methyl-1,3-propanediol	8.5	<i>Gluconobacter oxydans</i>	[87]
3HIB	BCAA degradation	glucose	5.1	<i>Saccharomyces cerevisiae</i>	[88]
3HIB	BCAA degradation	isobutane	0.413	<i>Yarrowia lipolytica</i>	[89]
3HIB	aldolase	formaldehyde + propanal	2.5	<i>E. coli</i>	[90]
3HIB	sleeping beauty mutase	glucose	0.069	<i>E. coli</i>	[91]
3H2MB	rBOX	glucose + propionate	1.08	<i>E. coli</i>	[21]

Conventionally, short-chain-length (scl) 3HAs like 3HIB and 3H2MB are bio-produced via the rBOX pathway (Figure 1.3). However, the rBOX pathway generally fails to produce  $\alpha$ -substituted 3HAs ( $\alpha$ -3HAs) because of the strict substrate specificity of thiolases. There are few reports of the bio-production of 3H2MB. Blaisse et al.<sup>21</sup> demonstrated the production of 3H2MB using a branched-chain specific thiolase, but the product exhibited S stereochemistry at C3 which is incompatible with biodegradation by PHA depolymerases. 3HIB bio-production is informed by the rich literature surrounding its conversion to methacrylic acid - a

monomer used in the production of acrylic. 3HIB production has been reported from a variety of substrates and pathways (Table 3.1 and Figure 3.1). The highest achieved titer was via the oxidation of 2-methyl-1,3-propanediol via endogenous metabolism in *Gluconobacter oxydans*.<sup>87</sup> However, there is no clear biological route for this substrate. Cesnik et al. engineered a pathway involving the condensation of formaldehyde and propanal followed by oxidation of 3-hydroxyisopropanal to 3HIB. The product diversity determining step in this pathway is the condensation reaction catalyzed by FSA<sup>D6Q</sup> - a mutant aldolase from *E. coli*. Like thiolases, FSA demonstrates strict specificity for substrates which lead to 3HAs without  $\alpha$ -substitution. Optimizing this pathway for 3HIB production and extending it to 3H2MB production would require additional aldolase engineering.<sup>92</sup> Seo et al. utilized *E. coli*'s sleeping beauty mutase pathway for 3HIB production.<sup>91</sup> Natively, the sleeping beauty mutase pathway converts succinyl-CoA to propionate via the action of a vitamin B<sub>12</sub>-dependent methylmalonyl-CoA mutase.<sup>93</sup> Using this pathway for the production of 3H2MB would require the action of methylmalonyl-CoA mutase on glutaryl-CoA. Biological synthesis of glutarate is established,<sup>94</sup> but the substrate permissivity of methylmalonyl-CoA mutase is not well-studied.

Microorganisms like *Pseudomonas taiwanensis*, *Saccharomyces cerevisiae*, and *Yarrowia lipolytica* possess natural pathways for valine degradation that produce 3HIB-CoA as an intermediate. This pathway has been co-opted for the production of 3HIB at titers as high as 5.1 g/L.<sup>88</sup> BCAA degradation routes are attractive platforms for the production of both 3HIB and 3H2MB. Specifically, valine and isoleucine degradation produce 3HIB-CoA and (2S,3S)-3H2MB-CoA as intermediates, respectively. The BCAA pathway represents marked improvements over the diol oxidation pathway, aldolase pathway, rBOX pathway, and sleeping beauty mutase pathway because it can be used to produce both monomers from a bioaccessible feedstock without enzyme engineering. However, the BCAA pathway must be modified to initiate synthesis from an unrelated carbon feedstock and for the production of 3H2MB with biodegradation compatible stereochemistry at C3.

The goal of this study is to design and implement a pathway from glucose to (2S)-3HIB and (2S,3R)-3H2MB in *E. coli*. The pathway we develop consists of two halves: (1) module 1 which converts glucose to branched acids and (2) module 2 which specifically converts the branched acids to 3HIB or 3H2MB using steps inspired by BCAA degradation. We take a bottom-up approach to pathway validation where we first validate module 1 and module 2 separately. Finally, we combine the entire pathway in *E. coli* to demonstrate the production of both advantaged plastic monomers from glucose.



**Figure 3.1.** Previously reported biological routes to 3-hydroxyisobutyric acid and 3-hydroxy-2-methylbutyric acid. Abbreviations used include: Acat3 - thiolase (*A. suum*), Acd1 - acyl-CoA dehydrogenase (*Pseudomonas aeruginosa* PAO1), Bch - thioesterase (*Bacillus cereus*), BckAD - branched-chain  $\alpha$ -keto acid dehydrogenase (*Pseudomonas aeruginosa* PAO1), EchA - enoyl-CoA hydratase (*Pseudomonas aeruginosa* PAO1), HadH - ketoreductase (*A. suum*), HchA - thioesterase (*Pseudomonas aeruginosa* PAO1), MMCR - methylmalonate semialdehyde reductase (*Sulfolobus acidocaldarius*), MCE - methylmalonyl-CoA epimerase (*Propionibacterium freudenreichii*), MCM - methylmalonyl-CoA mutase (*E. coli*), Pct - propionyl-CoA transferase (*Clostridium propionicum*), 3HIBDH - 3HIB dehydrogenase (*E. coli*)

## 3.2 Materials and Methods

### 3.2.1 Strain construction

All strains used are described in Tables 3.2-3.6. Plasmid construction details can be found in Table 3.5. *E. coli* MG1655 (DE3)  $\Delta endA\Delta recA$  was used as the background strain for all production experiments unless otherwise noted. *E. coli* DH5 $\alpha$  was used for cloning and plasmid propagation. Strain 565 was lysogenized using the  $\lambda$ DE3 lysogenization kit (Novagen). Gene blocks for the following genes were ordered from Integrated DNA Technologies: *acdH* (*Streptomyces avermitilis*), *acx4* (*Arabidopsis thaliana*), *ilvGM* (*Klebsiella aerogenes*), MACS (*Methanosarcina acetivorans*), *phaJ* (*Aeromonas caviae*), PVLB05085 (*Pseudomonas taiwanensis* VLB120), PVLB10050 (*Pseudomonas taiwanensis* VLB120), and PVLB10075 (*Pseudomonas taiwanensis* VLB120). Sequences for these genes can be found in Table 3.4. The genes corresponding to Fjoh2967 (*Flavobacterium johnsoniae*), IbuA (*Rhodopseudomonas palustris*), KivD (*Lactococcus lactis*), and Pct (*Megasphaera elsdenii*) were amplified from plasmids described in Sheppard et al.<sup>95</sup> All other genes were amplified from genomic DNA.

Individual genes and synthetic operons were expressed using compatible duet vectors or pET vectors (Table 3.3) under the control of T7lac promoters and synthetic ribosome binding sites. Synthetic ribosome binding sites were designed using the Salis Lab RBS Calculator with a target translation initiation rate of 10,000.<sup>96</sup> Genes were amplified from their corresponding templates using custom oligonucleotides (Millipore Sigma) and Q5 DNA polymerase (NEB) or KOD HotStart Polymerase (EMD Millipore). Genes were inserted into the multiple cloning sites (MCSs) of plasmids via Gibson Assembly with the NEBuilder HiFi DNA Assembly Kit (NEB). Site-directed mutagenesis of PhaJ was carried out using the Q5 site-directed mutagenesis kit (NEB). Deletion of *ilvBN*, *metA*, and/or *tdh* from *E. coli*'s genome were carried out using  $\lambda$ -red recombination as described by Datsenko and Wanner.<sup>97</sup>

**Table 3.2.** List of background strains used

Strain Name	Relevant Genotype	Source
<i>E. coli</i> DH5 $\alpha$	F- endA1 glnV44 thi-1 recA1 relA1 gyrA96 deoR nupG $\phi$ 80dlacZ $\Delta$ M15 $\Delta$ (lacZYA-argF)U169, hsdR17(rK- mK+), $\lambda$ -	Prather Lab
<i>E. coli</i> MG1655	wild type K-12 strain F- $\lambda$ - ilvG- rfb-50 rph-1	Prather Lab
663	<i>E. coli</i> MG1655 with $\lambda$ DE3 prophage integrated into the genome	Prather Lab
715	<i>E. coli</i> MG1655 (DE3) $\Delta endA\Delta recA$	Prather Lab
565	<i>E. coli</i> MG1655 $\Delta endA\Delta ilvBN$	Prather Lab
844	<i>E. coli</i> MG1655 (DE3) $\Delta FadR$ pAtoDAEB::plac	Prather Lab

**Table 3.3.** List of plasmid backbones used

Plasmid	Relevant Genotype	Source
pETDuet-1	ColE1 (pBR322) ori, lacI, T7lac, Amp <sup>R</sup>	Novagen
pCOLADuet-1	ColA ori, lacI, T7lac, Kan <sup>R</sup>	Novagen
pACYCDuet-1	P15A ori, lacI, T7lac, Cm <sup>R</sup>	Novagen
pCDFDuet-1	Cl <sub>o</sub> DF13 ori, lacI, T7lac, Sm <sup>R</sup>	Novagen
pET29b	ColE1 (pBR322) ori, lacI, T7lac, Kan <sup>R</sup>	Twist Biosciences
pET28a	ColE1 (pBR322) ori, lacI, T7lac, Kan <sup>R</sup>	Drennan Lab (MIT)

### 3.2.2 Production experiments

Overnight cultures were grown in Luria-Bertani (LB) Broth (Difco) at 37 °C, 250 rpm, with supplementation of the appropriate antibiotic(s) (kanamycin 50 µg/mL, carbenicillin 100 µg/mL, streptomycin 50 µg/mL, or chloramphenicol 34 µg/mL). For production experiments, overnight cultures were spun down at 4500 rpm for 5 min and resuspended in 1X M9 salts (Millipore Sigma). M9 salts used for media formulation contained the following salts by concentration: 3 g/L KH<sub>2</sub>PO<sub>4</sub>, 0.5 g/L NaCl, 6.78 g/L Na<sub>2</sub>HPO<sub>4</sub>, and 1 g/L NH<sub>4</sub>Cl. Concentrated overnights were used to inoculate M9 + 1% glucose + 0.25% yeast extract (M9Y media) to an optical density at 600 nm (OD<sub>600</sub>) = 0.1. These cultures were grown according to: (1) condition A - 15 mL culture in 55 mL glass tube, (2) condition B - 50 mL culture in 250 mL baffled shake flasks, or (3) culture condition C - 7 mL cultures in 20 mL glass tubes. These cultures were grown at 30 °C and 250 rpm to early exponential phase (OD<sub>600</sub> 0.6 - 0.9). Subsequently, the cells were induced with 0.25 mM isopropyl β- d-1-thiogalactopyranoside (IPTG) and pathway carbon source was added if necessary. Additionally, 1 µM cobalamin (vitamin B<sub>12</sub>) was added for all isobutyrate recycle experiments. Samples were taken at ≈ 72 hr for growth and metabolite analysis via UV-VIS spectroscopy at 600 nm and high performance liquid chromatography (HPLC), respectively.

### 3.2.3 Metabolite detection

Metabolites were detected using an Agilent 1200 series HPLC (Agilent) equipped with a refractive index detector (RID). Acetate, 3HB, isobutyrate, 2-methylbutyrate, 3-hydroxy-3-methylbutyric acid, and 3HIB were detected using the Aminex HPX-87H column (Bio-Rad Laboratories) with 5 mM sulfuric acid mobile phase. Column temperature, RID temperature, and flow rate were set to 65 °C, 35 °C, and 0.6 mL/min, respectively. 3H2MB, 3-hydroxy-2-methylvaleric acid (3H2MV), and glucose were detected using a TSKgel OApak-A column (Tosoh Biosciences) with 0.75 mM sulfuric acid mobile phase. Column temper-

ature, RID temperature and flow rate were set to 40 °C, 35 °C and 0.8 mL/min, respectively. Standards for 3HIB, 3H2MB, and 3H2MV were purchased from Enamine. The 3H3MB standard was obtained from ThermoFisher Scientific. Standards for all other metabolites were obtained from Millipore Sigma. Commercial standards of each metabolite were used to construct standard curves to quantify metabolites in experimental samples.

### **3.2.4 Sodium dodecyl sulfate–polyacrylamide gel electrophoresis (SDS-PAGE)**

Overnight cultures in LB Broth were grown at 37 °C, 250 rpm for  $\approx$  18 hr. These cultures were diluted 1:1000 in M9Y media and grown according to culture condition B. Cultures were induced at  $OD_{600}$  0.6 - 0.9 with 0.25 mM IPTG and grown for 8 hr. After 8 hr, the cells were isolated via centrifugation at 4500 rpm for 10 min and resuspended in 1 mL Tris-HCl (pH = 8). The concentrated cells were combined 1:1 with a buffer containing Laemmli buffer and 1 mM dithiothreitol. This mixture was incubated at 95 °C for 5 min. Protein concentration determination was carried out using the Bradford assay with bovine serum albumin standards.<sup>98</sup> 15  $\mu$ g of total protein was run on a BioRad 10% MiniPROTEAN TGX Stain-Free gel (BioRad Laboratories) with the Mini-PROTEAN Tetra Cell electrophoresis set up.

### **3.2.5 Molecular docking**

Targeted docking with various substrates in the active site of PhaJ (PDB ID: 1IQ6) was carried out using AutoDock Vina.<sup>99</sup> Briefly, docking was centered around H36 - the catalytic residue of PhaJ. The crystal structure of PhaJ was prepared for analysis by removing water molecules, adding polar hydrogens, and Kollman charges. Three-dimensional conformers corresponding to each substrate of interest were generated using Avogadro.<sup>100</sup> The docking simulation was run with the following parameters: exhaustiveness = 32, energy range = 4, box size = 40 x 40 x 40.

**Table 3.4.** Gene block sequences for 3H1B and 3H2MB production strains

Gene Name	Sequence
<i>acdH</i>	<p>ATGGACCACCGTCTCACCCCGAGCTGGAAGAACTCCGCCGCACGGTCGAGGAGTTTCGCGCACGAC            GTCGTGCCCCCAAGATCGGGCGACTTCTACGAGCGGCACGAGTCCCGTACGAGATCGTCCGCGA            GATGGGCCGCATGGGCCTGTTCCGGGCTGCCGTTCCCGGAGGAGTACGGCGGCATGGGCGGGGACT            ATCTGGCGCTCGGCATCGCCCTCGAAGAACTCGCCCGCTCGACTCCTCCGTCGCCATCACCTGG            AGGCCGGGTCTCACTGGGCGCGATGCCGATCCACCTCTTCGGGACGGACGCGCAGAAGGCCGGAG            TGGCTCCCCCGGCTGTGTTCCGGCGAGATCCTCGGGCCTTCGGTCTCACCGAGCCGGACGGCGGC            TCGGACGCGGGCGCGACGCGCACGCGCCCGCTGGACGAGTCGACGAACGAATGGGTGATCAAC            GGCACCAAGTGCTTCATACCAACTCGGGCACCGACATCACGGGGTTGGTGACGGTCACGGCGGT            CACCGCCGGAAGCCCGACGGGAAACCGCTGATCCTCGATCATCGTCCCGTCCGGCACGCCCGG            GTTACCGTTCGCGGCCCGTACTCGAAGGTCCGGTGGAAACGCCTCGGACACCCGCGAGCTGTCTT            CGCCGACGTCCGCGTCCCGGCCGGAACCTGCTGGGCGAACAGGGCCGCGGGTACGCGCAGTTCCT            GCGGATCCTCGACGAGGGACGGATCGCCATCTCGGCCCTGGCCACCGGGCTCGCCAGGGCTGCGT            GGACGAGTCGGTGAAGTACGCCGGGAAACGGCACGCGTTCGGGGCGAACATCGGGGCGTACCAGG            CCATCCAGTTCAAGATCGCCGATATGGAGATGAAGGCGCACATGGCCCGCTCGGCTGGCGTGAC            GCCGCTCCCGCTGGTCCCGGCGAGCCCTCAAGAAGGAGGCGGCGATCGCAAGCTCTACTCG            TCCACGGTCGCGTCGACAACGCCCGGAGGCCACCCAGATCCACGGCGGCTACGGCTTCATGAAC            GAGTACCCGGTGGCCCGGATGTGGCGGACTCCAAGATCCTGGAGATCGGCGAGGGCACAGCGA            GGTGCAGCGGATGCTGATCGCAAGGGAGTTGGGGCTCGTGGGCTGA</p>
<i>acx4</i>	<p>ATGGCAGTGTTATCGTCAGCGGATCGTGCGTCTAACGAAAAGAAAGTGAATCCAGCTATTTTCA            TCTCCGCCTATGGAGATGTCTGTGGCCTTCCACAAGCAACACCAGCCAGCACTTTTCCACCGT            GTACGAGCGATTACTATCACTTCAACGATCTGCTCACCCCGAAGAACAGGCGATCCGCAAGAAA            GTGCGCGAATGCATGGAAAAGGAAGTAGCTCCGATCATGACAGAGTACTGGGAGAAAGCCGAATT            TCCGTTTACATTACCCCGAAACTGGGTGCAATGGGAGTGGCTGGTGGGAGCATCAAAGGCTATG            GATGCCCCGGCTTGTGATTACCGCGAATGCTATTGCCACCGCAGAGATTGCACGCGTTGATGCC            AGTTGCTAACGTTTATTCTGGTCCATTCAAGCCTGGGTATGCTGACCATCGTTTTGTGTGGCTC            TGAAGCGCAGAAAGAGAAATACTTACCGTCTTGGCGCAACTGAACACTGTAGCGTGTGGGGCC            TGACGGAAACCGGATAACGGCTCTGACGCGTCGGGTCTGGGTACCACAGCAACCAAAGTTGAAGGC            GGTTGGAAAATCAATGGTCAGAAACGCTGGATTGGCAATAGCACGTTTTGCGGATCTGCTCATTAT            CTTTGCCCGTAATACGACGACTAACAGATTAACGGCTTTATCGTGAAGAAGGATGCTCCAGGCC            TGAAAGCGACCAAGATTCCGAACAAAATCGGTCTGCGCATGGTTCAGAATGGCGACATTCTTCTG            CAGAACGTGTTGTTCCGGATGAGGATCGCTTGGCCGGCGTCAACTCCTTCCAAGACACCAGTAA            AGTGTAGCCGTTAGCCGTGTCATGGTTGCCGCAACCTATCGGAATTTTCGATGGGCATCTACG            ACATGTGTGATCGTATCTGAAAGAACGGAAACAGTTTGGTGCTCCTTTAGCGGCCTTCCAGCTG            AATCAACAGAACTTGTGCAGATGCTGGGAATGTACAAGCGATGTTTCTTATGGGCTGGCGTCT            GTGCAAACTCTATGAAACGGGCCAGATGACTCCCGGACAGGCTTCGCTGGGGAAGGCATGGATTA            GTTCCAAAGCCCGTGAACCCGCTCATTAGGTGCTGAACTGCTGGGCGGCAATGGGATTCTGGCA            GACTTTCTGGTGCCTAAAGCGTTCTGCGATTTGGAACCGATCTATACCTATGAGGGGACTTACGA            CATTAAACCCCTCGTAACCGTCCGGAAGTACGGGTATTGCGAGTTTCAAACCGGCAACACGCA            GCCGGCTGTAA</p>



<i>ilvGM</i>	<p>ATGAACGGGGCGCAGTGGGTGGTACATGCTTTGCGAACACAGGGAGTCGACACGGTATTTGGCTA  TCCGGGTGGCGGATTATGCCGTTTACGATGCTTTGTATGACGGCGGCGTGAACACCTGCTGT  GTCGGCAGGCAAGGCGCCCAATGGCCGCCATCGTTATGCCCGCGCAGCCGGCAAACTGGTG  TTTGCATCGCCACTTCCGGCCCTGGCGCCACCAACCTGATCACCGGTTTGGCTGACGCGTTACTT  GATTCTGTACCTGTTGTCGCCATCACCGGTCAAGTGGCGGCGCCGTTTATCGGCACCGATGCTTT  TCAGGAAGTGGACGTTCTTGGTTTGTGCGTGGCCTGCACCAAACACAGTTTCTCGTGCAGTCGT  TGGAAGAGCTGCCGCGCGTCAATGCGGAAGCTTTCCAGGTGGCAAACCTCAGGCCGCTCTGGCCCG  GTACTGGTTGATATTTCCAAAAGATATCCAGTTGGCTAAAGGCGAATTAGATCCGATTCTCCAC  CGTCCCTGATGATGTTGAGTTCGGCACACACAAGTCGAGCAGGCGTTAGCGATGCTTGGCAGT  CCCACAAGCCAATGCTGTACGTGGGCGGCGGTGTTGGAATGGCACAGGCGGTACCGGCCGTGCGC  GAATTTCTGGCGGTGACGCAGATGCCGTTAACCTGCACCCTGAAAGGGTTGGGTGCCGTGCGCGC  GGATTATCCGTATTACCTTGGCATGCTGGGTATGCACGGAACCAAGGCAGCAAACCTGGCGGTGC  AGGAGTGGCATTATTAATCGCCGTGCGCGCCGTTTTGATGACCGGTTACCGGAAGCTGAAT  ACTTTTGCCCGCACGCCAAAGTAATCCATATGGATATTGACCCGGCTGAGCTGAACAACTGCG  CCAGGCGACGTGCGCTTAACCGGAGATTTAAACGCCATGCTGCCGGCGTTGACGAGCCGTTGG  CCATCGATGCGTGGCGGAGCACAACGCGCAGCTGCGCGCGGAGCAGCCTGGCGTTACGATCATC  CCGGCAGGCAATCTACGCGCCGCTGTTGCTCAAGCAGCTTCCGATCGAAACCGGCGGATTGC  GTCGTGACGACCGATGTCGGCCAGCACCAAATGTGGTGGCCAGCACATGACCTATAACCCGCCCG  GAAAACCTCATCACTTCCAGCGGCCTCGGCACCATGGGTTTTGGTCTGCCGCGAGCCGTTGGCGC  GCAGGTGGCTCGCCCGACGATACGTTATCTGTATCTCCGGCGATGGCTCTTTCATGATGAACG  TGCAGGAGCTGGGCACCGTTAAGCGCAAGCAATTACCGTTGAAAATCGTGTCTGGATAACCAA  CGTTTAGCATGTTTCCAGTGGCAGCAGCTGTTTTTCCAGGAGCGTTACAGCAAAACCGCT  TACCGATAATCCTGATTTTTCTACGCTGGCCAACGCTTTTTGGCATTCCAGGCCAGCACATCACCC  GTAAGACCAGGTTGAAGCGGCACCTGCACACCATGCTTTCGAGCCAGGGGCCATACTGCTTCAT  GTCTCAATCGATGAACTTGAGAATGTCTGCCGTTGGTGGCCCGCGCGCCAGTAATGCAGAAAT  GCTGGAGAAATATCATGATGCAACATCAGGTGCTTTACAGGCTCGCTTCAACCCGAAACCTT  AGAACGCTGCTGCGCGTGGTGGCCATCGCGTTTTCAAATTTGCTCAATGAATATGAAAACCG  CGTCGGATGCGCAAAACATAAATATCGAGCTGACCGTTGCCAGCCAGCGGCCCGTCAATTA  TTAGTCAGTTACGCAAACCTGGTCGACGTCGCTGCGTGCAGATCCAGCAACCCACATCACAACA  AATCCGCGCTGA</p>
<i>MACS</i>	<p>cctctagaataattttgtaactttaagaaggagatataATGACTTCCTTGCTGAGCCAATTTGTTTCCAAAACCGA  TTTCGAATCCTACGAGGATTTCCAGGAAAACCTCAAATCCTGGTCCCTGAAAACCTCACTTTG  CTATGATGTGGTCGATGTCTATGCAAGAGATTCTCCTGAAAAGCTTGCCATGATCTGGTGTGAC  GATTACGGGAATGAGAAAATCTTCACTTTCAAAGATCTCAAGTACTACAGCGATAAAGCTGCAAA  TTTTCTTTGTAAGCACGGCATAGGCAAAGCGACTATGTAATGCTTACCTTAAAGAGCCGCTATG  ATTTCTGGTACTGCATGCTGGGGCTACACAAGCTCGGAGCAATAGCCGTGCTGCAACCCACATG  CTGAAAACCCGGGATATAGTATACAGAATCGAAAAGCCGGTTGAAGATGATTGCTGCTGCATCGC  CGAAGACGATGTTCCGGAACAGGTAGATGAAGCCCATGCCGAATGCGGGGATATCCTCTCAAGA  AAGCCAAGGTAGGAGGAGATGTCCTGGAAGGCTGGATTGATTTCAAGAAAGAACTTGAGGAAAGT  TCCCGGATTTTCGAGCGTCCGACAGCGAGGTTTCAACAAAGAAGCAAGACATCTGTCTGGTCTA  TTCTCTCCGGAACCGCCGGTTTTCCGAAAATGGTAGAGCACGACAACACCTATCCACTCGGCCA  CCTCTGACCGAAAATACTGGCAGAATGTGAAGACGACGGGCTGCACTACCCGTTGACGACA  GCGGATGGGGTAAATGTGTCTGGGGCAAGCTCTACGGGCAAGTGGATAGCTGGTTGTGCGGTCTTT  GTCTATGACTATGACAGGTTTGAAGCCAAAATATGCTTGAAGGCTCCAAGTATGGAGTTAC  GACTTTCTGTCTCCACCCACGATCTATCGTTTTCTGATCAAAGAAGACCTCTCCATTATAATT  TCAGCACTCTGAAATATGCGGTTGTTGACGGCGAACCCCTCAACCCTGAAGTCTTTAACCGCTTC  CTTGAGTTTACCGGAATCAAACCTTATGGAAGGTTTGGGCAAACCGAGACCGTTGTTACGATTGC  GACCTTCCCTGGATGGAACCCAAGCCCGGATCTATCGGAAAACCCACCCCTGGATATAAGATCG  AGCTCATGGACAGGGATGGCAGGCTCTGCGAGGTGCGGAGAAGAAGGGGAAATCGTCATCAACACA  ATGGAAGGAAAACCTGTGGGACTTTTTGTCCACTATGGAAGGATCCTGAAAGGACAGAGGGAC  CTGGCACGACGGCTACTACCATACCGGAGATATGGCTGGATGGATGAAGACGGTTATCTCTGGT  TTGTGGGAAGGCTGACGATATAATCAAGACCTCAGGATACAAGGTGCGGCCCTTTGAAGTGGAA  AGCGCTCTTATCCAGCACCCGGCTGTGCTTGAAGTGTGCTATCACGGGAGTCCCGACCCCTGTCAG  AGGTGAGTCATTAAGGCGACCATTTGACTTACAAAGGATTATACGCCGAGTGACTCCCTAAAA  ACGAGTCCAGGATCATGTGAAAAATGTCACGGCTCCTTACAAGTATCCCAGGATTATTGAATTC  GTTCCCGAACTACCGAAAACCATCAGCGGAAAATCCGACGGTGAATCCGTCGAAATCCGTGACAAGGACCA  GAGCCAATGATgaaccatctaccacaagtaggatgatggcagtggttatcgtcagcgg</p>
<i>phaJ</i>	<p>cccatcttagtatattagttaagataaagaaggagatataATGAGCGCACAAATCCCTGGAAGTAGGCCAGAAGGCCCGT  CTCAGCAAGCGGTTCCGGGCGGCGGAGGTAGCCGCTTCGCCGCGCTCTCGGAGGACTTCAACCC  CTGCACCTGGACCCGGCTTCCGCCACACCGCGTTTCGAGCGGCCATAGTCCACGGCATGCTG  CTCGCCAGCTCTTCTCCGGGCTGCTGGGCCAGCAGTTGCCGGGCAAGGGGAGCATCTATCTGGG  TCAAAGCCTCAGCTTCAAGCTGCCGCTTTTGTGCGGGACGAGGTGACGGCCGAGGTGGAGGTGA  CCGCCCTTCGCGAGGACAAGCCCATCGCCACCCTGACCACCCGATCTTACCCAAGGCGGCGCC  TCGCCGTGACGGGGGAAGCCGTGGTCAAGCTGCCTTAAccaactatcccgaatcttcagtcaccaagaggtattcatg  agtcaggcgctaataaattactgacat</p>

<i>PVLB05085</i>	ATGAGCATCCATTGTGAGGTCCTTACCGGCGCCGATGGCGCGGCATCGGCATCGCCACCTTGA CGCACC <sup>5</sup> GAAAGCATTAAATGCCCTGAATTTGCCAATGATTGAGGTA <sup>10</sup> CTGGCAGAGCATCTGCAG CGTGGGCGCATGACCCCGGGTGGTATGTGTTTTACTGCGCGGGTCTGGCTAAGGCATTTTGC GCAGGTGGGGACGTTTCGTCTCTTGCCCAAGCCTGTCGTGAACATCCTGGTCCGTTCCGCGCT TGCCGCGACCTTTTTTGGCGGGAGTACTCTTTGGACTATATGTTACACACGTACCCGAAGCCTT TACTTTGCTGGGGTCATGGCCACGTA <sup>15</sup> CTGGGCGGCGGGATGGGGCTTCTGCAAGGAGCAGGGGT CGTATCGTCA <sup>20</sup> CCCCCTCCTCCCGCTTAGCGATGCCTGAGATTTCTATTGGACTGTATCCCGACGT TGGAGCATCGTGGTTTCTGGCCCGCTTACCTGGTCGCTGGGTTTATTTTTAGGCTTGACGGGG CGCCGATCAACGCTCGCGACGCCATTGATCTGGGATTAGCCGACCGTTTCTTGGGGAAACATCAA CAAGAGGCACTTATTGAAGA <sup>25</sup> ACTTCTTCAGTTAAATTGGCAAGAGCAA <sup>30</sup> ACTGAGTTGCAACTTAA TTCATTGCTTAAGGCCGAACAACACCGTGCCTGTGCAGAATTGCCGAAGCACAATGGTTGCCAC GTCGCGGTATGATTGATGAGCTTCTTGATGTTGCAGACCCAGCGTCTGCCTGGCGTGC <sup>35</sup> TTAGAG GGCTTAAACAACATTCGACCCCTGCTTGGCCGAAGCAGGTCAGCGCTGCATGAAGGGTGTCC CTTAACAGCGCATTTGGTGTGGGAACAGATCCGCCGCGCCCGTCACTT <sup>40</sup> GAGCTTAGCCCAAGTTT TCCAGATGGAGTACACTATGTCATTGAACTGTTGTCTCACCCGAATTTAGTGAAGGCGTACGT GCACGCTTGCCTTGATAAAGACAACCAACCTCATTGGCACTGGCCAGATATCGACAAGTCCCATT GGCAGTGGTTGAAGCTCATTTTGTAAAGTTTGGGAAGGACGCCATCCCTTAGCTGACTTAGCCT AG
<i>PVLB10050</i>	GTGACTGATTACAGTGCTTTTAAAGTTGAGCAA <sup>5</sup> ACTGACAATATCGCGCATGTGCAAATCAATCG CCCCGAAAAAATCAATGCAATGAACGCTGCGTTCTGGGAAGAAATCGTCGACATCTTTCAATGGA TTGATGATACCGACGCTGTGCGCGCTGTA <sup>10</sup> GTAAATTAGTGGGGCTGGAAAGCATTCTCCAGCGGA ATTGACTTAATGATGTTAGCTAGTCTGGCTGGACAAATGGGCAAGGACGTGCGACGTAACGCGCG CTTGCTGCTCGCACAATCCTTCGCTTACAAGCAAGTTTCAACGCAGTACGATAATTGCCGAAGC CGGTCTTGTCTGCAATTCAAGGATATTGCATCGGAGGCGCGATTGATCTGGT <sup>15</sup> CAGCGCTTGTGAC ATGCGCTATTGCAGCCAGGACGCCAGTTC <sup>20</sup> CCATCAAGGAGATTGATATGGGGATGGCAGCGGA CGTCGGGACTTTACAGCGTCTGCCGCGCATTATCGGAGACGGAATGATGCGT <sup>25</sup> GAGCTTGCTTCA CCGGACGTATGGTCGACGCTGATGAAGCTCTGCGCATCGGATTAGTCAATCGTGTGATGATGAC CAGGCAGCTCTTTTGGACGGGGTATTGCTATTGCTCGCGAAATTGACGTAAGTCA <sup>30</sup> CCCATCCGC AGTCGCGGGGACCAAAGAGATGCTGTCTTATATGCGCGATCACCGTATCGATGATGGTTTAGAAT ATATTGCTACCTGGAATGCGGCTATGCTTCA <sup>35</sup> GTCTGAGGACTTGCCTGTCGAGTTGCAGCCAT ATGAGCAAACAAAAACCCACCTTCGCCGATTGA
<i>PVLB10075</i>	ATGGATTTTGCTATAGTCCGAAAGTGAAGCGCTGCGTGAGCGTGTAGCAGCATTATGGATAC GCACGTGTACCCTGCTGAGCCAGTTTTCGAGCGTCAAGTTGCCGAGGGGATCGTGGCAGCCTA CCCGGATCATGGAGGAATTGAAGGCGAAAGCAGCAGTGCCGAAGGCTTGTGGAATTTATTCTTGCCG GAATCGGAATATGGCGCTGGGTTGTCAAACCTT <sup>5</sup> GAGTACGCGCCGCTTGCCGAAATTTATGGGTGCG CTCGTTGCTGGGCCCCGAACCCTTTAATTGTTCTGCGCCGATACTGGTAACATGGAGGTTCTGG TTCGCTATGGAAGCGAGGCCCAAAGCGTCA <sup>10</sup> GTGGCTT <sup>15</sup> GAGCCTCTTCTGCGCGGAGAGATCCGC TCCGGCTTCCGATGACGGAGCCTGATGTCGCGTCTCCGACGCAACTAATATGGCCATCCCGC GGTACGCGACGGT <sup>20</sup> GATGAATGGGTTATTAATGGCCGTAAGTGGTGGACATCCGGCGCTTGTGATC CTCGTTGTAAGTAATGATCTTTATGGGGCTGT <sup>25</sup> CGAACCTGATGGCCCTCGCCATCAGCAACAT TCGATGGTATTGGTTCCAACAGACGCACCGGGAGTAAACATCGTTCGCCCCGCTGCCTGTGTTGCG GTATGACGACGCGCCACACGGACACGCCGAAGT <sup>30</sup> GCTTTTTGAAGATGTTGCGGTACCTTACGAAA ACGTAATCTTGGT <sup>35</sup> GAGGGGCGCGTTTTCGAGATCGCCAGGGCGCTGCTGGGCCCTGGTCGTATC CATCACTGTATGCGTAGCATCGGCATGGCAGAGCGCGCTT <sup>40</sup> GAGCTGATGTGTCTGCTTCCGT CGAACGCACCGCCTTTGGACGTCCACTGGCAGT <sup>45</sup> TTAGGAGTAAACATTGACAAGATTGCCGATA GCCGCATGGAAATTTGACATGGCGCGCTT <sup>50</sup> GCTTACATTGAAGGCCCTACATGATGGATACAGTC GGGAATAAAGTTGCCCGTTCCGAAATCGCACA <sup>55</sup> AATTAAGTAGTGGCGCCCAATGTCGCAC <sup>60</sup> TAA AGTAATCGACCGTGCTATCCAGATT <sup>65</sup> CATGGCGGTGCAGGTGTTTCTGGGGACTTTCCGTTAGCTT ATATGTATGCCATGCAGCGCACATTACGTTT <sup>70</sup> AGCTGACGGACCCGATGAGGTGCATCGTGCAGCC ATCGGGAAGTATGAGATTGGCAAATACGTTCCACCGAGTATGTTGCGCTAG

**Table 3.5.** 3HIB and 3H2MB plasmid construct descriptions

Name	Description	Primers
pET(-) (PVLB05085-pct)	pETDuet-1 with synthetic operon containing PVLB05085 and <i>pct</i> in MSC 2 separated by the RBS:GCAGGAGGAAGTTACGGTA	PVLB05085_f_051:GAGATATACATATGAGCATCCA TTGTGAGGTCCTTACC; PVLB05085_r_026_070:C TTTTCTCATTACCGTAACTTCTCTGCTAGGCT AAGTCAGCTAAGGGATG; <i>pct</i> _f_026:CCTAGGCAGG AGGAAGTTACGGTAATGAGAAAAGTAGAAATCATT ACAGC; <i>pct</i> _r_028:CAGCAGCTAGGTTAATTAAT TATTTTTTCTAGTCCCATGGg; <i>bb</i> _f_047:CCCATGG GACTGAAAAAATAATTAATTAACCTTAGGCTGCTG; <i>bb</i> _r_046:GTAAGGACCTCACAAATGGATGCTCATAT GTATATCTCCTTCTTATACTTAAC <sup>5</sup> TAATATA

pET(PVLB10075-PVLB10050)-(PVLB05085-pct)	pET(-)(PVLB05085-pct) with PVLB10075 and PVLB10050 in MCS 1 separated by the synthetic RBS sequence:CTCAAGGAGTACCGCCC	PVLB10076_f_050:GAGATATACCATGGATTTTGCC TATAGTCCGAAAAGTGCAAGC; PVLB10075_r_022: gcggtactccttgagCTAGCGCAACATACTCGGTGG; PVLB10050_f_023:gctagCTCAAGGAGTACCGC CCGTGACTGATTACAGTGCTTTTAAAGTTG; PVLB10050_r_024:gttcgaCTTAAGTCAATCGGCGAA GGTGGG; bb_f_043:CAAAAACCCACCTTCGCCGAT TGACTTAAGTCTGAACAGAAAAGTAATC; bb_r_042:C TTTCGGACTATAGGCAAAATCCATGGTATATCTCC TTCTTAAAGttaaac
pET(pct)	pETDuet-1 with <i>pct</i> in MCS 1	pct_f_100: TTTAAGAAGGAGATATAATGAGAAAA GTAGAAATCATTACAGC; pct_r_103: CGATTACTT TCTGTTTCGATTATTTTTTCAGTCCC; bb_f_102:TG GGAAGTAAAAAATAATCGAACAGAAAAGTAATCGTA TTGTACAGC; bb_r_101:GATTTCTACTTTTCTCAT TATATCTCCTTCTTAAAGTTAAACAAAATTATTTT TAGAGGGGA
pET(pct)-(phaJ-tesB)	pET(pct) with a synthetic operon containing <i>phaJ</i> gene block and <i>tesB</i> from <i>E. coli</i> added to MSC 2 RBS sequence: CCAACTATCCCGTAATTTTCAGTCA CCAAGAGGTATTC	tesB_f_104_127: CGTAATTTTCAGTCACCAAGA GGTTATCATGAGTCAGCGCTAAAAAATTTACTG; tesB_r_105: GCTCAGCGGTGGCAGCAGTTAATTGT GATT; bb_f_106: AATCACAATTAAGTCTGCCAC CGCTGAG; bb_r_107: TATATCTCCTTCTTATACT TAACTAATATACTAAGATGGGGAATTGTTATCCGC
pET(pct)-(phaJ)	removed <i>tesB</i> from pET(pct)-(phaJ-tesB)	bb_f_155:CTGCTGCCACCGCTGAGC; bb_r_156: T TAAGCAGCTTGACCACGG
pET(-)(phaJ)	<i>pct</i> removed from pET(pct)-(phaJ)	bb_f_290: TCGAACAGAAAGTAATCGTATTGTACA C; bb_r_289:TATATCTCCTTCTTAAAGTTAAACAA AATTATTTCTAGAGG
pET(pct)-(phaJ <sub>PS</sub> )	<i>phaJ</i> from <i>Pseudomonas syringae</i> in MCS 2 of pET(pct)	phaJ <sub>PS</sub> _f_215: TTAAGTATAAGAAGGAGATATatgg ggatgcctttgtac; phaJ <sub>PS</sub> _r_215: CTCAGCGGTGGCAG CAGttacacgaacacacaactcaaaag; bb_f_220: aactttgacct tgtgtttcgtgtaaCTGCTGCCACCGC; bb_r_221: gcatccc atATATCTCCTTCTTATACTTAACTAATATACTAA GATG
pET(pct)-(PVLB10050)	<i>PVLB10050</i> added to MCS 2 of pET(pct)	PVLB10050_f_211: AAGAAGGAGATATAGTGACT GATTACAGTGCTTTTAAAG; PVLB10050_r_212:G CTCAGCGGTGGCAGCAGTCAATCGGCGAAGGTGG; bb_r_087: CACTGTAATCAGTCACTATATCTCCTT CTTATACTTAACTAATATACTAAGATG; bb_f_216: CAAAAACCCACCTTCGCCGATTGACTGCTGCCACC GC
pET(pct)-(phaJ <sub>CN</sub> )	<i>phaJ<sub>CN</sub></i> from <i>Cupriavidus necator</i> added to MSC 2 of pET(pct)	phaJ <sub>CN</sub> _f_217: TTAAGTATAAGAAGGAGATATatgg cagatctcatgggg; phaJ <sub>CN</sub> _r_218: AGTTATTGCTCAG CGGTGGCAGCAGTcagggaagcggc; bb_r_214: agatc tgccatATATCTCCTTCTTATACTTAACTAATATACT AAGATG; bb_f_213:GCGCTTTCCTGACTGCTGCC ACCGC
pACYC(acx4)	pACYCDuet-1 vector with <i>acx4</i> in MSC 1	bb_r_281: GGTATATCTCCTTATTAAGTTAAACA AAATTATTTCTAC; bb_f_282: CTTAAGTCGAACA GAAAGTAATCGTATTG
pACYC(acx4)-(katE)	pACYC(acx4) with <i>katE</i> from <i>E. coli</i> in MCS 2	katE_f_283: AGAAGGAGATATACATatgTCGCAAC ATAACGAAAAGAAC; katE_r_285:GCAGCCTAGGTT AATTAATcaGGCAGGAATTTGTCAATC; bb_f_285: TGACAAAATTCTGCTgaTTAATTAACCTAGGCTG CTGC bb_r_286:ATGTTGCGAcATGTATATCTCC TTCTTAACTTAACTAATATACTAAG
pACYC(acox3)	pACYCDuet-1 with <i>acox3</i> from <i>Yarrowia lipolytica</i> in MCS 1	acox3_f_293:TAACITTAATAAGGAGATATAatgatc cccccaacctc; acox3_r_294:TACTTTCTGTTTCGACTT AAGctattcctcgtccagctcg; bb_f_295:gctggacgaggaatag CTTAAGTCTGAACAGAAAAGTAATCG; bb_r_296: TA TATCTCCTTATTAAGTTAAACAAAATTATTTCT AC

pACYC(fadE)	pACYCDuet-1 with <i>fadE</i> from <i>E. coli</i> in MCS 2	<i>fadE_f_268</i> :AAGGAGATATACATatgATGATTTTTGAGTATTCTCGCTAC; <i>fadE_r_269</i> : CAGCAGCCTAGGTTAATTAAGttaCGCGGCTTCAACTTTC; <i>bb_f_270</i> :GAAAGTTGAAGCCGCGtaaCTTAATTAACCTAGGCTGCTG; <i>bb_r_271</i> : ACTCAAATCATcatATGTATATCTCCTTCTTATACTTAACATAATATACT
pCOLA(-)( <i>etfBA</i> )	pCOLADuet-1 with <i>etfBA</i> from <i>Pseudomonas putida</i> KT2440 added to MSC 2	<i>etfBA_f_231</i> : ATAAGAAGGAGATATACATATGAAGGTTCTTGTAGCTGTC; <i>etfBA_r_232</i> : GCAGCAGCCTAGGTTAATTAATCAGACCAGCTTTTCCA <i>Gbb_r_234</i> :CAAGAACCTTCATATGTATATCTCCTTCTTATACTTAACATAATATACT; <i>bb_f_233</i> : CTGGAAAGCTGGTCTGATTAATTAACCTAGGCTGCTGC
pCOLA( <i>acd</i> )-( <i>etfBA</i> )	pCOLA(-)( <i>etfBA</i> ) with <i>acd</i> from <i>Pseudomonas putida</i> KT2440 added to MSC 1	<i>acd_f_225</i> :TAACTTTAATAAGGAGATATAatgctggtaaatgacgagc; <i>add_r_225</i> :TACTTTCTGTTCCGACTTAAGTcaaagattcgcgcaatg; <i>bb_r_227</i> :ttaccagcatTATATCTCCTTATTAAAGTTAAACAAAATTATTTCTACAG; <i>bb_f_228</i> :caatcttgaCTTAAGTCGAACAGAAAGTAATCG
pACYC( <i>etfD</i> )	pACYCDuet-1 with <i>etfD</i> from <i>Pseudomonas putida</i> KT2440 in MCS 1	<i>etfD_f_364</i> :ACTTTAATAAGGAGATATAATGAGTAGGAGAGAACCAGTG; <i>etfD_r_263</i> : ACTTTCTGTTCCGACTTAAAGTTACATGTTCCGATAGTTCCGG; <i>bb_f_280</i> : CGCTGGCGGGCCGAACCTATCCGAACATGTAACTTAAGTTCG; <i>bb_r_366</i> : TATATCTCCTTATAAAGTTAAACAAAATTATTTCTAC
pCOLA( <i>acd</i> )-( <i>etfAB</i> )	replace <i>etfBA</i> in MSC 2 of pCOLA( <i>acd</i> )-( <i>etfBA</i> ) with <i>etfAB</i> from <i>Pseudomonas putida</i> KT2440	<i>etfab_f_223</i> :AGTATAAGAAGGAGATATACATATGAGCGACATTATCCGC; <i>etfab_r_224</i> :GTGGCAGCAGCCTAGGTTAATTAATCAGCGCAGGACACC; <i>bb_r_229</i> :ATGTCGCTCATATGTATATCTCCTTCTTATACTTAACATAATATACT; <i>bb_f_230</i> :AGGGTGTCTGCGCTGATTAATTAACCTAGGCTGCTGC
pCOLA( <i>acdH</i> )-( <i>etfBA</i> )	replace <i>acd</i> from pCOLA( <i>acd</i> )-( <i>etfBA</i> ) with <i>acdH</i> from <i>Streptomyces avermitilis</i>	<i>acdH_f_235</i> :TAACTTTAATAAGGAGATATAATGGACCACCGTCTCAC; <i>acdH_r_236</i> :GATTACTTTCTGTTCGACTTAAAGTCAGCCCACGAGCCC; <i>bb_r_237</i> :GAGCGGTGGTCCATTATATCTCCTTATAAAGTTAAACAAAATTATTTTC; <i>bb_f_238</i> :GGGCTCGTGGGCTGACTTAAGTCGAACAGAAAGTAATCG
pET28a( <i>lcmF</i> )	pET28a with <i>lcmF</i> from <i>Cupriavidus metallidurans</i>	Plasmid gifted from Cathy Drennan's lab at MIT
pET28a( <i>lcmF</i> )_carb	pET28a( <i>lcmF</i> ) with kan marker replaced by carb marker	<i>carb_f_490</i> :tcacgttaagggtatttggctcatTTACCAATGCTTAATCAGTGAGG; <i>carb_r_491</i> :TCGGGAAATGTGTTTGTTTTATTTTTCTAAATACATTCAAATATGTATC; <i>bb_r_488</i> :TGATTAAGCATTGGTAAATGACCAAAATCCCTTAACGTG; <i>bb_f_489</i> :TATTTGAATGTATTTA GAAAAATAAACAAACACATTTCCCCGAAAAGTG
pET(pct)-( <i>phaJ</i> <sup>L65A</sup> )	truncated module 2 pathway with L65A mutant PhaJ ( <i>Aeromonas caviae</i> )	<i>bb_f_381</i> : CTTCTCCGGGgcgCTGGGCCAGC; <i>bb_r_382</i> : AGGCTGGCGAGCAGCATG
pET(pct)-( <i>phaJ</i> <sup>V130G</sup> )	truncated module 2 pathway with V130G mutant PhaJ ( <i>Aeromonas caviae</i> )	<i>bb_f_521</i> : GGAAGCCGTGggcAAGCTGCCTT; <i>bb_r_522</i> : CCCGTCACGGCGAGGG
pET(pct)-( <i>phaJ</i> <sup>Y76A</sup> )	truncated module 2 pathway with Y76A mutant PhaJ ( <i>Aeromonas caviae</i> )	<i>bb_r_415</i> : TTGCCCGGCAACTGCTGG; <i>bb_f_416</i> : GGGAGCATCgccCTGGGTCAAAGCCTCAG
pET(pct)-( <i>phaJ</i> <sup>Y76S</sup> )	truncated module 2 pathway with Y76S mutant PhaJ ( <i>Aeromonas caviae</i> )	<i>bb_r_415</i> : TTGCCCGGCAACTGCTGG; <i>bb_f_418</i> : GGGAGCATCtccCTGGGTCAAAGCCTCAG
pET(pct)-( <i>phaJ</i> <sup>Y76F</sup> )	truncated module 2 pathway with Y76F mutant PhaJ ( <i>Aeromonas caviae</i> )	<i>bb_r_415</i> : TTGCCCGGCAACTGCTGG; <i>bb_f_417</i> : GGGAGCATCtccCTGGGTCAAAGCCTCAG
pET( <i>ibuA-acx4</i> )-( <i>phaJ</i> )	<i>ibuA</i> inserted into in place of <i>pct</i> in pET(pct-acx4)-( <i>phaJ</i> ) with synthetic RBS:tgaacctctcaccacaagtaggagat	<i>ibuA_f_501</i> : AAATAATTTTGTTTAACTTTAAGAA GGAGATATAatgggcagcagccatc; <i>ibuA_r_502</i> : ATACTCTACTTGTGGTGAGATGGTTCAatgctgcagaagaag ag; <i>bb_f_503</i> : ctcttctctcagcctgaTGAACCATCTCAC CACAAG; <i>bb_r_289</i> : TATATCTCCTTCTTAAAGTTAAACAAAATTATTTCTAGAGG

pET(MACS-acx4)- (phaJ)	MACS inserted in place of <i>pct</i> in pET(pct-acx4)-(phaJ) with synthetic RBS:TGAACCATCTCACCACAAGTAG GAGTAT	bb_f_507: TGAACCATCTCACCACAAGTAG; bb_r_289: TATATCTCCTTCTTAAAGTTAAACAAA ATTATTTCTAGAGG
---------------------------	--	--

**Table 3.6.** List of 3HIB and 3H2MB production strains

Strain Name	Plasmid 1	Plasmid 2	Plasmid 3	Plasmid 4	Background
sKB001	pET(PVLB10075-PVLB10050)-(PVLB05085-pct)	-	-	-	715
sKB002	pET(pct)-(phaJ <sub>tesB</sub> )	-	-	-	715
sKB003	pET(pct)-(phaJ <sub>AC</sub> )	-	-	-	715
sKB004	pET(pct)-(phaJ <sub>PS</sub> )	-	-	-	715
sKB005	pET(pct)-(PVLB10050)	-	-	-	715
sKB006	pET(pct)-(phaJ <sub>CN</sub> )	-	-	-	715
sKB007	pET(pct)-(phaJ <sub>AC</sub> )	pACYC(acx4)	-	-	715
sKB008	pET(pct)-(phaJ <sub>AC</sub> )	pACYC(acx4)-(katE)	-	-	715
sKB009	pET(pct)-(phaJ <sub>AC</sub> )	pACYC(acox3)	-	-	715
sKB010	pET(pct)-(phaJ <sub>AC</sub> )	pACYC(fadE)	-	-	715
sKB011	pET(pct)-(phaJ <sub>AC</sub> )	pCOLA(acd)-(etfBA)	pACYC(etfD)	-	715
sKB012	pET(pct)-(phaJ <sub>AC</sub> )	pCOLA(acd)-(etfAB)	pACYC(etfD)	-	715
sKB013	pET(pct)-(phaJ <sub>AC</sub> )	pCOLA(acdH)-(etfBA)	pACYC(etfD)	-	715
sKB014	pCDF(alsS)-(ilvCD) <sup>A</sup>	pACYC(kivD)-(fjoh2967)	-	-	715
sKB015	pCDF(alsS)-(ilvCD)	pACYC(kivD)-(fjoh2967)	pCOLA-Tecm-lcg	-	715
sKB016	pCDF(alsS)-(ilvCD)	pACYC(kivD)-(aldH)	pCOLA-Tecm-lcg	-	715
sKB017	pCDF(alsS)-(ilvCD)	pACYC(kivD)	pCOLA-Tecm-lcg	-	715
sKB018	pCDF(ilvGM)-(ilvCD)	pACYC(kivD)-(fjoh2967)	pCOLA-Tecm-lcg	-	715
sKB019	pCDF(ilvGM)-(ilvCD)	pACYC(kivD)-(aldH)	pCOLA-Tecm-lcg	-	715
sKB020	pCDF(ilvGM)-(ilvCD)	pACYC(kivD)	pCOLA-Tecm-lcg	-	715
sKB025	pCDF(ilvGM)-(ilvCD)	pACYC(kivD)-(aldH)	pCOLA-Tecm-lcg	pET(pct-acx4)-(phaJ <sub>AC</sub> )	715
sKB029	pCDF(alsS)-(ilvCD)	pACYC(kivD)-(aldH)	pET(pct-acx4)-(phaJ <sub>AC</sub> )	-	715
sKB038	pCDF(ilvGM)-(ilvCD)	pACYC(kivD)-(aldH)	pCOLA-Tecm-lcg	pET(ibuA-acx4)-(phaJ <sub>AC</sub> )	715
sKB039	pCDF(ilvGM)-(ilvCD)	pACYC(kivD)-(aldH)	pCOLA-Tecm-lcg	pET(MACS-acx4)-(phaJ <sub>AC</sub> )	715

<sup>A</sup> Plasmid taken from Sheppard et al.<sup>95</sup>

sKB040	pCDF(ilvGM)-(ilvCD)	pACYC(kivD)-(aldH)	pCOLA-Tecm-lcg	-	565(DE3)
sKB041	pCDF(ilvGM)-(ilvCD)	pACYC(kivD)-(aldH)	pCOLA-Tecm-lcg	-	663 $\Delta$ metA
sKB042	pCDF(ilvGM)-(ilvCD)	pACYC(kivD)-(aldH)	pCOLA-Tecm-lcg	-	663 $\Delta$ tdh
sKB043	pCDF(ilvGM)-(ilvCD)	pACYC(kivD)-(aldH)	pCOLA-Tecm-lcg	-	565(DE3) $\Delta$ metA
sKB044	pCDF(ilvGM)-(ilvCD)	pACYC(kivD)-(aldH)	pCOLA-Tecm-lcg	-	663 $\Delta$ tdh
sKB045	pCDF(ilvGM)-(ilvCD)	pACYC(kivD)-(aldH)	pCOLA-Tecm-lcg	-	663 $\Delta$ metA $\Delta$ tdh
sKB046	pCDF(ilvGM)-(ilvCD)	pACYC(kivD)-(aldH)	pCOLA-Tecm-lcg	-	565(DE3) $\Delta$ metA $\Delta$ tdh
sKB047	pCDF(pct) <sup>B</sup>	pET28a(lcmF)	-	-	715
sKB048	pCDF(ilvGM)-(ilvCD)	pACYC(kivD)-(aldH)	pCOLA-Tecm-lcg	pET28a(icmF) _carb	715
sKB050	pCDF(ilvGM)-(ilvCD)	pACYC(kivD)-(aldH)	pCOLA-Tecm-lcg	pET28a(icmF) _carb	844
sKB051 <sup>C</sup>	pET(pct)-(phaJ <sup>L65A</sup> )	-	-	-	715
sKB052	pET(pct)-(phaJ <sup>V130G</sup> )	-	-	-	715
sKB053	pET(pct)-(phaJ <sup>Y76A</sup> )	-	-	-	715
sKB054	pET(pct)-(phaJ <sup>Y76S</sup> )	-	-	-	715
sKB055	pET(pct)-(phaJ <sup>Y76F</sup> )	-	-	-	715
sKB064 <sup>D</sup>	pET(pct)	-	-	-	715
sKB069	pET()- (phaJ)	-	-	-	715

<sup>B</sup>Plasmid taken from Sheppard et al.<sup>95</sup>

<sup>C</sup>Strains sKB051-sKB055 were constructed by Kelcey Allen.

<sup>D</sup>Strains sKB064 and sKB069 constructed by Kelcey Allen

### 3.3 Results and Discussion

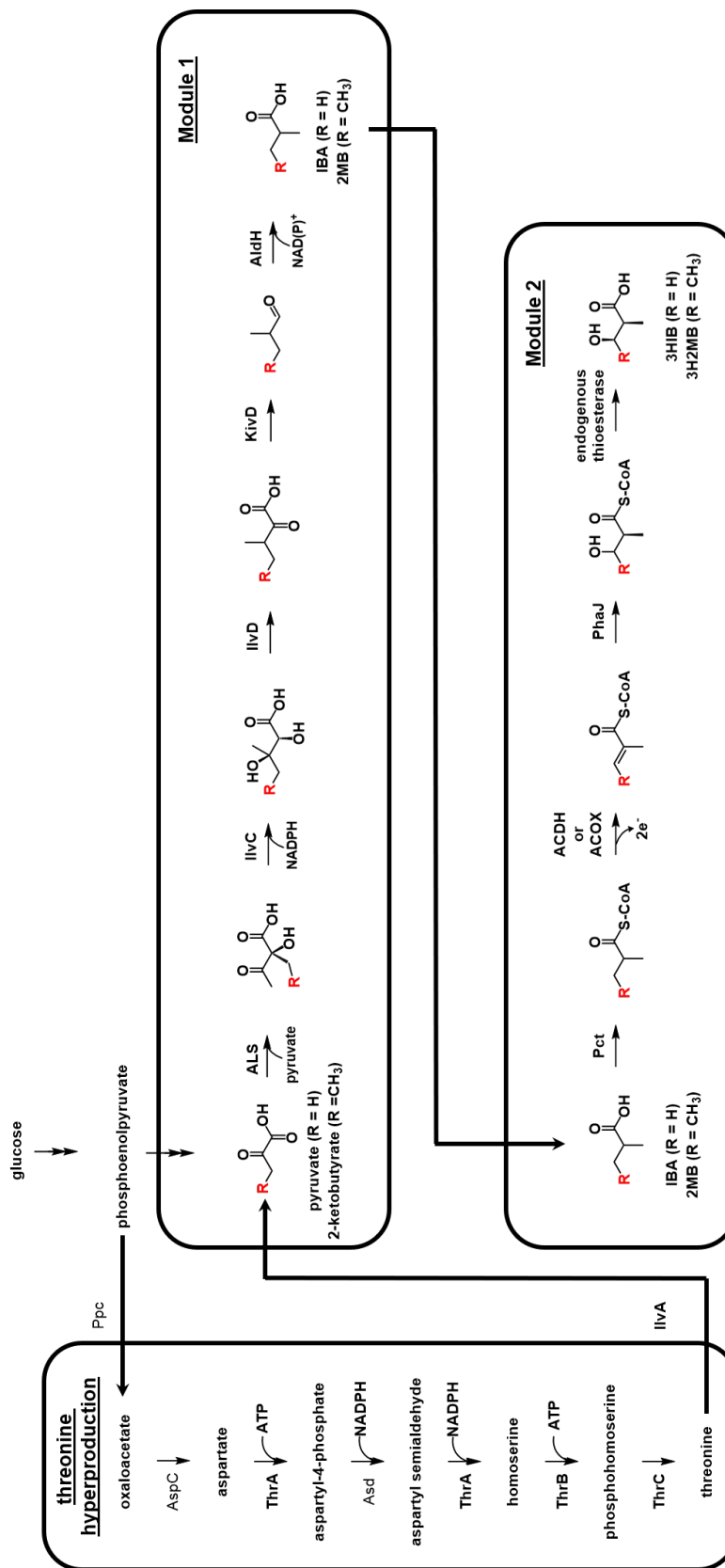
#### 3.3.1 Designing a pathway to $\alpha$ -3HAs

The proposed biological pathway provides a route from glucose to 3HIB and 3H2MB in recombinant *E. coli* (Figure 3.2). This pathway begins with the conversion of glucose to pyruvate or threonine via endogenous metabolism. Heterologous steps convert pyruvate and threonine to isobutyrate (IBA) or 2-methylbutyrate (2MB), respectively. Finally, four heterologous steps inspired by BCAA degradation generate 3HIB and 3H2MB from IBA and 2MB, respectively. Critical to the efficacy of this pathway is the modification of a previously developed biological route to IBA<sup>95</sup> for 2MB production and its combination with a new pathway that includes a branched chain permissive (R)-enoyl-CoA hydratase and acyl-CoA oxidase/acyl-CoA dehydrogenase.

Module 1 involves the conversion of glucose to IBA or 2MB. Briefly, the IBA pathway involves the condensation of pyruvate by the acetolactate synthase (ALS) from *Bacillus subtilis* – AlsS. Next, the ketol-acid reductoisomerase IlvC and dihydroxy acid dehydratase IlvD from *E. coli* convert the condensation product to a 2-keto acid. The 2-keto acid is decarboxylated via KivD from *Lactococcus lactis* and oxidized by an aldehyde dehydrogenase – Fjoh2967 from *Flavobacterium johnsoniae* or AldH from *E. coli* – to yield IBA.<sup>95</sup> Threonine hyperproduction is required for the biosynthesis of 2MB. The IBA pathway can be modified for threonine hyperproduction by overexpressing genes using the pCOLA-Tecm-Icg plasmid developed by Tseng et al.<sup>101</sup> The plasmid contains genes encoding ThrA<sup>G433R</sup> (feedback resistant, fused aspartate kinase/homoserine dehydrogenase from *E. coli*), ThrB (homoserine kinase from *E. coli*), and ThrC (threonine synthase from *E. coli*) to generate threonine from glucose. Threonine is then converted to 2-ketobutyrate via IlvA, a feedback resistant threonine deaminase from *Corynebacterium glutamicum*. From this point, the steps in the original IBA pathway and module 1 production of 2MB mirror each other.

Inspired by BCAA catabolism pathways present in many bacteria, module 2 oxidizes IBA or 2MB to yield 3HIB or 3H2MB, respectively. This is done via four steps: (1) the activation of the branched acid from module 1 by the propionyl-CoA transferase Pct (*Megasphaera elsdenii*), (2) dehydrogenation of the acyl-CoA by an acyl-CoA oxidase (ACOX) or acyl-CoA dehydrogenase (ACDH), (3) stereospecific hydration of the enoyl-CoA to a (3R)-3-hydroxy acid by PhaJ, and (4) hydrolysis of this product to an  $\alpha$ -3HA by endogenous thioesterases.

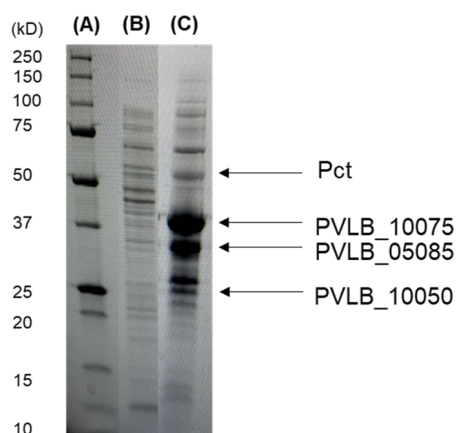




**Figure 3.2.** Biological route to 3-hydroxyisobutyric acid and 3-hydroxy-2-methylbutyric route glucose. Abbreviations used: Ppc - phosphoenolpyruvate carboxylase (*E. coli*), AspC - aspartate aminotransferase (*E. coli*)

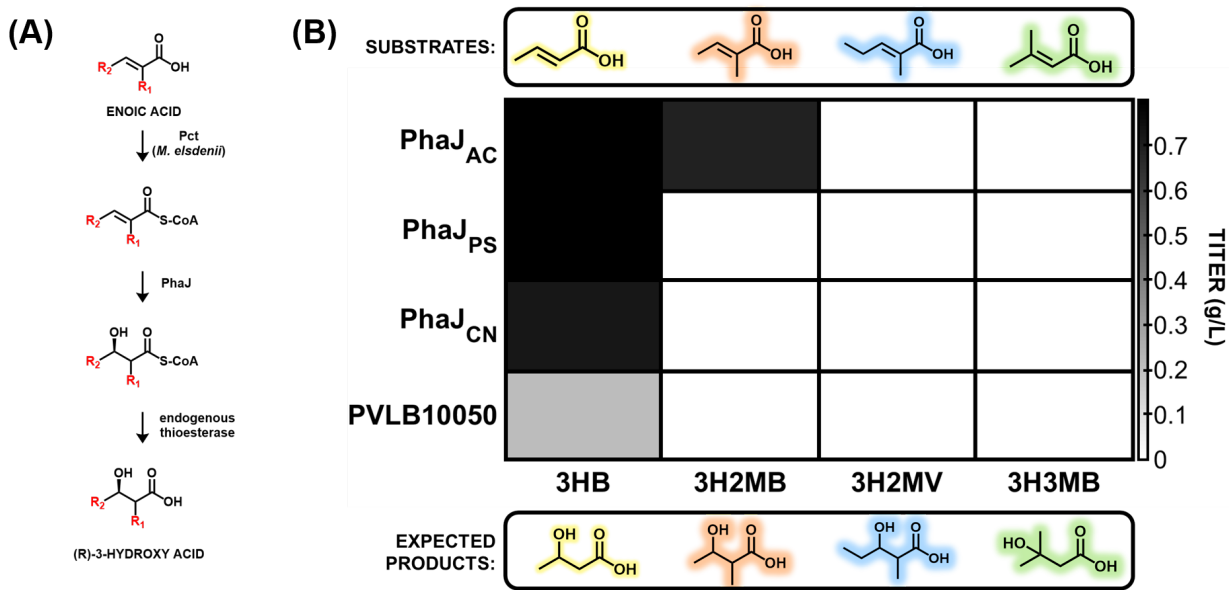
### 3.3.2 Validating the production of $\alpha$ -substituted 3-hydroxy acids from branched acids

As a first step in the bottom-up approach to pathway validation for 3HIB and 3H2MB, we investigated production of these monomers from branched acids. Enzyme homologs for each module 2 pathway step were chosen from *Pseudomonas taiwanensis* VLB120 – an organism with proven 3HIB production capabilities from IBA.<sup>23</sup> Briefly, Lang et al. hypothesized that conversion of IBA-CoA to 3HIB proceeded via the following steps: dehydrogenation by PVLB10075, hydration of methacryl-CoA by PVLB10050, and removal of the CoA group to generate the free acid by PVLB05085. Soluble protein expression of these enzymes was confirmed via SDS-PAGE (Figure 3.3). However, *E. coli* harboring this version of module 2 with Pct was unable to convert IBA to 3HIB (data not shown).



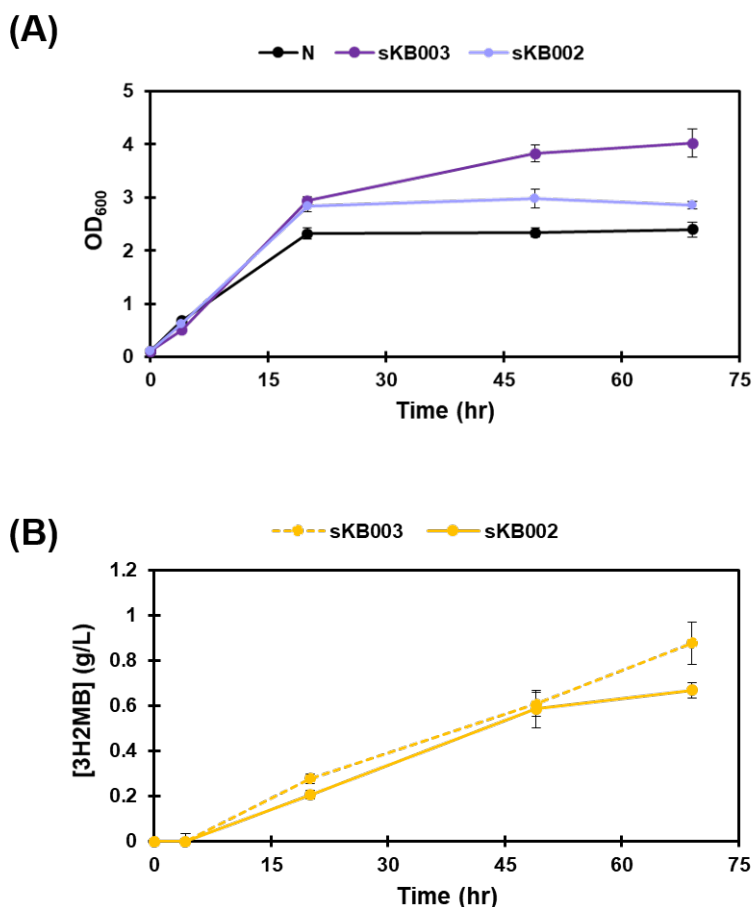
**Figure 3.3.** SDS-PAGE analysis of module 2 enzymes from *Pseudomonas taiwanensis* (A) Ladder (B) lysate from empty vector negative control (C) lysate from sKB001

To pinpoint the cause of pathway issues, a truncated version of the  $\alpha$ -3HA pathway was developed based on a pathway developed by others.<sup>18</sup> This shortened pathway bypasses the dehydrogenation step, instead converting enoic acids to the corresponding  $\alpha$ -3HA. Because the precursor enoic acid for 3HIB (methacrylic acid) is a toxic, valuable chemical, the version of the truncated pathway for the production of 3H2MB was investigated. This truncated module 2 pathway involves the activation of tiglic acid, its hydration to 3H2MB-CoA and deactivation to 3H2MB (Figure 3.4a). This shortened pathway served as a good point for pathway troubleshooting because it has fewer steps, making it easier to determine problematic ones. Additionally, it makes use of enzyme homologs with documented functionality.



**Figure 3.4.** Enoic Acids to 3-hydroxy acids production experiment. sKB003-sKB005 were cultivated according to culture condition A with 2 mM enoic acid added every 24 hr. Abbreviations used: CN = *Cupriavidus necator*, AC = *Aeromonas caviae*, PS = *Pseudomonas syringae*, PT = *Pseudomonas taiwanensis* VLB120

Because PhaJ is the stereospecificity determining enzyme in the pathway, initial production experiments focused on testing the ability of PhaJ variants of this pathway to catalyze the conversion of tiglic acid to 3H2MB. PhaJ homologs were identified from characterized (R)-enoyl-CoA hydratases in the literature.<sup>102</sup> Of the four PhaJ variants of the truncated pathway tested, only the variant possessing PhaJ from *Aeromonas caviae* was capable of producing 3H2MB from tiglic acid (Figure 3.4b). Other variants produced 3HB from crotonate indicating that pathway inefficacy for 3H2MB production in these cases was due to PhaJ substrate specificity. Finally, none of the PhaJ-variant pathways tested worked in the conversion of 2-methyl-2-pentenoic acid to 3H2MV or the conversion of 3-methyl-3-butenoic acid to 3H3MB - indicating that PhaJ determines the product range in this pathway. PhaJ mutagenesis will be required to reach longer  $\alpha$ -3HAs and  $\beta$ -branched 3HAs.



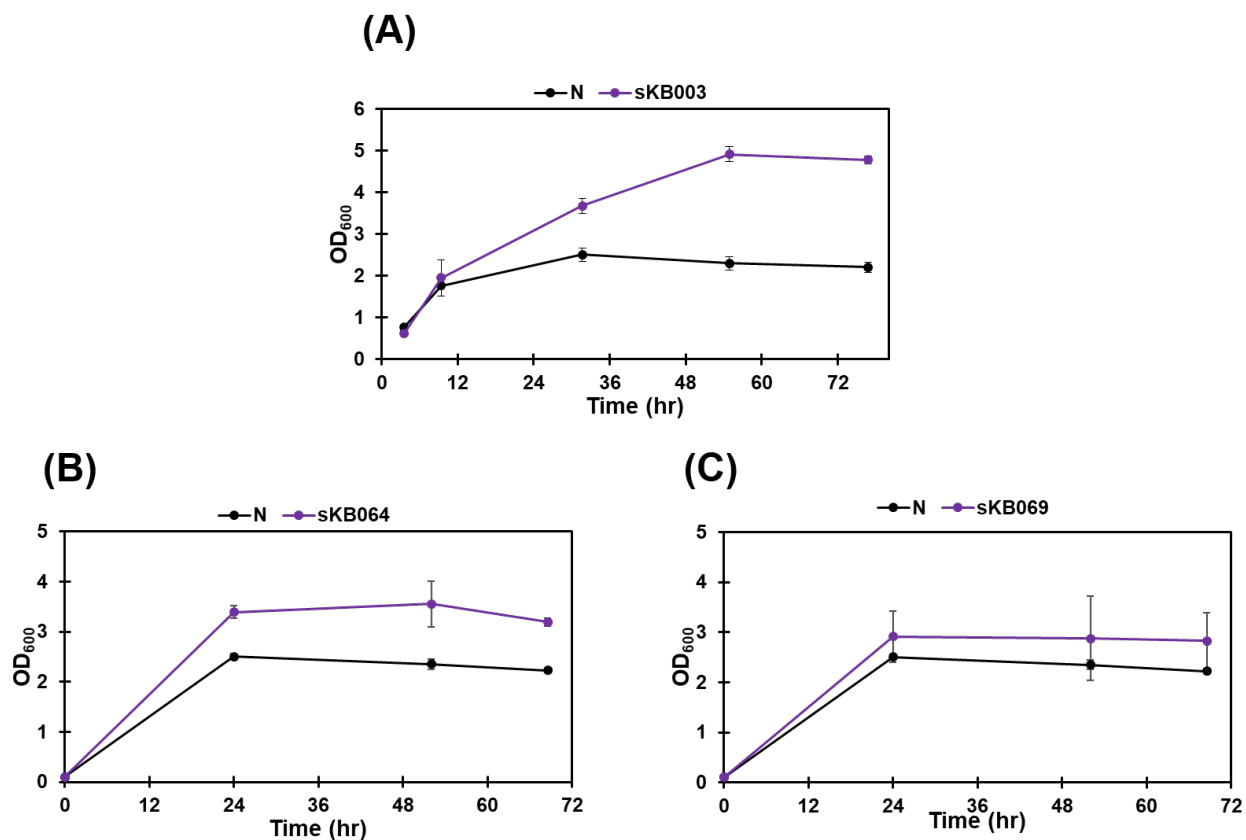
**Figure 3.5.** Tiglic Acid to 3H2MB Shake Flask Production Experiment. sKB002 and sKB003 was cultivated according to culture condition B with 2 mM tiglic acid added every 24 hr. (A) Growth curve of empty vector negative control vs sKB002 and sKB003 (B) 3H2MB titers from production strains sKB002 and sKB003. Abbreviations used: N = empty vector negative control

Additional characterization of the truncated module 2 pathway revealed (1) the production strain grows better than an empty vector negative control (Figure 3.5a) and (2) overexpressing *tesB* does not significantly improve 3H2MB titers (Figure 3.5b)<sup>E</sup>. The highest 3H2MB titers achieved by truncated module 2 strain with and without *tesB* overexpression were  $878 \pm 90$  mg/L and  $668 \pm 30$  mg/L, respectively. Anomalous, the truncated module 2 production strains maintained their growth advantage in the absence of tiglic acid (Figure 3.6a)<sup>F</sup>. However, the overexpression of Pct alone does confer a growth advantage (Figure 3.6b-c). This may suggest that Pct participates in CoA-activation in *E. coli*'s endogenous metabolism in a way that reduces cofactor utilization to bolster growth. Finally, 3H2MB production from the truncated module 2 pathway

<sup>E</sup>P-value for differences between 3H2MB titers with and without *tesB* overexpression < 0.05. P-value calculated using student's two tailed t-test with unequal variances.

<sup>F</sup>Experiments in Figure 3.6 were conducted by Kelcey Allen

in the absence of *tesB* overexpression is most likely due to activity from more than 12 other thioesterase paralogs in *E. coli*.<sup>103</sup>



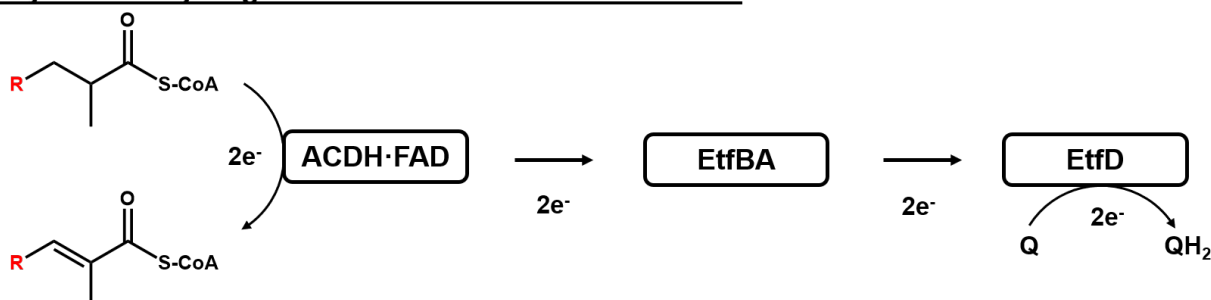
**Figure 3.6.** Examining the growth advantage of strains expressing the truncated module 2 pathway. sKB003, sKB064, and sKB069 were cultivated using condition B with 2 mM tiglic acid added every 24 hr if necessary. (A) Growth of empty vector negative control vs sKB003 in the absence of tiglic acid (B) Growth of empty vector negative control vs strain only expressing *pct* (C) Growth of empty vector negative control vs strain only expressing *phaJ*. Abbreviation used: N = empty vector negative control

Experimental efforts next turned to implementing module 2 for 3HIB and 3H2MB production from IBA and 2MB, respectively. The enzymatic step separating the two pathways is the  $\alpha$ ,  $\beta$ -dehydrogenation of an acyl-CoA to an enoyl-CoA. This step is catalyzed by an ACDH or an ACOX. In this reaction, electrons are funneled from the acyl-CoA to an enzyme bound flavin adenine dinucleotide (FAD). These electrons are ultimately shuttled to the respiratory chain through accessory electron transfer flavoproteins (ETFs) by ACDHs.<sup>104</sup> Alternatively, ACOXs utilize oxygen as a final electron acceptor, producing H<sub>2</sub>O<sub>2</sub> as a byproduct (Figure 3.7).

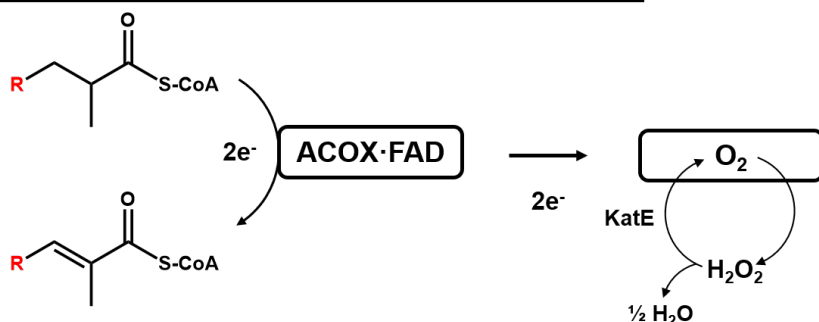
ACDH and ACOX homologs were identified by mining BRENDA for enzymes with documented activity on branched acyl-CoAs. ACDH homologs identified include: Acd (*Pseudomonas putida* KT2440)<sup>105</sup> and

AcdH (*Streptomyces avermitilis*).<sup>106</sup> Since little is known about bacterial ETF systems, two ETF systems were identified from *Pseudomonas putida* KT2440 by BLASTing its genome using *Sus scrofa* ETF as query. Two sets of ETFs were identified: (1) EtfB (locus tag = PP4202), EtfA (locus tag = PP4201), and EtfD (locus tag = PP4203) where *etfBA* and *etfD* are transcribed via divergent promoters that are spatially distant from Acd on the genome and (2) EtfA (locus tag = PP0312) and EtfB (locus tag = PP0313) which are in the same operon as dimethylglycine catabolism genes. Additionally, FadE (*E. coli*) was selected as a candidate ACDH because it is believed to utilize intra-enzyme domains for electron transfer instead of accessory ETFs.<sup>107</sup> ACOX homologs identified include: Acx4 (*Arabidopsis thaliana*)<sup>108</sup> and ACOX3 (*Yarrowia lipolytica*).<sup>109</sup>

### Acyl-CoA Dehydrogenase Electron Transfer Mechanism

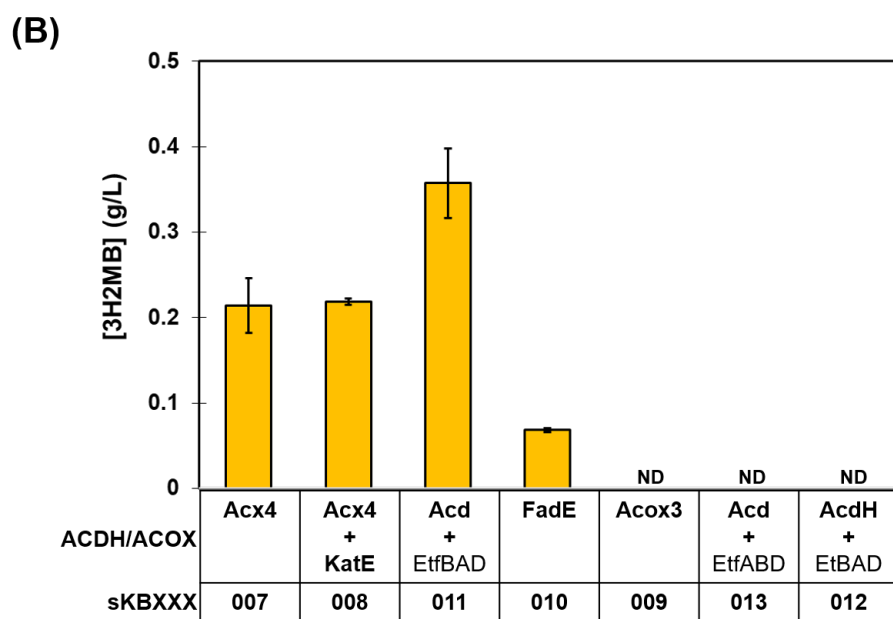
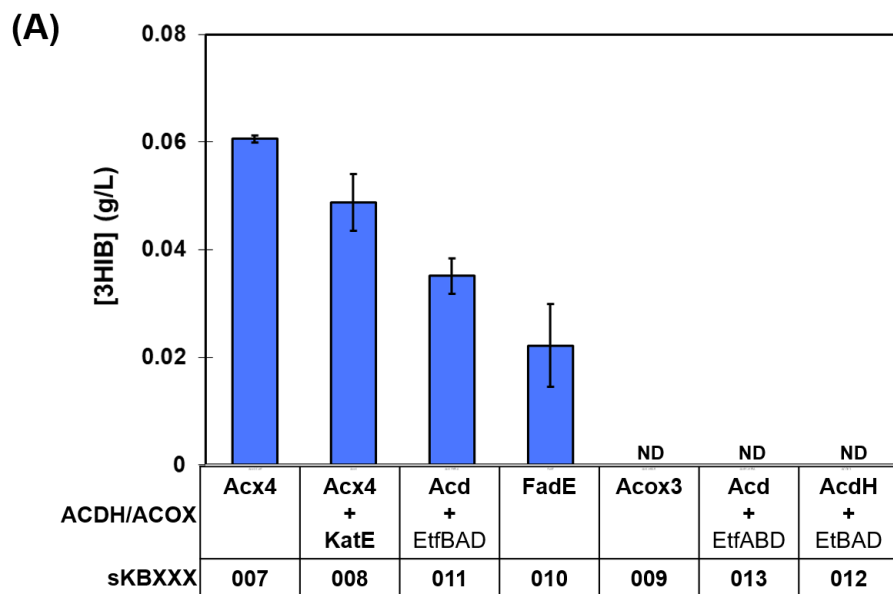


### Acyl-CoA Oxidase Electron Transfer Mechanism

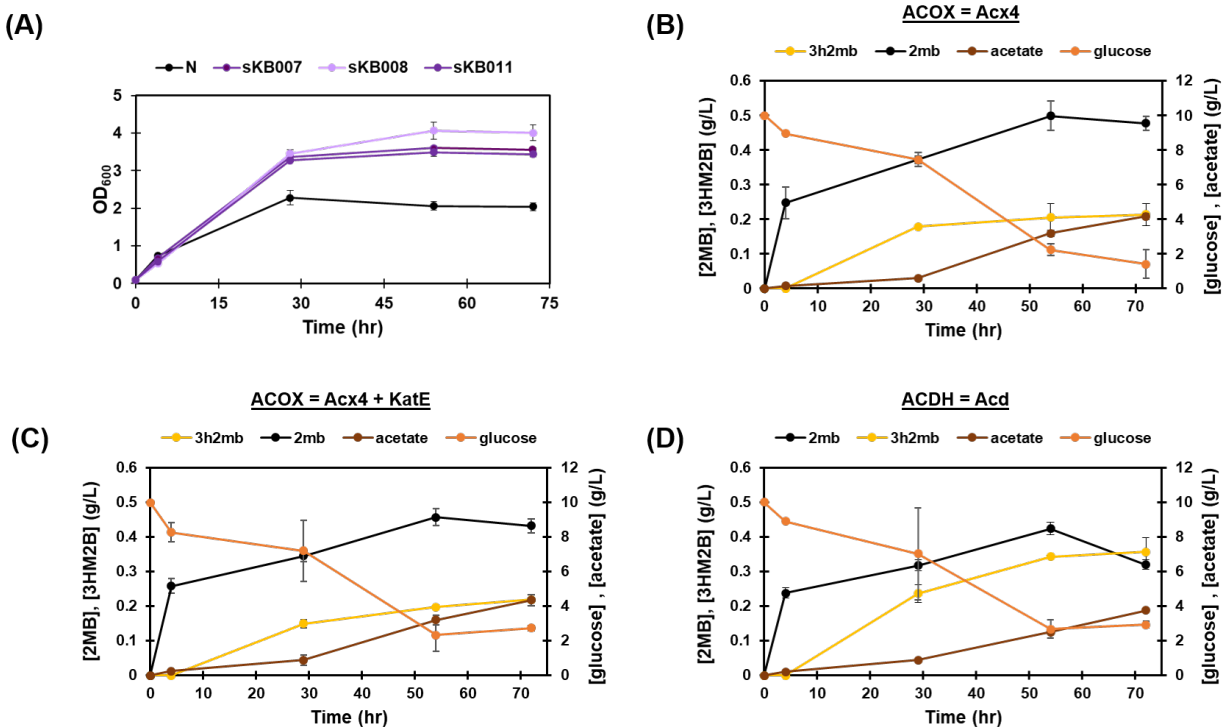


**Figure 3.7.** Electron transfer in acyl-CoA dehydrogenases and acyl-CoA oxidases. ACDH oxidizes acyl-CoAs, shuttling electrons to EtfBA, then EtfD with the final electron transfer involving the reduction of ubiquinone (Q) to ubiquinol (QH<sub>2</sub>). ACOX oxidizes acyl-CoAs using oxygen as a final electron acceptor. In another reaction catalyzed by a catalase like KatE, hydrogen peroxide can be used to regenerate oxygen. Abbreviations used: EtfA (electron transfer flavoprotein subunit alpha), EtfB (electron transfer flavoprotein subunit beta), and EtfD (electron transfer flavoprotein-ubiquinone oxidoreductase)

Results from production experiments in strains harboring these dehydrogenase enzyme variants of the module 2 pathway are shown in Figure 3.8. Strains expressing versions of the pathway with Acd-EtfABD, AcdH-EtfBAD, and ACOX3 produced no 3HIB or 3H2MB. Causes for the inefficacy of these versions of the module 2 pathway are related to (1) incorrect electron transfer system (Acd-EtfABD and AcdH-EtfBAD) and



**Figure 3.8.** 3-Hydroxyisobutyric acid and 3-hydroxy-2-methylbutyric acid production from branched acids. sKB007-sKB013 were cultivated using condition B with 2 mM IBA or 2MB added every 24 hr. Abbreviations used: ND = not detected



**Figure 3.9.** Dynamic production run data for selected module 2 strains. sKB007, sKB008, and sKB011 were cultivated according to culture condition B with 2 mM 2MB added every 24 hr.

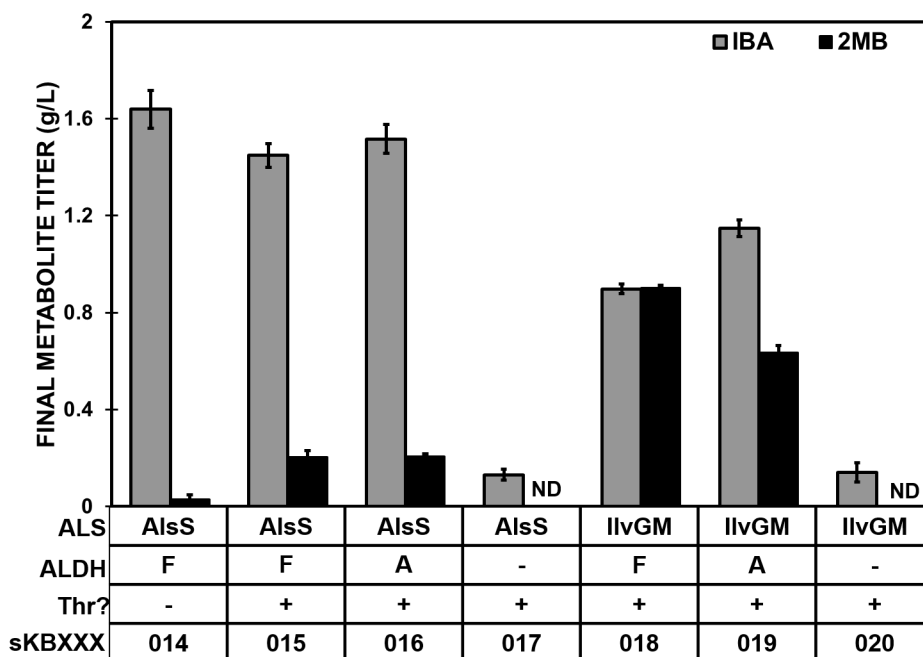
insoluble protein expression (ACOX3). Interestingly, FadE is able to catalyze the dehydrogenation reaction without overexpressing accessory ETFs. This observation, in combination with the absence of genes encoding for ETFs in *E. coli*'s genome lends credence to Campbell and Cronan's hypothesis<sup>107</sup> that FadE may contain intra-enzyme domains for electron transfer. However, yields for 3HIB and 3H2MB are only 3.5% and 9.6% the maximum theoretical yield, respectively. The low  $\alpha$ -3HA titers exhibited by FadE versions of module 2 are attributed to substrate specificity. FadE acts primarily on straight chain acyl-CoAs with carbon backbones  $\geq 4$  from fatty acid degradation.

Compared to FadE, strains possessing Acx4 or Acd-EtfBAD produced more  $\alpha$ -3HAs (Figure 3.8 and 3.9). However 3H2MB titers were substantially less than that exhibited by truncated module 2 strains fed tiglic acid. This suggests that the dehydrogenation step is a pathway bottleneck. To our knowledge, 3H2MB production by versions of module 2 containing Acd-EtfBAD represents the first time that a complete ACDH system has been expressed heterologously and it shows that EtfBAD (annotated as PP4201-PP4203 in *Pseudomonas putida* KT2440's genome) is a sufficient electron transfer system for this ACDH. 3HIB titers were lower than 3H2MB titers for all versions of module 2 tested indicating that dehydrogenation enzymes specific



for shorter substrates could be used to increase titer here. Low 3HIB titers are also likely due to the acute toxicity of its pathway precursor molecule - methacrylic acid. There was no significant difference between 3HIB or 3H2MB titers when *katE* – a gene encoding for catalase - was overexpressed to scavenge toxic H<sub>2</sub>O<sub>2</sub> in versions of module 2 with Acx4. This suggests that H<sub>2</sub>O<sub>2</sub> generated by Acx4-mediated versions of module 2 was low or that another endogenous H<sub>2</sub>O<sub>2</sub> scavenging system like the alkyl hydroperoxide reductase (AhpCF) or bifunctional catalase (KatG) was being used.<sup>110</sup> Clearly, the (R)-enoyl-CoA hydratase and the dehydrogenation enzymes are key factors in controlling pathway efficacy,  $\alpha$ -3HA titer, and product range.

### 3.3.3 Engineering branched acid specificity from glucose



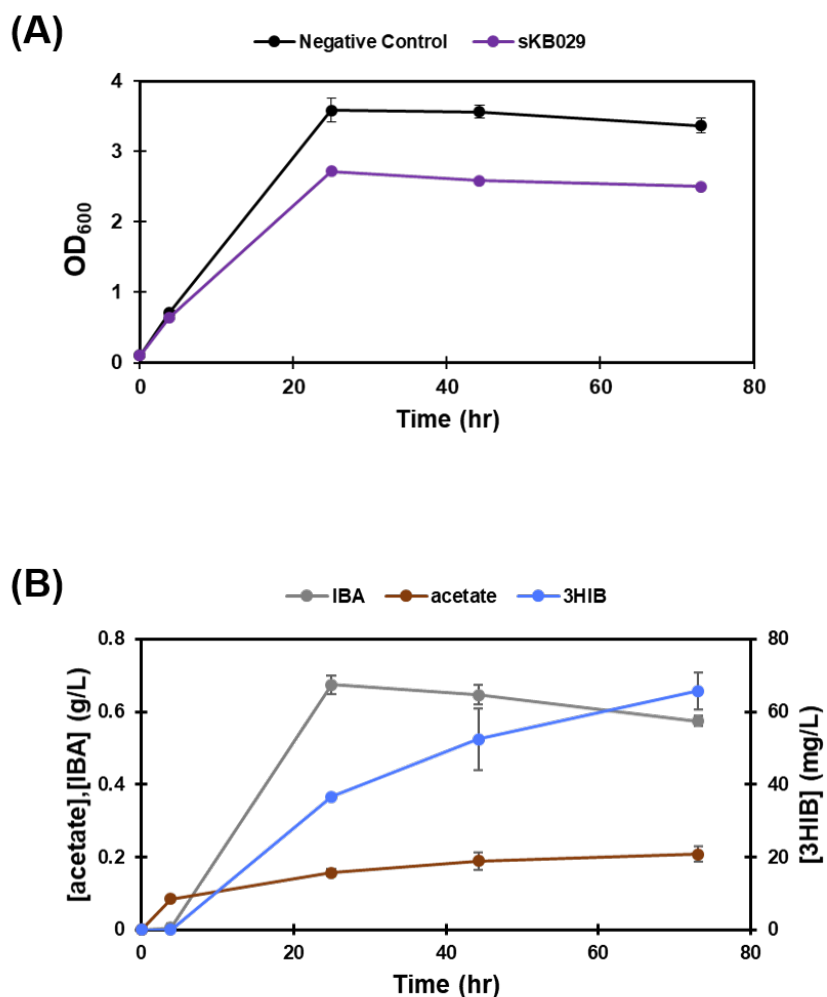
**Figure 3.10.** Isobutyrate and 2-methylbutyrate production from glucose. sKB014 – sKB020 were cultivated according to culture condition A. F = isobutyraldehyde dehydrogenase Fjoh2967, A = AldH, Thr? = Is threonine hyperproduction pathway present?

Following the bottom up approach to pathway validation, module 1 was next engineered for branched acid specificity. Module 1 of the pathway involves the conversion of glucose to IBA or 2MB. IBA production from the previously developed IBA strain<sup>95</sup> was demonstrated in this study at  $1.7 \pm 0.1$  g/L (Figure 3.10). Threonine hyperproduction improved 2MB titer nearly 7x over the IBA producer developed by Sheppard et al. However, IBA was still the dominant product. To further tune module 1 for 2MB production, versions of the pathway with ALDH and ALS homologs more specific for 2MB production were investigated. AldH –

an aldehyde dehydrogenase from *E. coli* with broader specificity than the isobutyraldehyde dehydrogenase employed in the original IBA pathway – was tested in the module 1. No significant difference in 2MB specificity modulation was observed between module 1 pathway variants with AldH or Fjoh2967. Next, versions of module 1 with the ALS IlvGM from *Klebsiella aerogenes* were analyzed. IlvGM reportedly prefers the condensation reaction which leads to 2MB formation 1,333x more than AlsS from *Bacillus subtilis*.<sup>111</sup> *E. coli* harboring module 1 with IlvGM exhibited a 2MB titer of  $0.9 \pm 0.01$  g/L which is the highest of all the module 1 variants tested. Dhande et al.<sup>112</sup> previously reported 2MB titers as high as 2.59 g/L, but their experiments were run with 4x more glucose than the ones presented here. Despite these modifications, IBA titer remains high in module 1 strains engineered for 2MB specificity. Additional metabolic engineering efforts are required to reduce the formation of IBA in 3H2MB production strains.

### 3.3.4 3HIB and 3H2MB production from glucose in *E. coli*

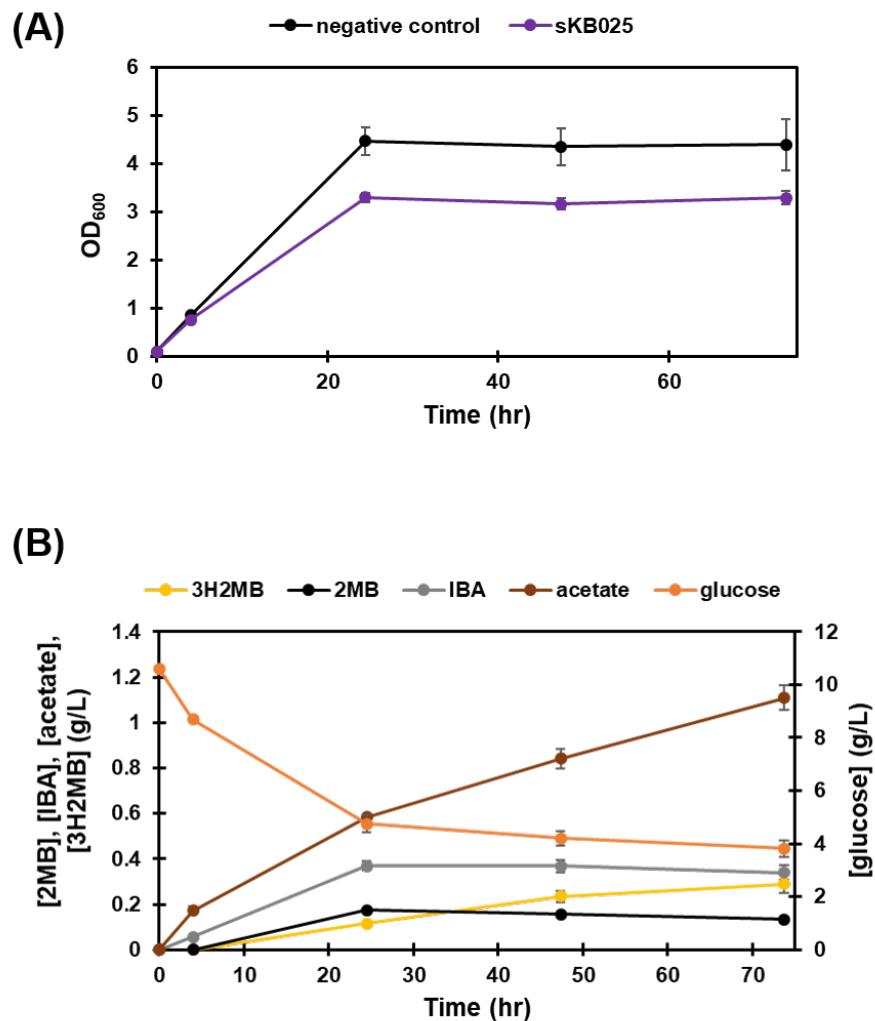
Versions of module 1 specific for IBA or 2MB were combined with the Acx4 version of module 2 to yield recombinant *E. coli* capable of producing 3HIB or 3H2MB from glucose. Acx4 versions of module 2 were chosen despite their reduced titer compared to Acd versions due to the difficulty of cloning Acd's complete electron transfer system in the context of the full pathway. Only versions of module 1 with AldH were examined since it is a broader specificity enzyme which lends itself to the application of this pathway for other compounds. These strains were grown as previously described and  $\alpha$ -3HA production from glucose was measured. Both 3HIB and 3H2MB production from glucose were observed. 3HIB production was observed at titers as high as  $66 \pm 5$  mg/L with full consumption of fed glucose (Figure 3.11). This titer is comparable to 3HIB production from strains with module 2 only fed IBA. The 3HIB production strain showed IBA buildup indicating that module 2 conversion of IBA to 3HIB is limiting in this system. Substantially higher 3HIB titers have been reported in bacteria which naturally possess the valine degradation pathway (Table 3.1). This suggests that the main limiting factor for 3HIB production from our pathway is module 2 enzyme activity on pathway substrates.



**Figure 3.11.** 3-hydroxyisobutyric acid production from glucose in recombinant *E. coli*. sKB029 was cultivated according to culture condition B (A) Growth curve of sKB029 and empty vector negative control (B) Metabolite profile for sKB029

The highest 3H2MB titer achieved by cells expressing the full pathway was  $290 \pm 40$  mg/L (Figure 3.12). To our knowledge, this is the first time that 3H2MB has been biologically produced from an unrelated carbon source. This titer is on par with the titers exhibited by strains with module 2 only fed 2MB. The 3H2MB full pathway strain exhibited IBA and 2MB build up. Additionally, the growth advantage exhibited by strains with shorter iterations of this pathway disappears in the full pathway strains (Figure 3.11a and 3.12a). 2MB build-up suggests that activation by Pct may be a limiting step in the full pathway. Pct catalyzes the *reversible* activation of short-chain acids to acyl-CoAs (Figure 3.2). Thus, there is some equilibrium constant which bounds the amount of 2MB-CoA that forms intracellularly. Replacing Pct with an irreversibly acting enzyme could drive flux towards the production of 3H2MB. The disappearance of the growth advantage associated

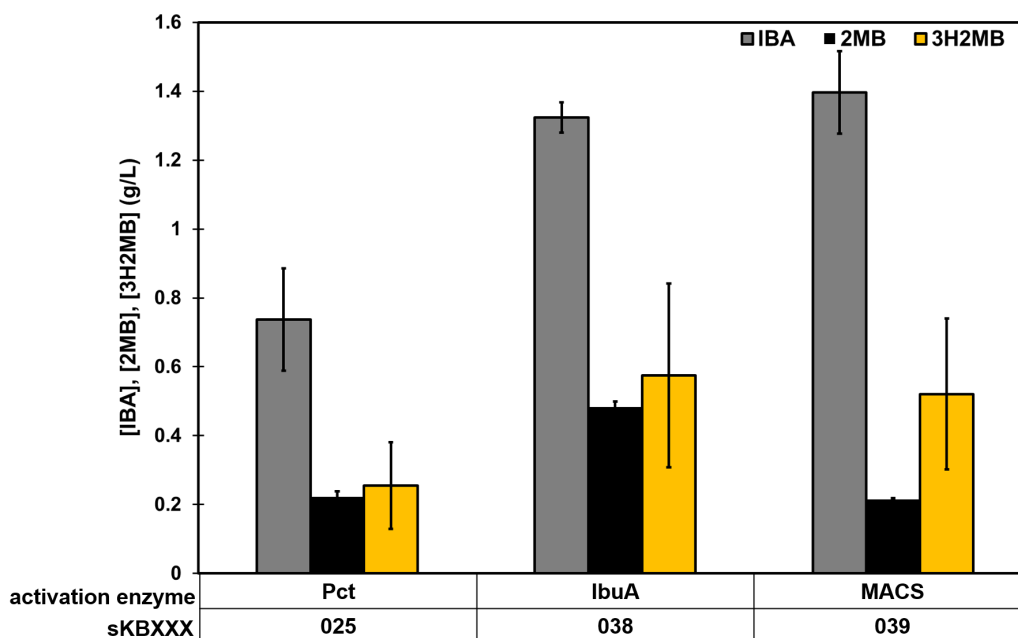
with shorter versions of our pathway may be due to the metabolic burden associated with overexpressing the genes that encode the entire pathway. The most abundant by-product formed during 3H2MB production is IBA. IBA forms from the condensation of two molecules of pyruvate by an ALS. *E. coli* MG1655 has two active ALSs - IlvBN and IlvIH. Additionally, the 3H2MB pathway involves the overexpression of *ilvGM* (*Klebsiella aerogenes*). Most likely, the action of all three enzymes contributes to the production of IBA. Improving 3H2MB titers from our pathway will rely on reducing IBA production and 2MB accumulation.



**Figure 3.12.** 3-hydroxy-2-methylbutyric acid production from glucose in recombinant *E. coli*. sKB025 was cultivated according to culture condition B (A) Growth curve of sKB025 and empty vector negative control (B) Metabolite profile for sKB025

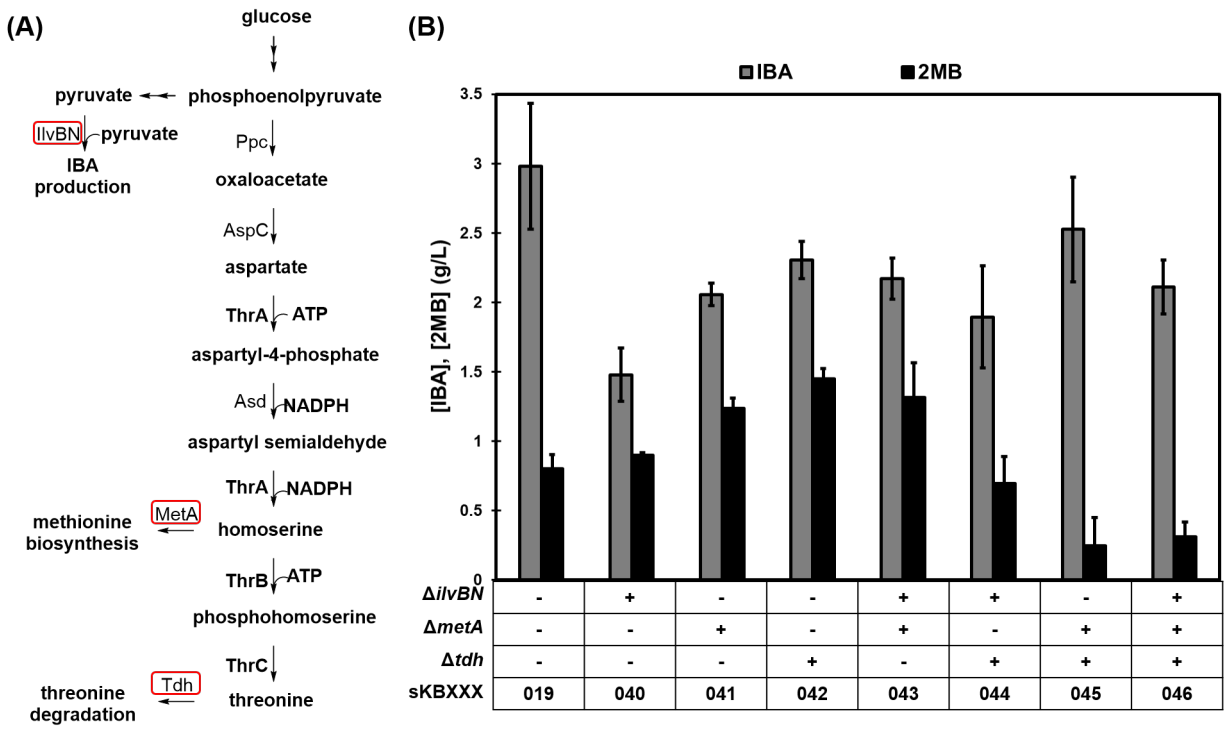
### 3.3.5 Optimizing 3H2MB production from glucose by improving precursor supply and use

This report represents the first time 3H2MB has been produced from an unrelated carbon source in *E. coli*. Based on this success and the documented improved material properties of 3H2MB-based biopolymers,<sup>22,75</sup> we chose to optimize our route for 3H2MB production. Major impediments to 3H2MB titer included IBA production and 2MB accumulation. To reduce 2MB accumulation from strains harboring the full 3H2MB pathway, alternative activation enzymes were investigated for module 2. Pct reversibly activates short-chain acids using the CoA moiety from an acetyl-CoA. Alternatively, acyl-CoA synthetases irreversibly ligate CoA and an acid to yield acyl-CoAs at the expense of ATP. IbuA (*Rhodopseudomonas palustris*) and MACS (*Methanosarcina acetivorans*) were selected from the literature for pathway inclusion based on their demonstrated activity on branched acids.<sup>113,114</sup> Preliminary experiments show higher 3H2MB titers in production strains with IbuA in place Pct (Figure 3.13). However, this difference is not statistically significant. Additional experiments must be carried out to ascertain the effects of replacing Pct with IbuA.



**Figure 3.13.** Effects of activation enzyme choice on 3-hydroxy-2-methylbutyric acid production. sKB025, sKB038, and sKB039 were grown according to culture condition B.

Another route to improve 3H2MB production is by deleting competing pathways to target compound formation. Module 2 is orthogonal to *E. coli*'s native metabolism and the branched acyl-CoAs it produces are unlikely substrates for endogenous fatty acid metabolism. Thus, major competing pathways to 3H2MB production are the routes that prevent 2MB production from module 1. The main competing pathways to 2MB



**Figure 3.14.** Improving 2-methylbutyric acid production by deleting competing pathways. sKB019 and sKB040-sKB046 were cultivated according to culture condition A (A) Competing Pathways to 2MB (B) Final IBA and 2MB titers from module 1 knockout strains

formation are methionine biosynthesis, threonine degradation, and the native activity of IlvBN on pyruvate which leads to the formation of IBA (Figure 3.14a). The first committed step in methionine biosynthesis and threonine degradation are carried out by Tdh (threonine dehydrogenase) and MetA (homoserine O-succinyltransferase). The genes encoding IlvBN, MetA, and Tdh were combinatorically deleted from *E. coli*'s genome and the production of IBA and 2MB from these knockout strains overexpressing the 2MB specific version of module 1 were tested (Figure 3.14).

sKB042 with  $\Delta tdh$  only exhibited the highest 2MB titer of  $1.4 \pm 0.1$  g/L (Figure 3.14). This represents an 81% increase over the base strain. Cann and Liao<sup>115</sup> previously examined the effects of deleting *metA*, *tdh*, and *ilvBN* from *E. coli*'s genome for the production of 2-methylbutanol - another product derived from threonine metabolism. They found that deleting *tdh* and *metA* resulted in the highest 2-methylbutanol titer. However, they did not test the  $\Delta tdh$  variant. The better performance of the *tdh* knockout over the double or triple knockouts in our study may be due to: (1) IlvBN's capacity to also work in the production of 2MB, (2) higher flux through the threonine degradation pathway compared to methionine biosynthesis since it's being overproduced in the 3H2MB pathway, and (3) growth defects associated with deleting essential genes like

*metA*. sKB040 with  $\Delta ilvBN$  only, exhibited the largest decrease in IBA titer - going from  $3 \pm 0.5$  g/L to  $1.5 \pm 0.2$  g/L IBA. The action of *IlvBN* on pyruvate is the only endogenous pathway that leads to the formation of IBA. Thus, additional engineering efforts are needed to further reduce IBA formation.

### 3.3.6 Developing a novel isobutyrate recycle system

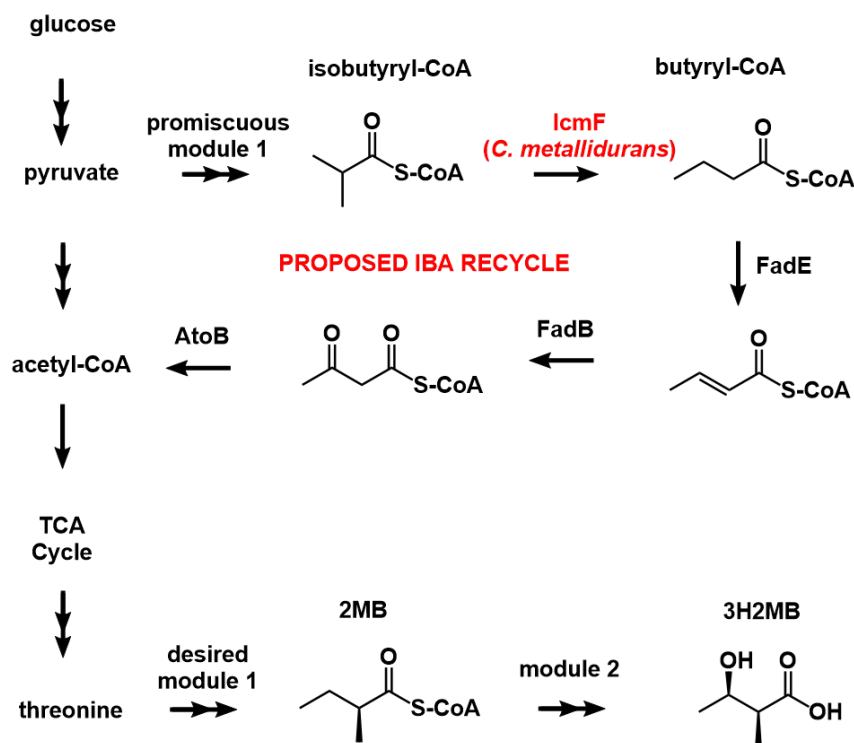
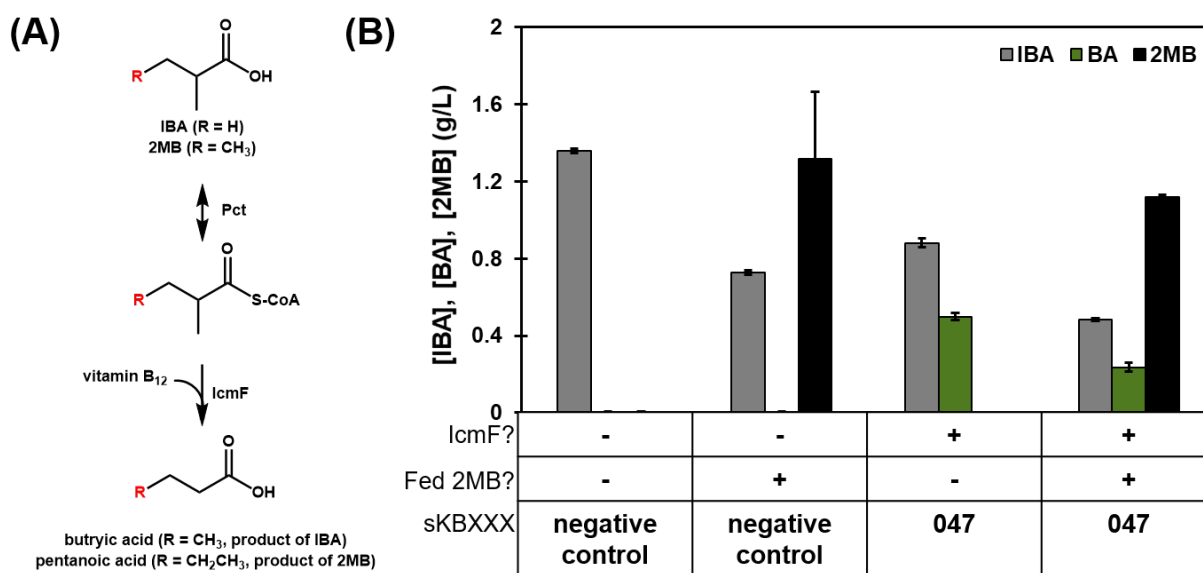


Figure 3.15. Isobutyrate recycle system

A major byproduct of 3H2MB production from glucose is IBA – a product formed from the native activity of *IlvBN* on pyruvate. Deleting *IlvBN* did not eliminate IBA production (Figure 3.14), so we pursued the design and implementation of an IBA recycle (Figure 3.15). In this recycle, an isobutyryl-CoA mutase converts isobutyryl-CoA to butyryl-CoA. Native short-chain fatty acid degradation machinery in *E. coli* converts butyryl-CoA to acetyl-CoA where it can re-enter the  $\alpha$ -3HA pathway for 3H2MB production. Specifically, FadE dehydrogenates butyryl-CoA - the product of *IcmF* action on isobutyryl-CoA. Next, FadB (bifunctional enoyl-CoA hydratase/3-hydroxyacyl-CoA dehydrogenase) converts the resulting enoyl-CoA to acetoacetyl-CoA. AtoB (thiolase) cleaves acetoacetyl-CoA to two molecules of acetyl-CoA. The *IcmF*-mediated IBA recycle converts IBA to two molecules of acetyl-CoA. Importantly, this recycled carbon cannot reenter metabolism for the production of IBA, but it can lead to increased threonine production.

The key enzyme in this recycle is the isobutyryl-CoA mutase. Isobutyryl-CoA mutases catalyze the vitamin B<sub>12</sub>-dependent isomerization of isobutyryl-CoA to butyryl-CoA.<sup>116</sup> Cracan et al.<sup>117,118</sup> characterized several mutases and found IcmF from *Cupriavidus metallidurans* to be the most active on IBA-CoA. Thus, we chose this homolog for inclusion in our IBA recycle. The IBA recycle was first validated in sKB047 to confirm the ability of cells overexpressing *icmF* to convert exogenously fed IBA to butyrate (BA) (Figure 3.16a). Cells overexpressing *icmF* converted IBA to BA (Figure 3.15b). All fed IBA was not consumed - most likely because of the reversibility of pathway steps. Further, when fed both IBA and 2MB, no pentanoic acid production was observed. The expected product for IcmF action on 2MB is pentanoic acid. Thus, IcmF specifically converts IBA to BA.

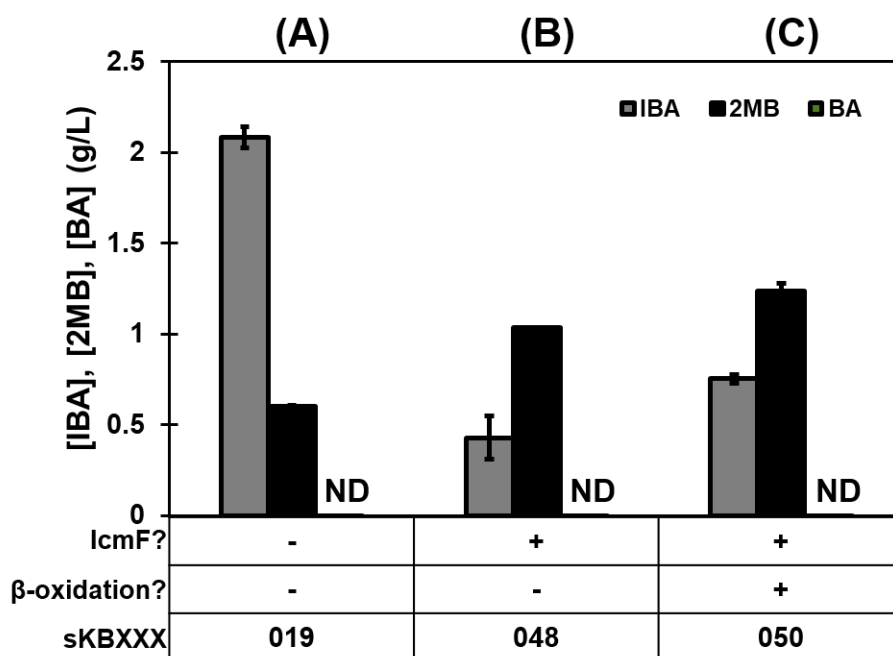


**Figure 3.16.** Conversion of isobutyrate to butyrate acid by cells with an isobutyryl-CoA mutase. sKB047 was cultivated according to culture conditions A with fed IBA or IBA and 2MB. Negative control represents an empty vector negative control

Next, acid production was monitored from sKB019 and sKB048 to compare the IBA production in module 1 strains with and without *icmF* overexpression. sKB048 with IcmF produced 80% less IBA than sKB019 (Figure 3.17). Anomalously, no BA accumulation was observed in sKB048 even though *atoB*, *fadE*, and *fadB* shouldn't be expressed under the given culture conditions. The enzyme products of these genes are required for BA's recycle back to central carbon metabolism. In the initial conception of the recycle, the final version would be expressed in a strain 844 (Table 3.2) with  $\Delta fadR$  and constitutive expression of *atoC*. *FadE* and *fadB* expression are repressed by FadR and this repression is only alleviated in the presence of long chain fatty



acids. Further, AtoC is a transcriptional activator for *atoB* expression that is only turned on in the presence of acetoacetyl-CoA.<sup>119</sup> We hypothesize that leaky expression of *atoB*, *fadE*, and *fadB* allows for the efficacy of the recycle in sKB048. To test this, quantitative reverse transcription PCR targeting *fadB* and *atoB* could be carried out during a production experiment in sKB048. We tested the recycle in the background strain 844 and saw no significant difference between IBA production in sKB048 and sKB050. Nevertheless, the IcmF-mediated IBA recycle is an effective tool to reduce byproduct formation from module 1. Future experiments on the IBA recycle would center on testing its ability to boost 3H2MB titer in the context of the full pathway.



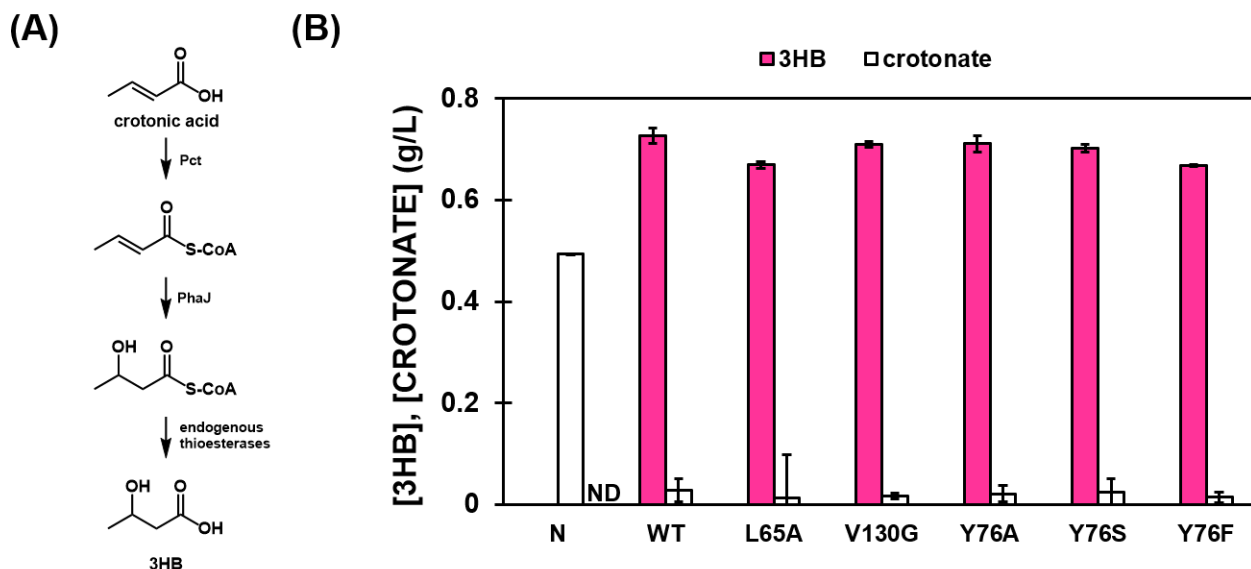
**Figure 3.17.** Testing the isobutyrate acid recycle in 2-methylbutyrate production strains. sKB019, sKB048, sKB050 were cultivated according to culture condition B.

### 3.3.7 PhaJ for the production of other 3HAs

Early experiments in truncated versions of module 2 demonstrated that PhaJ controls the product range of the  $\alpha$ -3HA pathway. Specifically, PhaJ (*Aeromonas caviae*) catalyzed the conversion of tiglic acid to 3H2MB, but was unable to work on longer chain  $\alpha$ -substituted 3HAs or 3HAs with  $\beta$ -branching. Natively, PhaJ catalyzes the stereospecific conversion of C4-C6 enoyl-CoAs - with highest affinity for crotonyl-CoA.<sup>102</sup> To expand the product range of our pathway to produce 3H2MV, we investigated mutating PhaJ for increased promiscuity. According to Tsuge et al., PhaJ's acyl-CoA binding site is surrounded by the side chains of

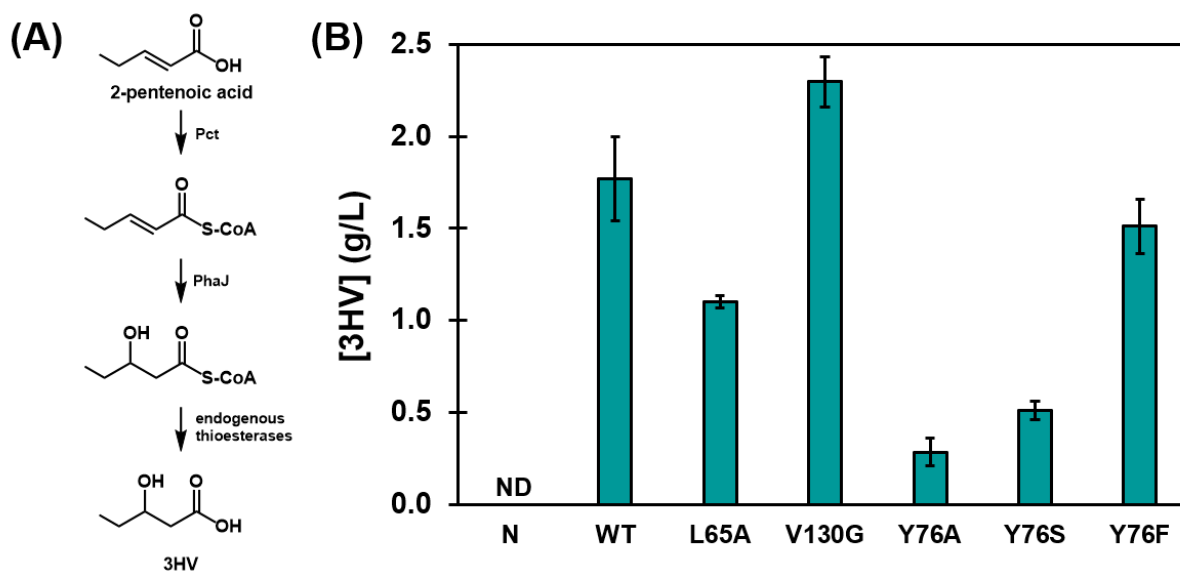
S62, L65, P70, Y76, and V130. Further, they identified L65A and V130G PhaJ mutants as having increased activity on longer substrates. Applying these findings to our study, we chose to test five PhaJ mutants (L65A, V130G, Y76A, Y76S, Y76F) in the truncated module 2 pathway to identify a mutant capable of acting in the production of 3H2MV. Tsuge et al. did not test Y76 mutants, but manual inspection of acyl-CoA's docked in PhaJ's binding site showed that this residue's bulkiness may prevent PhaJ from accepting larger substrates.

We tested the ability of strains carrying PhaJ mutants of the truncated module 2 pathway to convert various enoic acids to their corresponding 3HAs.<sup>G</sup> All mutants retained the native ability to convert crotonate to 3HB with nearly 100% substrate conversion (Figure 3.18). We next tested the ability of sKB051-sKB055 to convert 2-pentenoic acid to 3-hydroxyvaleric acid (3HV). 3HV is the straight chain analogue of 3H2MV. Comparing 3HV and 3H2MV production from the truncated module 2 pathway could provide valuable insight into how PhaJ mutants separately facilitate the production of longer or wider 3HAs. Interestingly, the L65A and Y76 mutants exhibited decreased 3HV titers compared to wild type (Figure 3.19). 3HV titer in Y76 mutants decreased in order of side-chain size. This suggests that the bulkiness of this residue is important for catalyzing the hydration of larger substrates. The V130G mutant produced  $\approx 30\%$  more 3HV than WT suggesting that replacing valine with the smaller residue glycine at this position allows PhaJ to accept longer substrates.



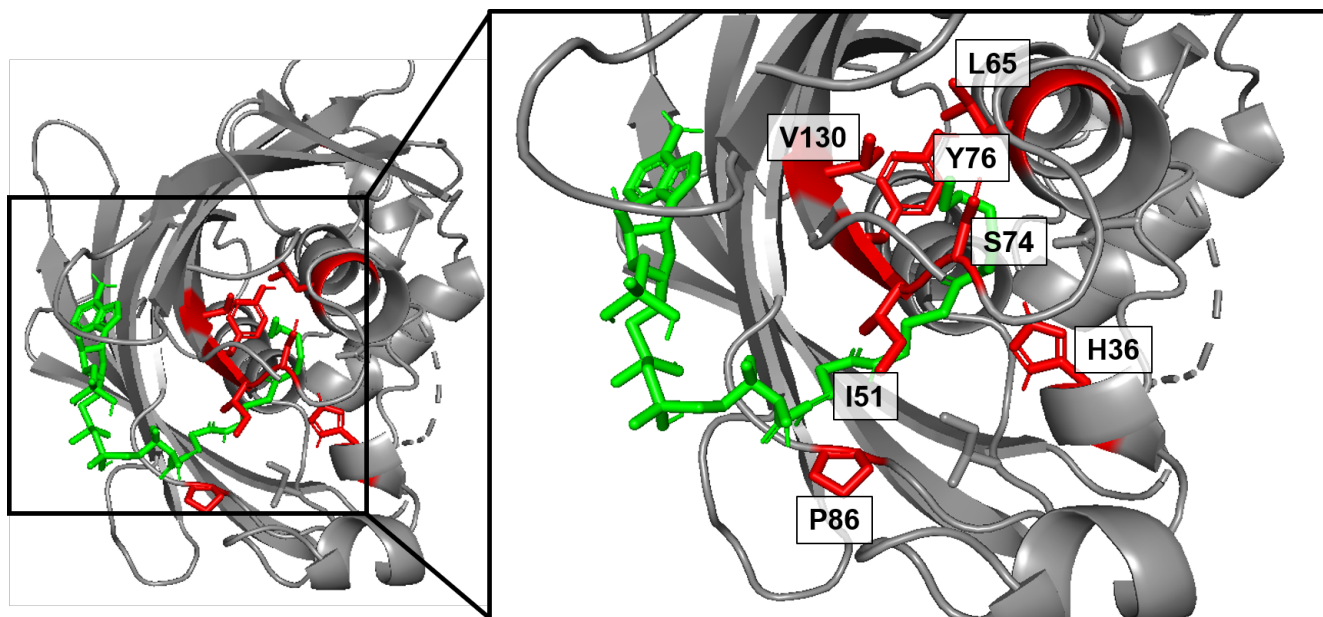
**Figure 3.18.** Examining enoyl-CoA hydratase mutant activity on crotonate. (A) Conversion of crotonate to 3HB by truncated module 2 (B) sKB051-sKB055 were grown according to culture condition c with 2 mM crotonate supplemented every 24 hr. Abbreviations used: N = empty vector negative control, WT = wild type

<sup>G</sup>All experiments in this subsection were conducted by Kelcey Allen.

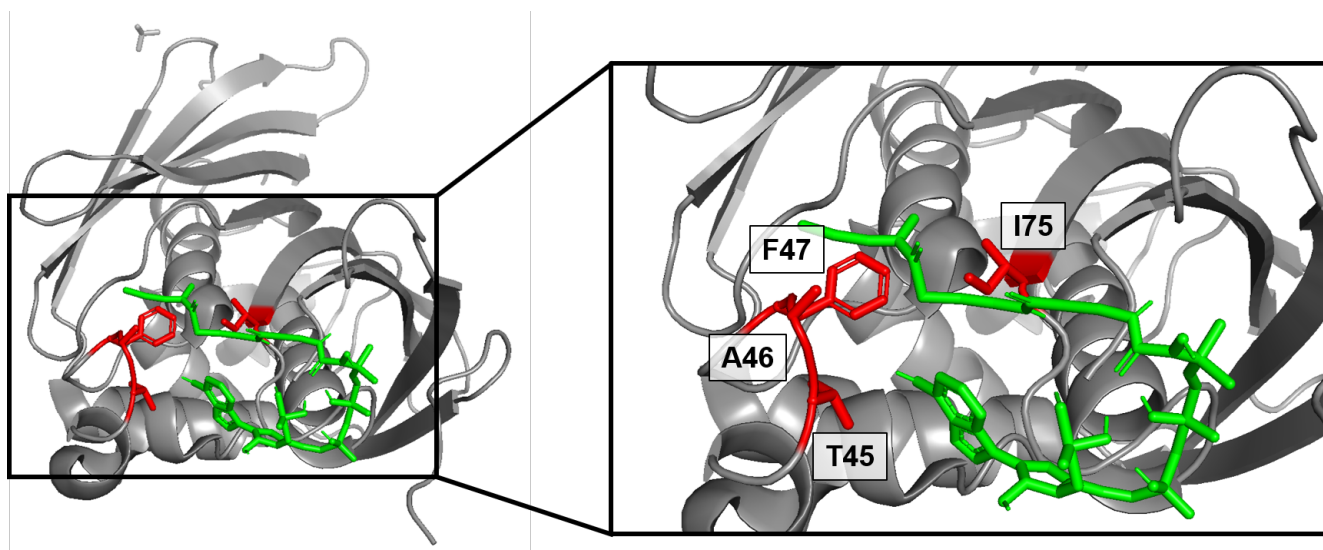


**Figure 3.19.** Examining enoyl-CoA hydratase mutant activity on 2-pentenoic acid. (A) Conversion of 2-pentenoic acid to 3HV by truncated module 2 (B) sKB051-sKB056 were grown according to culture condition c with 2 mM 2-pentenoic acid supplemented every 24 hr. Abbreviations used: N = empty vector negative control, WT = wild type

When fed 2-methyl-2-pentenoic acid, no 3H2MV production was observed from any mutants. To identify additional mutants to broaden PhaJ's substrate specificity, AutoDock Vina<sup>99</sup> was used to generate a substrate docking model of wild type PhaJ with 2-methyl-2-pentenyl-CoA. As a first step in validating the docking procedure, octenyl-CoA was docked with PhaJ. The docking model for PhaJ with octenyl-CoA agreed with the one reported by Tsuge et al.<sup>120,121</sup> - identifying L65, V130, Y76, and S74 as interacting with octenyl-CoA (Figure 3.20). 2-methyl-2-pentenyl-CoA was next docked with PhaJ to identify residues which might confer activity on this longer, wider substrate. One docking model for this substrate indicated that the alkyl chain of 2-methyl-2-pentenyl-CoA interacts with I75, F47, A46, and T45 (Figure 3.21). Future studies would focus on testing these mutants in the context of the truncated module 2 pathway to determine their ability to catalyze the production of other 3HAs.



**Figure 3.20.** Docking octenoyl-CoA into the active site of PhaJ. PhaJ is shown as ribbons in grey. Octenoyl-CoA is shown in green. Residues that interact with octenoyl-CoA are shown in red.



**Figure 3.21.** Docking 2-methyl-2-pentenoyl-CoA into the active site of PhaJ. PhaJ is shown as ribbons in grey. 2-methyl-2-pentenoyl-CoA is shown in green. Residues that interact with 2-methyl-2-pentenoyl-CoA are shown in red.

## 3.4 Conclusions

In conclusion, this work demonstrates the production of 3HIB and (2S,3R)-3H2MB - biopolymer building block molecules - from glucose in *E. coli*. This pathway consists of two modules: module 1 which specifically converts glucose to IBA or 2MB and (2) module 2 which oxidizes these branched acids via steps inspired by BCAA degradation to 3HIB and 3H2MB, respectively. We show in module 1 that the choice of ALS is the key determinant driving branched acid specificity. In module 2, we showed that choice of dehydrogenation enzymes is key to the pathway's efficacy. Additionally, we identified a branched-chain permissive (R)-enoyl-CoA hydratase that produces biodegradation-compatible stereochemistry in the final product. As proof-of-concept, this pathway was optimized for 3H2MB production by deleting competing pathways, balancing flux between modules, and preliminary investigation of a novel by-product recycle. Thiolase-independent pathways like the ones presented in this study are promising alternatives to the rBOX pathway for the production of biopolymer building blocks that lead to plastics with improved properties.

## Chapter 4

# Design and feasibility analysis of pathways to 3-methyl-1,5-pentanediol

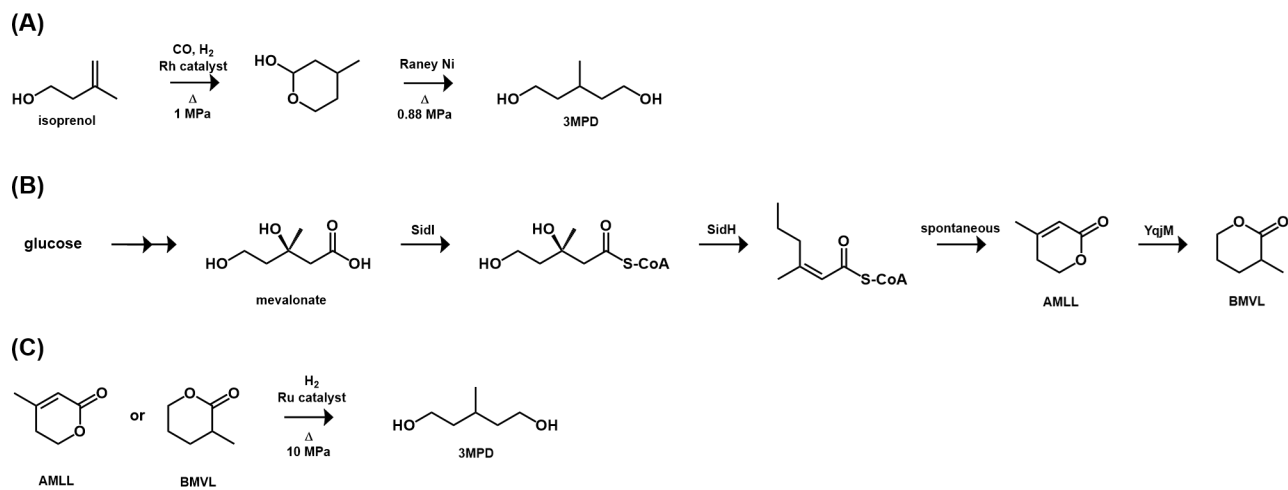
### Abstract

3-methyl-1,5-pentanediol (3MPD) is an attractive monomer for the production of biodegradable copolyesters. There are well-established chemical routes to this compound, but they rely on petroleum-derived feedstocks, require elevated temperatures and pressures, and produce several byproducts. In this chapter, we design three biological routes to 3MPD via manual *de novo* design and prioritize one route based on pathway length, co-factor utilization, and perceived enzyme availability. The prioritized route is based on a previously designed route to 3-methylpentanol (3MP) where a mutant 2-isopropylmalate synthase allows for the production of 2-keto-4-methylhexanoate from a leucine precursor. We extend this pathway to 3MPD via a single hydroxylation step catalyzed by AlkBGT (*Pseudomonas putida* GPo1). Feasibility analysis of this pathway focused on determining the ability of AlkBGT to hydroxylate 3MP. Initial experiments showed that overexpressing *AlkBGT* caused a growth defect. Optimizing the *alkBGT* plasmid or media composition restored growth. However, no 3MPD production was observed. We next probed substrate transport into the cell as a cause of pathway inefficacy using permeabilized cells and alternative transporters. However, no 3MP to 3MPD conversion was observed in any of the tested systems. These data suggest that AlkBGT cannot act in the conversion of 3MP to 3MPD. Future work should probe other hydroxylation enzymes at this step with the ultimate goal of developing a biological route from glucose to 3MPD.

## 4.1 Introduction

Copolyesters formed from the condensation of diols and diacids have application in various fields. Bacteria have been leveraged for the production of both classes of biopolymer building block molecules. Polybutylene adipate terephthalate (PBAT) is the most popular bioderived copolyester by production capacity. In recent years, PBAT garnered immense attention because it exhibits material properties comparable to PET, with improved biodegradability.<sup>122</sup> However, PBAT exhibits reduced biodegradability compared to other biopolymers like PHAs. This opens the door for the exploration of other diol-diacid copolyesters with improved degradation properties. 3-methyl-1,5-pentanediol (3MPD) is a promising copolyester building block. In internal experiments, our industrial sponsor showed that certain copolyesters containing 3MPD exhibit tunable biodegradation (data not shown). Thus, we pursued the design and feasibility analysis of pathways to this novel biopolymer building block.

3MPD is conventionally synthesized in a two-step process where (1) isoprenol is hydroformylated to 2-hydroxy-4-methyltetrahydropyran with a rhodium catalyst followed by (2) hydrogenation in the presence of a Raney nickel catalyst (Figure 4.1a).<sup>123</sup> This process begins with a petroleum-derived feedstock (isoprenol), requires elevated temperature and pressure, and produces several byproducts. Xiong et al. reported the production of  $\beta$ -methyl- $\delta$ -valerolactone (BMVL) - a compound structurally related to 3MPD - from glucose in *E. coli*. Their route begins with the production of mevalonate followed by its dehydrogenation to anhydromevalonolactone (AMLL) via steps from siderophore biosynthesis. AMLL is then reduced to BMVL by YqjM - a mutant enoate-reductase from *Bacillus subtilis* (Figure 4.1b).<sup>124</sup> BMVL is structurally very similar to 3MPD and Xiong et al.'s progress lays the groundwork for developing biological pathways to C5,  $\beta$ -branched compounds like 3MPD. However, their pathway produced 270 mg/L BMVL with the accumulation of more than 10 g/L mevalonate pointing to the need for additional pathway engineering. Spanjers et al. connect BMVL to 3MPD production through a chemical route where bio-derived mevalonate is sequentially hydrogenated to AMLL or BMVL and then to 3MPD (Figure 4.1c). They showed the production of 3MPD from both lactones with selectivities as high as 89%. However, their method still employed high temperatures and pressures.<sup>125</sup> Combined, these works highlight the need for a complete biological route from a renewable feedstock to 3MPD.



**Figure 4.1.** Previously developed routes to 3-methyl-1,5-pentanediol. Abbreviations used: SidI (acyl-CoA ligase from *Aspergillus fumigatus*), SidH (enoyl-CoA reductase from *A. fumigatus*)



## 4.2 Materials and Methods

### 4.2.1 Strain construction

*E. coli* DH5 $\alpha$  was used for cloning and plasmid propagation. *E. coli* MG1655 (DE3)  $\Delta endA\Delta fadD$  was used at the background strain for all production experiments. A gene block for *alkL* (*Pseudomonas putida* GPo1) was ordered from Integrated DNA technologies. Additionally, the pET29b(alkBGT) plasmid was custom synthesized by Twist Biosciences. Sequences for these genes can be found in Table 4.1. All other genes were amplified from genomic DNA. Plasmid construction details can be found in Tables 4.2 - 4.3. Individual genes and synthetic operons were expressed using compatible duet vectors or pET vectors under the control of T7lac promoters (Table 3.3) and synthetic ribosome binding sites. Synthetic ribosome binding sites were created using the Salis Lab RBS Calculator with a target translation initiation rate of 10,000.<sup>96</sup> Genes were amplified from their corresponding templates using custom oligonucleotides (Millipore Sigma) and Q5 DNA polymerase (NEB) or KOD HotStart Polymerase (EMD Millipore). Genes were inserted into the MCSs of plasmids via Gibson Assembly with the NEBuilder HiFi DNA Assembly Kit (NEB). Specific details for the construction of each plasmid can be found in Table 4.2.

**Table 4.1.** Gene block sequences for 3MPD production

Gene Name	Sequence
<i>alkB</i>	ATGTTAGAGAAGCATCGTGTTCTGGACTCTGCGCCTGAGTATGTGATAAGAAAAAGTACCTTTG GATCTTATCCACCTTGTGGCCGGCCACTCCGATGATCGGAATTTGGCTTGCTAATGAACTGGCT GGGTATCTTTATGGCCTGGTTTTATTAGTCTGGTATGGAGCATTGCCGTTATTAGATGCCATG TTTGGAGAAGACTTCAACAATCCGCCGGAAGAAGTTGTACCCAACTTAAAAAGGAACGCTATTA CCGTGTATTAACGTACTTAACAGTCCCAATGCACTACGCCGCTCTATTGTTTCTGCCTGGTGGG TTGGTACACAACCAATGAGCTGGTTGGAGATTGGCGCCCTTGCCCTGTGCGTTGGAATTGTCAAT GGACTTGCCTTGAACACCGGCCATGAATTGGGGCATAAGAAAGAACTTTTCGACCGTTGGATGGC AAAAATCGTCTGGCCGTAGTGGGTACGGGCACCTTTTTCATCGAGCACAAAGGGACATCATC GTGATGTAGCGACCCCGATGGACCCAGCCACATCTCGTATGGGTGAGTCAATCTATAAATTCTCC ATCCGTGAAATCCCAGGGGCTTTTTATCCGCGCTTGGGGTTTAGAAGAGCAGCGTCTTAGCCGCCG TGGGCAATCCGTGTGGTCATTTGATAACGAAATCCTTCAGCCGATGATTATCACTGTAATCTTGT ACGCTGTCTTACTTGCCTTATTTGGACCTAAAATGTTAGTCTTTTTGCCTATTCAAATGGCATT GGGTGGTGGCAGCTGACCAGCGCAACTATATTGAGCATTATGGTTTGCCTCGCCAGAAAATGGA GGATGGCCGTTATGAGCACCAGAAACCTCATCATAGCTGGAACCTCAATCATATTGTGAGTAACC TGGTTTTATTCCATCTGCAACGTCATAGTATCATCATGCTCATCTACTCGCTCGTATCAGAGC TTACGTGACTTTCTGGACTGCCCGCACTTCCGACTGGTTACCTGGGGCGTTCTTAATGGCTAT GATCCCGCAATGGTTCGGCTCTGTAATGGACCCAAAGTAGTCGACTGGGCTGGCGGTGACCTTA ACAAGATTCAAATCGACGACTCGATGCGTGAGACCTATCTGAAGAAATTTGGCACCAGCTCTGCG GGACACTCGTCTCCACCTCCGAGTGGCGTCATAG
<i>alkG</i>	ttgtaaacctccctcaagcgagatcttaaATGGCGTCATACAAATGTCCTGACTGTAACCTATGTGTATGATGAA TCAGCGGGTAATGTGCATGAAGGATTCTCCCTGGAACACCATGGCACTTGATTCCCGAGGACTG GTGCTGCCCTGACTGTGCAGTACGTGACAACTGGACTTTATGTTAATCGAATCAGGGGTTGGAG AGAAGGTGTTACGTCAACTCACACAAGTCCCAATCTGTCTGAAGTTTCGGGTACATCCCTTACC GCGGAGGCTGTGGTGGCCCCACATCATTGAAAAAGTTGCCTAGCGCCGACGTGAAAGGCCAGGA CCTGTATAAACTCAGCCTCCCCGCTCCGACGCACAAGTGGGAAAGCGTATCTGAAGTGGATTT GCATCACGTGCGGACATATTTACGACGAGGCTCTTGGTGATGAGGCTGAAGGCTTACACCCGGG ACTCGCTTTGAAGATATCCCAGACGATTGGTGCTGTCCCGACTGCGGAGCAACAAAGGAGGATTA CGTCTTGTACGAAGAGAAATGA

<i>alkT</i>	tcattagattttacaacaagctagaataggagaatatATGGCCATCGTAGTCGTAGGTGCGGGGACTGCCGGGGTTA ACGCGGCTTTCTGGTTACGCCAATACGGGTATAAAGGGCGAAATCCGCATCTTTTCGCGTGAGAGT GTCGCTCCCTACCAGCGCCCACCGTTGTCTAAGGCCTTCTTAACCAGTGAGATTGCCGAGAGTGC AGTTCCCTTGAAGCCAGAGGGCTTTTATACCAATAATAACATTACTATCTCCTTAAACACTCCGA TCGTGTCTATCGATGTGGGCCGCAAAATTGTAAGCAGCAAAGACGGGAAAGAGTACGCTTATGAA AAGTTGATCCTTGCGACCCCCGGCGAGCGCACGTGCGCTTACATGTGAAGGCTCTGAACTGAGCGG AGTATGTTATTTGCGTAGTATGGAGGATGCAAAGAACTTACGCCGTAACCTGGTGGAACTGTCCT CGGTGGTCTGTTCTGGGCGGGCGGTGTAATCGGCTTAGAGGTAGCCAGTCCCGCCGTGGGTTAGGC AAACGTGTAAACGGTAATCGAGGCAACCCCCGCGTTATGGCCCGTGTGGTCACTCCTGCCGCAGC TAATTTGGTCCGCGCGCTCTTGAGGCCGAAGGGATTGAGTTTAAAGTTGAACGCGAAGCTGACTT CGATTAAGGGCCGCAATGGCCACGTGGAACAGTGCCTTTTGAATCCGGAGAGGAGATCCAAGCC GATTTAATCGTCTGTCGATCGGTGCGATCCCTGAATTGGAGCTGGCGACAGAAGCAGCATTAGA GGTATCTAACGGTGTCTGTCGATGACCAAATGTGCACTTCGGATACTTCGATCTACGCAATTG GTGACTGCGCGATGGCTCGCAATCCATTTTGGGGCACTATGGTACGCCTGGAGACGATCCACAAT GCGGTAACACACGCTCAAATTGTAGCTTCTTCTATCTGTGGAACCTCGACCCCCGCGCCTACCC GCCGCTTTTTGGTCTGATTTAAAGGGAAATGGCGTTACAAGTTTAGGTGCTCTTAAAGACTATG ATAAAGTGGTAGTGGCGATCAATAATGAGACTCTTGAACCTGAAGTCTTAGCTTATAAGCAAGAA CGTTTAAATTGCTACTGAAACTATCAACCTTCCGAAGCGCCAGGGCGCATTGGCGGGTTCAATTA ATTGCCTGACTAG
<i>alkL</i>	ATCTTAGTATATTAGTTAAGTATAAGAAGGAGATATACATATGTCGTTTCAGTAACTATAAAGTCA TCGCAATGCCGATTAGTTGCTAACTTTGTTCTGGGGGCCGCGACAGCCTGGGCGAACGAAAAC TACCCCGCAAGTCGGCAGGTTATAATCAGGGAGATTGGGTTGCGTCTTTTAAATTTTTCAAAGT TTACGTGGAGAAGAAGTGGTACCTGAACGTCCGAGGGGGGGCCTTACCCAAATGCAGATGTTT CGATCGGAAACGACACAACGCTGACGTTTCGACATCGCCTACTTCGTAAGCTCAAACATCGCTGTA GATTTCTTTGTTGGCGTCCCCGACGCGCTAAATTCGAAGGCGAGAAGTGCATCTCCAGTCTTGG CCGTGTGTGAGAGGTCGATTACGGTCCGGCCATTTTATCGCTGCAATACCACTACGATAGTTTCG AGCGCTTGATCCATATGTTGGCGTCCGAGTTGGCCGCGTATTATTCTTTGACAAAACAGACGGA GCTTTGTGCTTTTCGACATCAAAGATAAATGGGCCCCCGCATTCCAAGTGGGTTTGGCTACGA CCTGGGCAACTCGTGGATGTTAAACTCCGACGTGCGCTACATCCCGTTCAAACGGATGTTACTG GCACCTTGGGGCCAGTGCCAGTCAGCACGAAAATCGAAGTGCATCCATTATTCTGTCCCTGGGT GCCTCATACGTGTTCTAATTAATTAACCTAGGCTGCTGCCACCGCTGAGCAATAACTAGCATAAC CCC

## 4.2.2 Production experiments

All production strains used in this chapter are described in Table 4.3. Overnight cultures were grown in LB Broth at 37 °C, 250 rpm, with supplementation of the appropriate antibiotic(s) (kanamycin 50 µg/mL, carbenicillin 100 µg/mL, streptomycin 50 µg/mL, or chloramphenicol 34 µg/mL). For production experiments, overnight cultures were spun down at 4500 rpm for 5 min and resuspended in 1X M9 salts (Millipore Sigma). Concentrated overnights were used to inoculate M9Y media or modified MOPS media to an OD<sub>600</sub> = 0.1. The modified MOPS media was described by Clomburg et al.<sup>41</sup> and includes: 125 mM MOPS, 20 g/L glycerol, 10 g/L tryptone, 5 g/L yeast extract, 100 µM FeSO<sub>4</sub>, 5 mM calcium pantothenate, 1.48 mM Na<sub>2</sub>HPO<sub>4</sub>, 5mM (NH<sub>4</sub>)<sub>2</sub>SO<sub>4</sub>, and 30 mM NH<sub>4</sub>Cl. These cultures were grown as 50 mL cultures in 250 mL baffled shake flasks. In early exponential phase, (OD<sub>600</sub> 0.6 - 0.9) cultures were induced with 0.25 mM IPTG and pathway carbon source was added if necessary. Samples were taken at ≈ 72 hr for growth and metabolite analysis via UV-VIS spectroscopy at 600 nm, HPLC, and gas chromatography-mass spectroscopy (GC-MS).

### 4.2.3 Permeabilized cell studies

The protocol for conducting 3MP consumption studies in permeabilized cells was modified from Schrewe et al.<sup>126</sup> 5 mL overnight cultures in LB broth were used to inoculate 50 mL cultures in modified MOPS media to  $OD_{600} = 0.1$ . These cultures were allowed to grow for 4 hr at 30 °C, 250 rpm, then induced with 0.25 mM IPTG. Cultures grew for 4 additional hours, then cells were harvested via centrifugation at 4500 rpm for 10 min. Concentrated cells were resuspended in 3 mL 50 mM phosphate buffer containing 0.25% (v/v) Triton X-100 and/or 2.5 mM EDTA to an  $OD_{600} = 0.9$ . Potassium phosphate buffer contains 34.7 mM  $K_2HPO_4$  and 15.2 mM  $KH_2PO_4$ . These cultures were incubated for 30 min at 30 °C and 250 rpm. 5 mM of 3MP and 10 g/L glucose was added to each culture to start the reaction which was allowed to proceed for 4 hr. Supernatant from these experiments was isolated for analysis via HPLC.

### 4.2.4 Fatty acid methyl ester derivitization

The fatty acid methyl ester (FAME) derivitization protocol was modified from Bonk and Tarasova et al.<sup>19</sup> 1 mL of experimental samples were spun down at 4500 rpm for 5 min to isolate supernatant. 1 mL of supernatant was mixed with 1.5 mL chloroform, 10  $\mu$ L of 0.5 M hexanoic acid as internal standard, and 1.5 mL 15% acidic methanol (methanol + 15% (v/v)  $H_2SO_4$ ) in a glass tube with threads wrapped with polytetrafluoroethylene tape. The glass vials were heated at 100 °C for 4 hr. The organic layer was removed and dried over anhydrous  $MgSO_4$ .

### 4.2.5 Metabolite detection

3MP and 3MPD were detected using an Agilent 1200 series HPLC (Agilent) equipped with an RID and an Aminex HPX-87H column (Bio-Rad Laboratories) with 5 mM sulfuric acid mobile phase. Column temperature, RID temperature, and flow rate were set to 65 °C, 35 °C, and 0.6 mL/min, respectively. FAMES were quantified using a gas chromatography system (Agilent 7890B) equipped with an Rxi-5Sil MS Column (Restek, 30 m, 0.25 mm ID, 0.25  $\mu$ m). The inlet and flame ionization detector (FID) were both set to 250 °C with a 10:1 split ratio. The temperature program for the GC oven was 50 °C hold for 5 min, ramp at 10 °C/min to 120 °C hold for 5 min, ramp at 15 °C to 220 °C hold for 10 min, ramp at 20 °C to 250 °C hold for 5 min. Standards for octanoic acid, hexanoic acid, and 8-hydroxyoctanoic acid were purchased from Millipore Sigma. A standard curve was generated by FAME derivitizing these standards.

**Table 4.2.** 3MPD plasmid construct descriptions

Name	Description	Primers
pCDF(-)(fadL)	<i>fadL</i> ( <i>E. coli</i> ) cloned into MSC 2	fadL_f_335: AGATATACATATGAGCCAGAA AACCTGTTTAC; fadL_r_336: CCTAGGTTA ATTAATCAGAACGCGTAGTTAAAGTTAGTAC; bb_f_344: TTAATTAACCTAGGCTGCTGC; bb_r_350: CTGGCTcatATGTATATCTCCTT CTTATACTTAACTAATATAC
pCDF(-)(alkL)	codon optimized <i>alkL</i> ( <i>Pseudomonas putida</i> ) GPo1 cloned into MSC 2	bb_f_528: TTCTAATTAATTAACCTAGGCTGCTGC; bb_r_527: CGACATATGTATATCTCCTTCTTATACTTAACTAATATACTAAG
pET29b(alkBGT) with T7lac promoter	codon optimized <i>alkBGT</i> with <i>alkB</i> and <i>alkG</i> separated by the synthetic RBS: ttgtaaacctccctc aagcgagatcttaa. <i>alkG</i> and <i>alkT</i> separated by the synthetic RBS: tcattagattttacaacaagctagaatag gagaatat	synthesized by Twist Biosciences
pET29b(alkBGT)_LacUV5	pET29b(alkBGT) with the T7lac promoter replaced by the LacUV5 promoter	bb_f_408: GGCTCGTATAATGgtgGGAATTGTGAGCGGATAAC; bb_r_409: GGAAGCATAAAGTGAAAATTTCCGCGGATCGAG
pET29b(alkBGT)_Trc	pET29b(alkBGT) with the T7lac promoter replaced by the Trc promoter	bb_r_406: GATGATTAATTGTCAAATTTCCGCGGATCGAGATC; bb_f_407: CGGCTCGTATAATgtgGGAATTGTGAGCGGATAAC
pET29b(alkBGT)_SC101 origin of replication	pET29b(alkBGT) with the ColE1 ORI replaced by the SC101 ORI from pSC101	sc101_r_004: AGGCCATTTATCGCCGGCATTACAGATCCTTCCGTATTTAGCCAG; sc101_f_003: TAGAAAAGATCAAAGGATCTTCGACAGTAAGACGGGTAAGCCTGbb_r_002: AGGCTTACCCGTCTTACTGTGGAAGATCCTTTGATCTTTTCTACG; bb_f_001: TGGCTAAATACGGAAGGATCTGAATGCCGGCGATAATGG
pET29b(alkBGT)_LacUV5_SC101	pET29b(alkBGT) with LacUV5 promoter and SC101 ORI	As previously described

**Table 4.3.** List of 3MPD production strains

Strain Name	Plasmid 1	Plasmid 2	Background
sKB033	pCDF(-)(fadL)	-	749
sKB034	pCDF(-)(fadL)	pET29b(alkBGT) with T7lac promoter	749
sKB035	pCDF(-)(fadL)	pET29b(alkBGT) with LacUV5 promoter	749
sKB036	pCDF(-)(fadL)	pET29b(alkBGT) with Trc promoter	749
sKB037	pCDF(-)(fadL)	pET29b(alkBGT) with SC101 origin of replication	749
sKB065	pCDF(-)(fadL)	pET29b(alkBGT) with SC101 origin of replication and LacUV5 promoter	749
sKB066	pET29b(alkBGT)	-	749
sKB067	pET(alkBGT) <sup>A</sup>	-	749

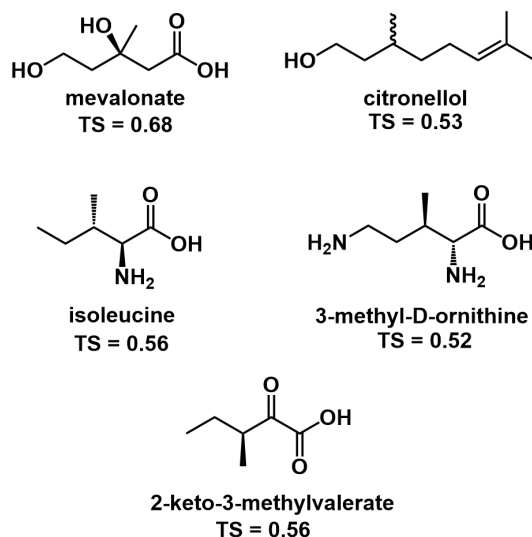
<sup>A</sup>This vector was obtained from Ramon Gonzalez's lab and is described in Clomburg et al.<sup>41</sup>

sKB068	pCDF(-)(alkL)	pET29b(alkBGT)	749
sKB073	pCDF(-)(fadL)	pET(alkBGT)	749
sKB074	pCDF(-)(alkL)	pET(alkBGT)	749

## 4.3 Results and Discussion

### 4.3.1 Designing biological pathways to 3-methyl-1,5-pentanediol

There are few examples of C5 and/or  $\beta$ -branched compounds in the microbial metabolome, so pathway design efforts for 3MPD were *de novo*. Initial efforts focused on using the retro-biosynthetic tool RetroPath 2.0<sup>70</sup> to devise a pathway to 3MPD. RetroPath 2.0 failed to yield any feasible pathways for 3MPD, so manual *de novo* design was pursued. First, KEGG SimComp<sup>127</sup> was used to identify the 30 most structurally similar compounds to 3MPD compounds from the microbial metabolome. From this initial list of 30 compounds, compounds without a main carbon backbone length of five or  $\beta$ -branching were removed from consideration based on the difficulty of conferring this chemistry enzymatically. This analysis yielded five compounds to pursue pathway design with: mevalonate, isoleucine, 2-keto-3-methylvalerate, citronellol, and 3-methyl-D-ornithine. We further reduced this list to mevalonate and 2-keto-3-methylvalerate (Figure 4.2). Isoleucine was removed from this list, since 2-keto-3-methylvalerate is an upstream metabolite that directly leads to isoleucine formation. Mevalonate is a central metabolite for isoprenoid biosynthesis in eukaryotes and its overproduction in chassis organisms has been engineered by others.<sup>128,129</sup>



**Figure 4.2.** Compounds structurally similar to 3-methyl-1,3-pentanediol in the microbial metabolome. Abbreviations used: TS = Tanimoto similarity score

To design a pathway from 2-keto-3-methylvalerate, we surveyed the literature to identify novel pathways branching from this compound.<sup>130</sup> Specifically, well-established biological routes exist that connect 2-ketoacids to alcohols that involve decarboxylation of the 2-ketoacid to an aldehyde, followed by further

reduction to an alcohol. This route was exploited by Zhang et al.<sup>131</sup> for the production of 3MP - a compound only one hydroxyl group dissimilar to 3MPD. Their route involves overexpressing isoleucine biosynthesis genes for the production of 2-keto-3-methylvalerate. They engineer a mutant LeuA\* (2-isopropylmalate synthase with G462D from *E. coli*) capable of extending 2-keto-3-methylvalerate to 2-keto-4-methylhexanoate (2K4MH). 2K4MH is next decarboxylated by a mutant decarboxylase (KivD with V461A/F381L from *Zygomonas mobilis*) and reduced by Adh6 (alcohol dehydrogenase from *Saccharomyces cerevisiae*) to produce 3MP. Two routes to 3MPD are envisaged using the Zhang et al. pathway as a starting point (Figure 4.3). The first route involves the hydroxylation of 3MP to 3MPD.<sup>132</sup> Another route involves decarboxylation of 2K4MH to 3-methylvaleric acid. 3-methylvaleric acid is then hydroxylated to 5-hydroxy-3-methylvaleric acid. Finally, 5-hydroxy-3-methylvaleric acid is reduced to 3MPD.

In a similar vein, a third pathway was designed from mevalonate (Figure 4.4). Xiong et al.<sup>124</sup> described the conversion of glucose to anhydromevalonyl-CoA which can be used as a starting point for a mevalonate-based pathway to 3MPD. The pathway to 3MPD from mevalonate begins with enzymatic steps from fungal siderophore biosynthesis that convert mevalonate to anhydromevalonyl-CoA. This intermediate is then reduced to 3MPD via three additional *de novo* steps: (1) the reduction of anhydromevalonyl-CoA by a cis-enoyl-CoA reductase, (2) the conversion of this hydroxy acyl-CoA to a hydroxy aldehyde by an aldehyde dehydrogenase, and (3) the reduction of this hydroxy aldehyde to 3MPD (Figure 4.4).

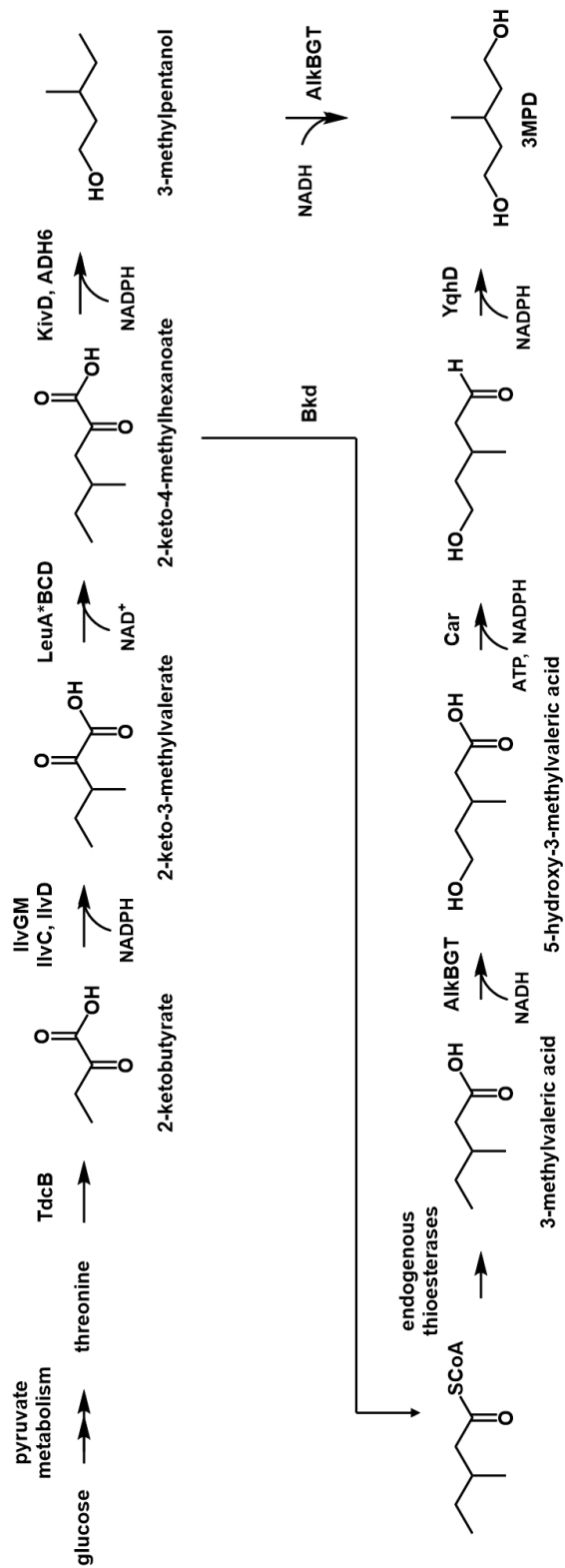
These three pathways for 3MPD production from glucose were prioritized for implementation based on enzyme availability, pathway length, and cofactor usage (Table 4.4). Pathway length refers to the number of successive pathway steps that have not been demonstrated *in vivo*. For example, the mevalonate based pathway has a pathway length of three since the steps up to anhydromevalonyl-CoA have been demonstrated by others.<sup>124</sup> Cataloging cofactor usage starts from the first heterologous step to *E. coli*. For the mevalonate pathway, cofactor cataloging begins after the production of acetoacetyl-CoA. Comparing pathway length and cofactor usage among the designed pathway, the 3MP pathway stands out based on its short length and low cofactor requirement. The 2K4MH and 3MP pathway both rely on a hydroxylase for the hydroxylation of an acid and alcohol respectively.  $\omega$ -Hydroxylation can be achieved via alkane monooxygenases like AlkB from *Pseudomonas putida* GPo1 or cytochromes P450. However, few examples exist for the hydroxylation of branched substrates like those that appear in the 2K4MH and 3MP pathways. Identifying an enzyme capable of carrying out these reaction steps would be integral to determining the feasibility of these pathways. There are well-characterized enzymes to catalyze all steps in the mevalonate pathway except for the

two steps converting anhydromevalonyl-CoA to a hydroxy aldehyde. Bld<sup>L273T</sup> has been used the conversion of C5 hydroxy acyl-CoAs to hydroxy aldehydes and could be leveraged in our pathway.<sup>35</sup> However, no enoyl-CoA reductases acting on cis-enoyl-CoAs have been described. The most well described enoyl-CoA reductase is the trans-enoyl-CoA reductase - Ter from *Treponema denticola*.<sup>133</sup> However, this enzyme cannot be used in our proposed pathway based on its strict specificity for the trans isomer. Based on its short length, low cofactor requirement, and perceived hydroxylase availability, the 3MP pathway was chosen for implementation.

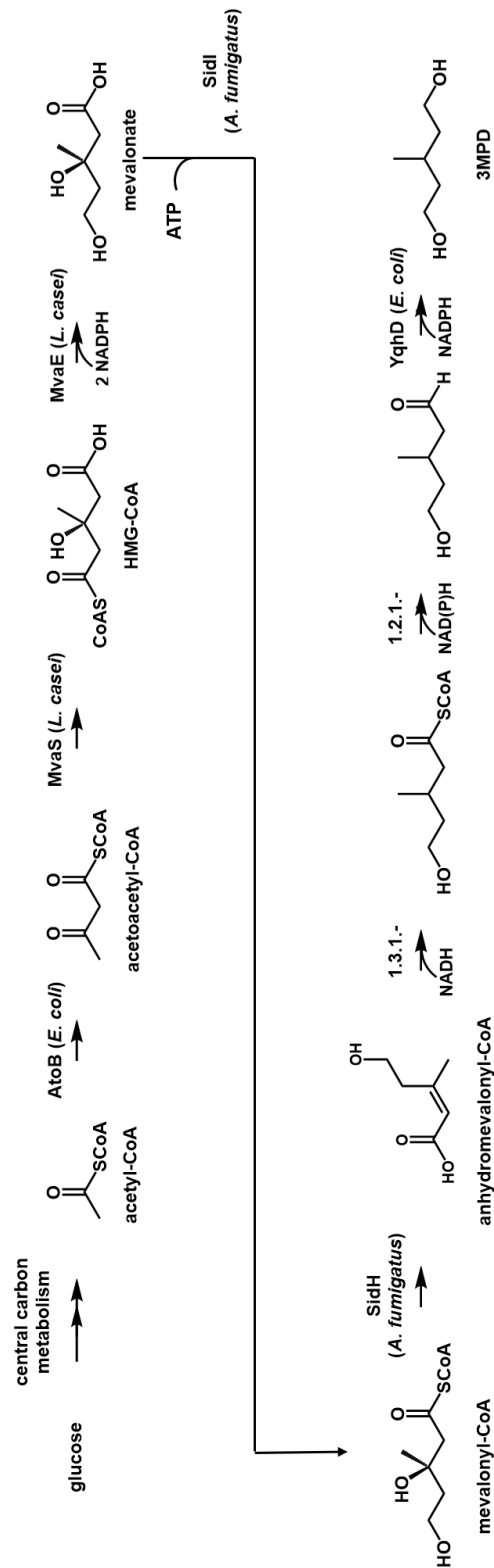
**Table 4.4.** Comparison of the 3-methyl-1,5-pentanediol pathways

Pathway	Pathway Length	NADPH	NADH	ATP	Enzyme Availability
2K4MH	5	2	-	1	hydroxylase
3MP	1	1	1	-	hydroxylase
mevalonate	3	2	3	1	cis-enoyl-CoA reductase





**Figure 4.3.** Proposed metabolic pathway from 2-keto-4-methylhexanoate to 3-methyl-1,5-pentanediol. Abbreviations used: TdcB (threonine dehydratase from *E. coli*); LeuB (3-isopropylmalate dehydrogenase from *E. coli*), LeuCD (3-isopropylmalate dehydratase from *E. coli*), Car (carboxylate reductase from *Nocardia iowensis*)

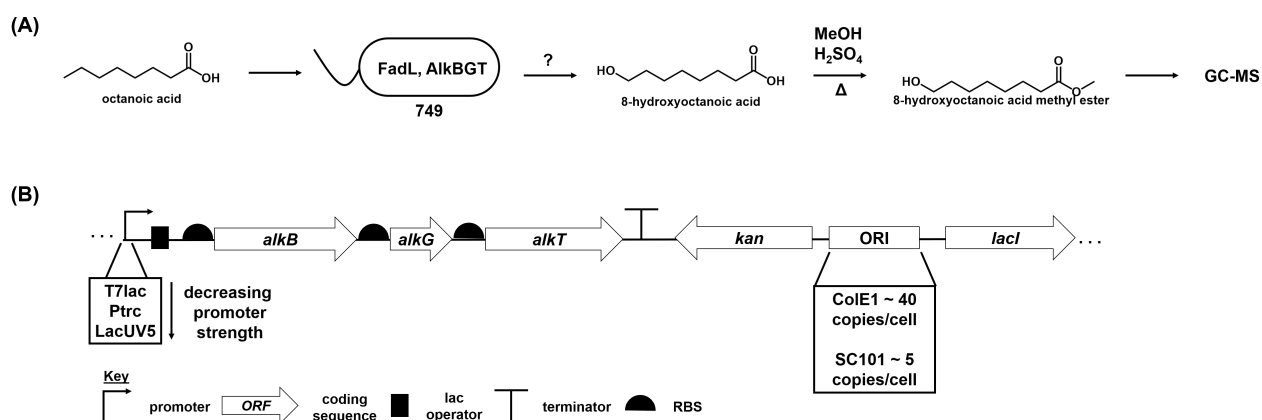


**Figure 4.4.** Proposed metabolic pathway from mevalonate to 3-methyl-1,5-pentanediol. Abbreviations used: MvaE (HMG-CoA reductase from *Lactococcus casei*), MvaS (HMG-CoA synthase from *Lactococcus casei*)

### 4.3.2 Determining the feasibility of the 3-methylpentanol-mediated pathway to 3-methyl-1,5-pentanediol

The 3MP pathway to 3MPD stands out for its short length and low cofactor requirement. The step without prior validation in this pathway is the hydroxylation of 3MP to 3MPD. Two classes of enzymes are known to carry out  $\omega$ -hydroxylation: CYP153As and alkane monooxygenases. CYP153As are cytochromes P450 that primarily hydroxylate long chain fatty acids. The most well-studied member of the alkane monooxygenases family is AlkB - a non-heme iron integral membrane protein that utilizes AlkG (rubredoxin) and AlkT (rubredoxin reductase) to insert oxygen derived from molecular oxygen onto the terminal end of various carbon substrates. AlkB from *Pseudomonas putida* GPO1 is well-studied and has been shown to work on alkanes, alcohols, FAMES, and fatty acids. Of note is its ability to convert 3-methylpentane to 3-methylpentanol.<sup>47</sup> Based on this, we investigated the ability of AlkBGT to hydroxylate 3MP to determine the feasibility of our 3MPD pathway.

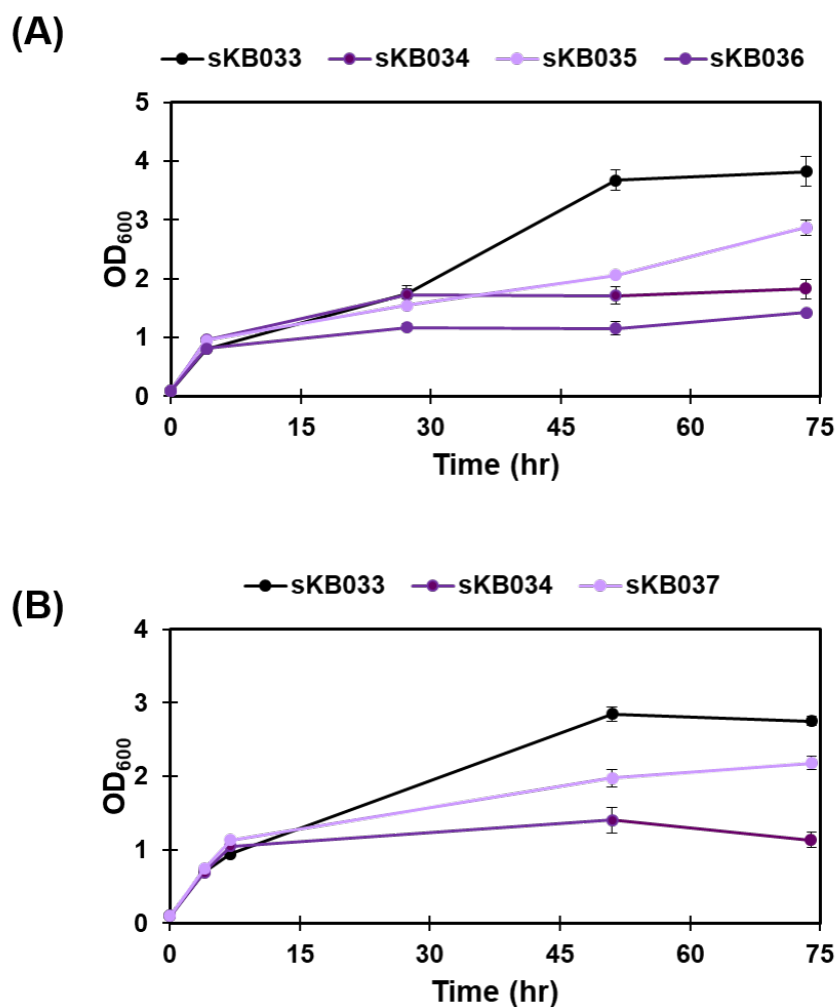
As a first step in validating the 3MP pathway for 3MPD production, we looked to confirm the activity of AlkBGT on the known substrate - octanoic acid - in *E. coli* (Figure 4.5). Production experiments were carried out in cells overexpressing the gene encoding a fatty acid transporter (*fadL*) and *alkBGT* fed octanoic acid. No octanoic acid consumption was observed. AlkBGT inefficacy on octanoic acid was also accompanied by a large growth defect (Figure 4.6a).



**Figure 4.5.** Assay design for determining the efficacy of AlkBGT for 3-methyl-1,5-pentanediol production. (A) Work flow for studying the conversion of octanoic acid to 8-hydroxyoctanoic acid by cells with AlkBGT (B) Plasmid design for *alkBGT* expression

Since poor growth could contribute to the observed inefficacy of AlkBGT, its expression was tuned by varying promoter strength and origin of replication (ORI) to reduce the metabolic burden of expressing the

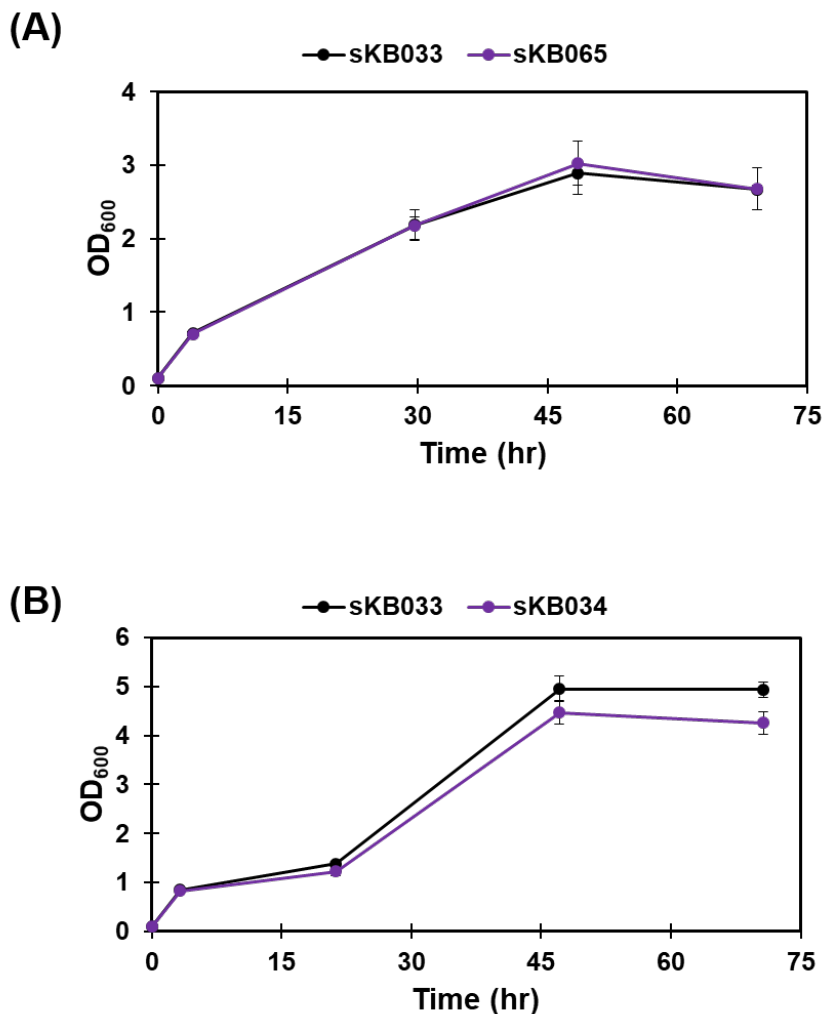
system. The original plasmid for *alkBGT* expression had this system under T7lac promoter control. The weaker LacUV5 and Trc promoter were also investigated. In addition to this, the low copy number ORI SC101 was investigated as replacement for the original medium copy number ORI - ColE1. Partial growth restoration was exhibited when the strong T7lac promoter was replaced with the LacUV5 promoter or when the ColE1 ORI was replaced with the SC101 ORI (Figure 4.6). Interestingly, growth from cells expressing *alkBGT* under the control of the Trc promoter was worse than the original vector – a phenomenon most likely due to leaky expression from this promoter. These changes in plasmid design yielded no changes in the efficacy of the AlkBGT system.



**Figure 4.6.** Measures to reduce growth burden associated with *alkBGT* overexpression (A) Expressing *alkBGT* under the control of promoters of varying strength (B) Expressing *alkBGT* on plasmid with varying copy number

Some engineering efforts did restore growth to strains overexpressing *alkBGT*. Octanoic acid consumption from a strain expressing *alkBGT* on a plasmid with LacUV5 and the SC101 ORI was tested. Growth

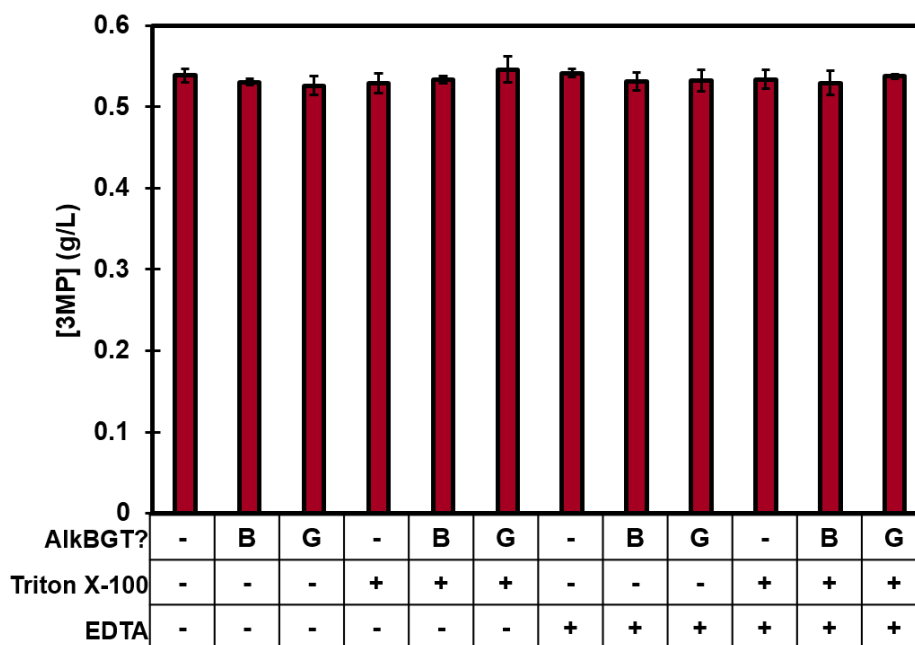
was restored to this strain (Figure 4.7a), but no octanoic acid consumption was observed. Similarly, when the original AlkBGT strain was grown in the rich growth medium described by Clomburg et al.,<sup>41</sup> growth was also restored (Figure 4.7b). However, no octanoic acid consumption was observed in this condition either.



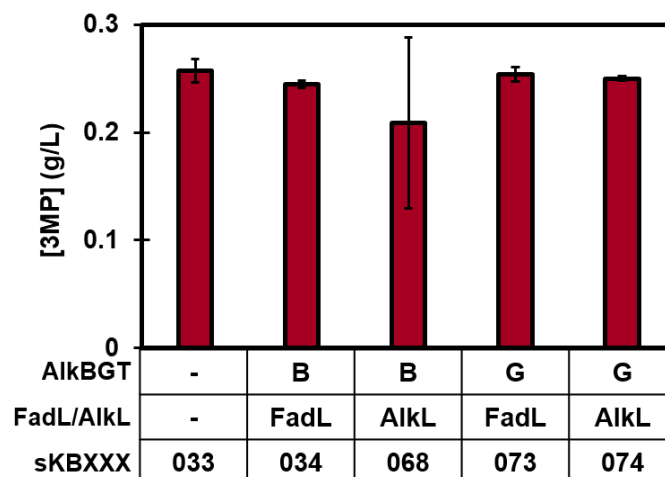
**Figure 4.7.** Measures to reduce growth burden associated with *alkBGT* overexpression (A) Expressing *alkBGT* a plasmid with the LacUV5 promoter and SC101 ORI (B) Growing T7lac promoter controlled *alkBGT* in complex growth media

Strains expressing AlkBGT did not demonstrate hydroxylation of a known substrate despite various engineering efforts to improve the growth defect associated with the system. Thus, we changed our focus to investigating substrate transport into the cell as the cause of inefficacy. In the original system, FadL - a long chain fatty acid transporter from *E. coli* was used for active transport of octanoic acid into the cell. To determine if transport into the cell was the cause of AlkBGT inefficacy, we conducted a new assay where we looked at the conversion of 3MP to 3MPD in cells permeabilized with EDTA and/or Triton X-100. Per-

meabilization agents like these disrupt the cell membrane allowing substrates that would otherwise need active transport into the cell to diffuse freely into the cytoplasm. In addition to incorporating permeabilized cells in place of FadL, we also examined the *alkBGT* expression plasmid reported by Clomburg et al.<sup>41</sup> Permeabilized cell studies in strains expressing *alkBGT* via our plasmid or the Clomburg plasmid showed no 3MP consumption or 3MPD production compared to a negative control (Figure 4.8). This indicates that AlkBGT cannot act in the conversion of 3MP to 3MPD. Alternatively, since AlkB is an integral membrane monooxygenase, permeabilization could affect its ability to fold and integrate properly into the membrane thus making it non-functional. To test this second hypothesis, we carried out an additional experiment where we replaced FadL with AlkL - the native transporter of the AlkBGT system. Again no 3MP consumption or 3MPD production was observed (Figure 4.9). Combined, these results suggest that AlkBGT cannot act in the conversion of 3MP to 3MPD or that it produces 3MPD below the limit of detection of our instrumentation.



**Figure 4.8.** 3-methylpentanol hydroxylation study in permeabilized cells. 749, sKB066, and sKB067 were permeabilized with Triton X-100 and/or EDTA. Abbreviations used: B = AlkBGT plasmid from this study, G = AlkBGT plasmid from Clomburg et al.<sup>41</sup>



**Figure 4.9.** 3-methylpentanol hydroxylation study in strains with FadL or AiKL. sKB033, sKB034, sKB068, sKB073, and sKB074 were grown in modified MOPS media according to culture condition B with 2.5 mM 3MP supplemented at T = 4 hr. Abbreviations used: B = AlkBGT plasmid from this study, G = AlkBGT plasmid from Clomburg et al.<sup>41</sup>

## 4.4 Conclusions

3MPD is a promising building block for the production of sustainable copolyesters. In this chapter, we proposed a biological pathway to this compound involving the hydroxylation of 3MP to 3MPD by AlkBGT. Initial experiments to test the hydroxylation capability of this enzyme system showed that overexpressing *alkBGT* caused a large growth defect. We showed that growth in cells overexpressing *alkBGT* could be recovered by optimizing plasmid design or media composition. Despite growth recovery, cells with AlkBGT did not exhibit the ability to catalyze hydroxylation on a known substrate. We probed substrate transport into the cell as a cause of pathway inefficacy using permeabilized cells and alternative transporters. However, no 3MP to 3MPD conversion was observed in any of the tested system. These data suggest that AlkBGT cannot act in the conversion of 3MP to 3MPD. Future work should probe other hydroxylation enzymes at this step.

## Chapter 5

# Conclusions, future directions, and outlook

### 5.1 Summary of thesis work

Environmental concerns associated with plastics consumption motivate the use of metabolically engineered microorganisms to produce renewably derived, degradable plastics. Metabolically engineered organisms can produce enantiopure biopolymer building blocks from renewable feedstocks without the complicated synthetic and purification schemes that are emblematic of traditional chemical synthesis. Further, biological pathways operate near physiological conditions, obviating the need for high temperatures and pressures that sometimes characterize chemical synthesis. However, canonical bio-based plastics exhibit disadvantages related to limited biodegradability (e.g. PLA) or thermal instability (e.g. P3HB). Developing novel metabolic pathways to plastic monomers which confer improved material properties to their corresponding plastics is integral for wider bio-based plastics adoption.

In this thesis we systematically identified industrially relevant plastic monomers for bio-production based on novelty, ease of chemical polymerization, maximum theoretical biological yield, and the expected improvements in material properties the monomer may confer in the context of a biopolymer. Through our analysis, we identified 3HIB and 3H2MB as advantaged monomers for biopolymer production primarily based on their ability to improve thermal stability in polymers. Next, we developed a platform pathway to both compounds from glucose. We implemented this pathway in *E. coli* and demonstrated the production of both compounds. To our knowledge, this is the first time 3H2MB has been produced from an unrelated carbon source.

Chapter 4 of this thesis introduces a new target biopolymer building block - 3MPD - that was prioritized



for bio-production by our industrial sponsors based on the biodegradability of its polymers. A pathway based on a previously developed pathway to 3MP was designed for this compound using *de novo* methods. The feasibility of this pathway was examined by probing the substrate specificity of AlkBGT for the hydroxylation of 3MP to 3MPD. Preliminary analysis showed that AlkBGT cannot carry out this conversion and troubleshooting this pathway step is ongoing. Overall, this thesis demonstrates the utility of novel pathway design to reach HAs and diols that lead to biopolymers with improved industrial application.

### 5.1.1 Prioritizing industrially relevant hydroxy acids for bio-production

Chapter 2 provides a systematic analysis of hydroxy acids for bio-production based on novelty, yield, ease of chemical polymerization, and material properties. We prioritized 17 HAs for bio-production based on these metrics. Our list of building blocks includes 2HAs,  $\omega$ HAs and  $\alpha$ -3HAs with connection to the microbial metabolome (Figure 2.4).  $\alpha$ -substituted 3HAs and  $\omega$ HAs stand out as advantaged monomers for PHA production based on their ability to enhance thermal stability. Specifically,  $\alpha$ -3HAs contain substituents at C2 which prevent thermal degradation via  $\beta$ -elimination mechanisms. Also,  $\omega$ HAs expand the thermal processing window when incorporated into PHAs with 3HAs. Through this analysis, 3HIB and 3H2MB were prioritized for biological production.

### 5.1.2 Engineering *E. coli* for the production of $\alpha$ -substituted 3-hydroxy acids

A pathway inspired by BCAA catabolism was designed and validated for 3HIB and 3H2MB production using a bottom up approach. Unlike traditional pathways to 3HAs, this pathway is thiolase independent which allows for  $\alpha$ -substitution which leads to more thermostable plastics. This pathway consists of two modules: (1) module 1 which encodes the specific conversion of glucose to IBA or 2MB and (2) module 2 which encodes the oxidative conversion of IBA and 2MB to 3HIB and 3H2MB, respectively. Using our bottom up approach, we first validated the conversion of enoic acids to their corresponding 3HA and identified PhaJ (*Aeromonas caviae*) as an (R)-enoyl-CoA hydratase capable of acting on branched acids in our pathway. Further, we showed that PhaJ determines the product range of our pathway and used molecular docking to identify potential mutations which might confer increased promiscuity to this enzyme. We next analyzed module 2 of the pathway for 3HIB and 3H2MB conversion from IBA and 2MB, respectively. The major enzyme in this pathway is the acyl-CoA dehydrogenase/oxidase. We identified three enzymes at this step

capable of acting in the production of 3HIB and 3H2MB. However, titers exhibited by the full module 2 pathway were only 1/3 the titers achieved by the truncated portion. This points to the dehydrogenation step as a major pathway bottleneck.

Next, we switched the specificity of a previously developed IBA pathway to 2MB production via the selection of a 2-ketobutyrate specific ALS. The best performing version of module 2 was combined with IBA or 2MB specific versions of module 1 to produce 3HIB or 3H2MB production strains, respectively. 3HIB and 3H2MB production from these strains was exhibited at titers as high as 66 mg/L and 290 mg/L, respectively. This pathway was optimized for 3H2MB production by deleting competing pathways to 3H2MB and via the development of a novel by-product recycle based on an isobutyryl-CoA mutase.

### **5.1.3 Design and feasibility analysis of pathways to 3-methyl-1,5-pentanediol**

Chapter 4 considered the biosynthesis of another promising plastic monomer – 3MPD. Three pathways were designed to this compound using *in silico* and heuristic methods. A pathway involving the hydroxylation of 3MP to 3MPD was prioritized based on pathway length, cofactor utilization, and perceived availability of hydroxylases. The feasibility determining step in this pathway is the conversion of 3MP to 3MPD and efforts in this chapter focused on determining the ability of AlkBGT to carry out this reaction. Preliminary experiments showed that overexpression of *alkBGT* caused a growth defect, which we ameliorated by optimizing plasmid design and media composition. Even after reducing the growth defect associated with *alkBGT*, cells with this system did not exhibit the ability to convert 3MP to 3MPD. Efforts are currently ongoing to determine the cause of pathway inefficacy.

## **5.2 Future directions**

### **5.2.1 Continued optimization of the 3-hydroxy-2-methylbutyric acid pathway**

From chapter 3, major bottlenecks to improved 3H2MB titer were 2MB accumulation and IBA production. Preliminary experiments incorporating irreversible activation enzymes in place of the reversible enzyme Pct suggest that the irreversible enzymes may improve 3H2MB titer. Further, we showed that deleting *tdh* significantly improves 2MB titer from cells with module 1 only. Future experiments should investigate how 3H2MB production differs from strains with and without *tdh* deleted.

We also designed and implemented a novel IBA recycle based on the isobutyryl-CoA mutase - IcmF. Incorporating this recycle into a module 1 production strain reduced IBA accumulation by 80%. Clearly the IBA recycle is an effective system to reduce byproduct formation. Future experiments on the IBA recycle should center on testing it's ability to boost 3H2MB titer in the context of a 3H2MB production strain. Further, we also showed that the IBA recycle was effective in cells without  $\beta$ -oxidation genes turned on - despite those genes being integral for recycle efficacy. Additional quantitative reverse transcription PCR experiments targeting *fadB*, and *atoB* should be carried out to determine if leaky expression of these genes supports the recycle in the absence of  $\beta$ -oxidation. More broadly, the IcmF-mediated recycle is a powerful tool to increase target product titer in any pathway with IBA as a byproduct.

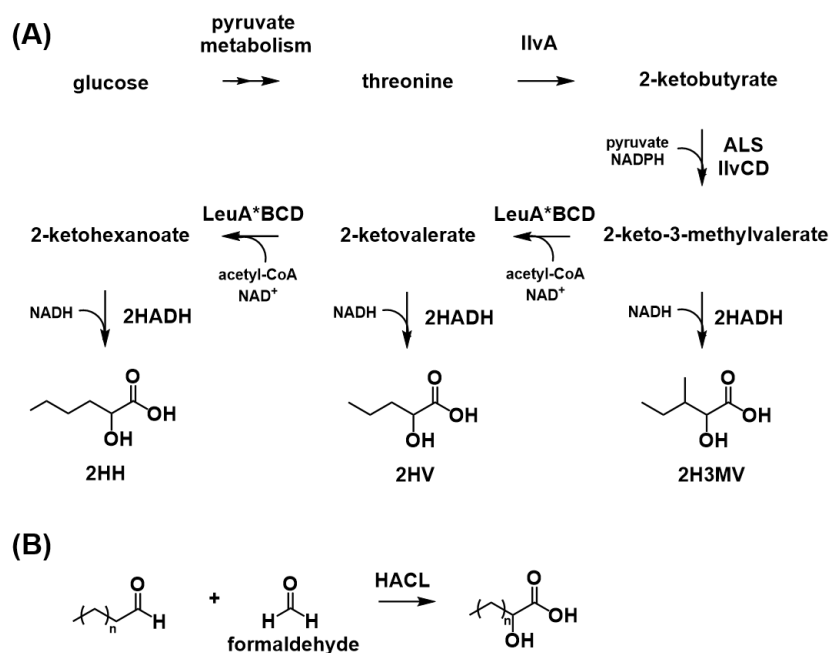
Outside of reducing 2MB and IBA accumulation, 3H2MB production could be increased by improving its growth. Strains with the module 2 pathway exhibited a growth advantage over an empty vector negative control. However, strains with the full pathway grew worse than the negative control. This growth reduction is most likely caused by the overexpression of this pathway across four plasmids. Future work could center on integrating the module 1 pathway onto *E. coli*'s genome via the method described by St. Pierre et al.<sup>134</sup> Additionally, the CICH method described by Tyo et al.<sup>135</sup> could be used to integrate multiple copies of this pathway into the genome. Integrating multiple copies of the pathway would allow for tunable, high level gene expression. In this way, the growth burden associated with expressing the entire pathway could be reduced and flux could be balanced between modules 1 and 2. Further, IBA and 2MB are precursors to other valuable products and strains containing these pathways integrated onto the genome are broadly applicable.

## 5.2.2 Bio-producing other hydroxy acids

This thesis demonstrates the efficacy of the 3HA pathway for 3HIB and 3H2MB. More broadly, the module 2 pathway could work for the production of any 3HA with  $\alpha$  and  $\beta$  hydrogens. Looking at the list of industrially relevant HAs (Figure 2.4), the 3HA pathway could be used to produce other 3HAs like 3H2MV and 3-hydroxy-2-methylhexanoic acid. Expanding the pathway's product range will rely on identifying PhaJ mutants. Our preliminary molecular docking experiments identified I75, F47, and T45 as important residues in the production of longer substrates. Future studies should focus on testing these mutants in the context of the truncated module 2 pathway to determine their ability to catalyze the production of other 3HAs. Given the bulkiness of phenylalanine and isoleucine, mutagenesis of these residues should be prioritized.

Outside of 3HAs, the findings in this thesis can also be used to reach other HAs. In addition to 3H2MB,

some 2HAs are accessible via pathways beginning with threonine metabolism. For example, 2HAs like 2HB and 2H3MV are accessible from threonine (Figure 1.4). Future work could center on extending 2-ketoacid pathways to reach other 2HAs using 2-ketoacid precursors for nonproteinogenic amino acids. Specifically, 2-hydroxyvaleric acid (2HV) and 2-hydroxyhexanoic acid (2HH) could be bio-produced using norvaline and norleucine biosynthesis intermediates, respectively (Figure 5.1a). This pathway involves 2-ketobutyrate (2KB) production via the native threonine biosynthesis pathway. 2KB is then acted on by LeuABCD to yield 2-ketovalerate or 2-ketohexanoate. Key to modulating 2HA chain-length in this pathway is the action of LeuA, a 2-isopropylmalate synthase. Mutations that allow for carbon chain length modulation via this enzyme have been identified and could be incorporated to reach these longer 2-ketoacids.<sup>131</sup> The final step in the proposed pathway involves the reduction of these 2-ketoacids to the corresponding HA by a 2HADH. Various 2HADHs with diverse substrate specificities have been identified and could be leveraged to reach 2HV and 2HH.<sup>136</sup> In another envisaged route, these straight chain 2HAs may also be reachable via Chou et al.'s 2-hydroxy-acyl-CoA lyase mediated route further motivating the exploration of these novel HAs (Figure 5.1b).<sup>30</sup>



**Figure 5.1.** Potential pathways to straight chain 2-hydroxy acids

### 5.2.3 Troubleshooting the 3-methyl-1,5-pentanediol pathway

We were unable to demonstrate the hydroxylation of 3MP to 3MPD, despite various troubleshooting efforts. AlkB is the only well-documented, substrate-permissive, non-heme hydroxylase and prospecting for hydroxylases in another enzyme family could reveal previously overlooked enzyme candidates for this step. CYP153A hydroxylases are a family of cytochromes P450 known to hydroxylate fatty acids and they represent a promising family of enzymes from which to find an enzyme for the 3MPD pathway. Further, these are soluble proteins not integral membrane proteins like AlkB which makes experimental validation of their activity on novel substrates easier. One of the most well-studied CYP153A hydroxylases is the fusion construct created from the heme domain of CYP153A33 from *Marinobacter aquaeolei* and the reductase domain of CYP102A from *Bacillus megaterium*.<sup>49</sup> This P450, along with CYP153A7 (*Sphingomonas* sp. HXN200)<sup>48</sup> were engineered for activity on a wide-variety of non-native substrates. Notably, CYP153A7 has been engineered for the conversion of butanol to 1,4-butanediol - a conversion very similar to the hydroxylation of 3MP to 3MPD.<sup>137</sup> In addition to these two, there are a wealth of other hydroxylases with demonstrated activity on shorter substrates whose efficacy on 3MP can be evaluated for inclusion in the 3MPD pathway (Table 5.1).

**Table 5.1.** CYP153As for inclusion in the 3-methyl-1,5-pentanediol pathway

Hydroxylase	Organism	Type	Primary Substrate	Reference
CYP153A7 <sub>D258E</sub>	<i>Sphingomonas</i> sp. HXN200	P450	octanoic acid	[48]
CYP153A7 <sub>I83M/I82T</sub>	<i>Sphingomonas</i> sp. HXN200	P450	butanol	[138]
CYP153A33 - CPR <sub>BM3</sub>	Hydroxylase from <i>M. aquaeolei</i> fused to reductase domain of CYP102A from <i>B. megaterium</i>	P450	octanoic acid	[49]
CYP153A6 <sub>A94V</sub>	<i>Mycobacterium</i> sp. HXN600	P450	pentane	[139]
BMO	<i>Thauera butanivorans</i>	monooxygenase	butane	[140]

## 5.3 Outlook

Every year, the chemical industry transforms billions of barrels of petroleum into plastics precursors which drive technological innovation and quality of life improvements. The chemical industry's reliance on petroleum is linked to a host of environmental issues including increased greenhouse gas emissions, pollution, and toxic waste generation. Metabolic engineering rewires microbial metabolisms for plastics

production with reduced carbon and energy footprints. The success (and short-comings) of biopolymers like PLA and P3HB sets the stage for the development of pathways to novel biopolymer building blocks.

Biopolymers represent less than 1% of global plastics use.<sup>2</sup> This slow uptake is the result of the complex interplay of policy, high costs, and the need for continued technological advancement. According to Shah and Gangadeen, "the social value of bioplastics outweighs its private value ... resulting in low investment attraction".<sup>141</sup> In other words, biopolymers exhibit undeniable environmental benefits over conventional plastics, but their industry is not competitive. Consolidating and extending policy that (1) incentivizes biopolymer use and investment, (2) encourages competitive substitution of conventional plastics with biopolymers, and (3) stimulates the growth of the industry are required to realize biopolymer private value. On the technology front, interdisciplinary research and development that engages bioengineers, chemical engineers, polymer chemists, material scientists, and environmental engineers is required to develop industrially useful, circular, low-cost biopolymers. This thesis lays a preliminary framework for engaging these diverse stakeholders in the discovery of novel, degradable biopolymers.

## References

- (1) Andrady, A. L.; Neal, M. A. Applications and Societal Benefits of Plastics. *Philosophical Transactions of the Royal Society* **2009**, *364*, 1977–1984.
- (2) OECD. *Global Plastics Outlook: Economic Drivers, Environmental Impacts and Policy Options*; tech. rep.; 2022.
- (3) Nicholson, S. R.; Rorrer, N. R.; Carpenter, A. C.; Beckham, G. T. Manufacturing Energy and Greenhouse Gas Emissions Associated with Plastics Consumption Emissions. *Joule* **2021**, *5*, 673–686.
- (4) Sheldon, R. A.; Woodley, J. M. Role of Biocatalysis in Sustainable Chemistry. *Chemical Reviews* **2018**, *118*, DOI: [10.1021/acs.chemrev.7b00203](https://doi.org/10.1021/acs.chemrev.7b00203).
- (5) Stephanopoulos, G. Synthetic Biology and Metabolic Engineering. *ACS Synthetic Biology* **2012**, *1*, 514–525.
- (6) Mozejko-Ciesielska, Justyna; Kiewisz, R. Bacterial Polyhydroxyalkanoates: Still Fabulous? *Microbiological Research* **2016**, *192*, 271–282.
- (7) Steinbüchel, A.; Valentin, H. E. Diversity of Bacterial Polyhydroxyalkanoic Acids. *FEMS Microbiology Letters* **1995**, DOI: [10.1016/0378-1097\(95\)00125-0](https://doi.org/10.1016/0378-1097(95)00125-0).
- (8) Agnew, D. E.; Pfleger, B. F. Synthetic Biology Strategies for Synthesizing Polyhydroxyalkanoates from Unrelated Carbon Sources. *Chemical Engineering Science* **2013**, *103*, 58–67.
- (9) Choi, S. Y.; Cho, I. J.; Lee, Y.; Kim, Y.-j.; Kim, K.-j.; Lee, S. Y. Microbial Polyhydroxyalkanoates and Nonnatural Polyesters. *Advanced Materials* **2020**, *32*, 1–37.
- (10) Rosenboom, J. G.; Langer, R.; Traverso, G. Bioplastics for a Circular Economy. *Nature Reviews Materials* **2022**, *7*, DOI: [10.1038/s41578-021-00407-8](https://doi.org/10.1038/s41578-021-00407-8).
- (11) Koller, M.; Mukherjee, A. A New Wave of Industrialization of PHA Biopolyesters. *Bioengineering* **2022**, *9*, DOI: [10.3390/bioengineering9020074](https://doi.org/10.3390/bioengineering9020074).
- (12) Ariffin, H.; Nishida, H.; Shirai, Y.; Hassan, M. A. Determination of Multiple Thermal Degradation Mechanisms of Poly(3-Hydroxybutyrate). *Polymer Degradation and Stability* **2008**, *93*, 1433–1439.
- (13) Singhvi, M. S.; Zinjarde, S. S.; Gokhale, D. V. Polylactic Acid: Synthesis and Biomedical Applications. *Journal of Applied Microbiology* **2019**, *127*, 1612–1626.
- (14) Bannister, K. R.; Prather, K. L. Engineering Polyester Monomer Diversity through Novel Pathway Design. *Current Opinion in Biotechnology* **2023**, *79*, 102852.
- (15) Tarasava, K.; Lee, S. H.; Chen, J.; Köpke, M.; Jewett, M. C.; Gonzalez, R. Reverse  $\beta$ -Oxidation Pathways for Efficient Chemical Production. **2022**, DOI: [10.1093/jimb/kuac003](https://doi.org/10.1093/jimb/kuac003).
- (16) Martin, C. H.; Dhamankar, H.; Tseng, H. C.; Sheppard, M. J.; Reisch, C. R.; Prather, K. L. A Platform Pathway for Production of 3-Hydroxyacids Provides a Biosynthetic Route to 3-Hydroxy- $\gamma$ -Butyrolactone. *Nature Communications* **2013**, *4*, 1414–1419.

- (17) Dhamankar, H.; Tarasova, Y.; Martin, C. H.; Prather, K. L. Engineering *E. Coli* for the Biosynthesis of 3-Hydroxy- $\gamma$ -Butyrolactone (3HBL) and 3,4-Dihydroxybutyric Acid (3,4-DHBA) as Value-Added Chemicals from Glucose as a Sole Carbon Source. *Metabolic Engineering* **2014**, *25*, 72–81.
- (18) Furutate, S.; Nakazaki, H.; Maejima, K.; Hiroe, A.; Abe, H.; Tsuge, T. Biosynthesis and Characterization of Novel Polyhydroxyalkanoate Copolymers Consisting of 3-Hydroxy-2-Methylbutyrate and 3-Hydroxyhexanoate. *Journal of Polymer Research* **2017**, *24*, 1–8.
- (19) Bonk, B. M.; Tarasova, Y.; Hicks, M. A.; Tidor, B.; Prather, K. L. Rational Design of Thiolase Substrate Specificity for Metabolic Engineering Applications. *Biotechnology and Bioengineering* **2018**, *115*, 2167–2182.
- (20) Torres-Salas, P.; Bernal, V.; López-Gallego, F.; Martínez-Crespo, J.; Sánchez-Murcia, P. A.; Barrera, V.; Morales-Jiménez, R.; García-Sánchez, A.; Mañas-Fernández, A.; Seoane, J. M.; Sagra Polo, M.; Miranda, J. D.; Calvo, J.; Huertas, S.; Torres, J. L.; Alcalde-Bascones, A.; González-Barrera, S.; Gago, F.; Morreale, A.; González-Barroso, M. D. M. Engineering Erg10 Hiolase from *Saccharomyces Cerevisiae* as a Synthetic Toolkit for the Production of Branched-Chain Alcohols. *Biochemistry* **2018**, *57*, 1338–1348.
- (21) Blaisse, M. R.; Dong, H.; Fu, B.; Chang, M. C. Discovery and Engineering of Pathways for Production of  $\alpha$ -Branched Organic Acids. *Journal of the American Chemical Society* **2017**, *139*, 14526–14532.
- (22) Furutate, S.; Kamoi, J.; Nomura, C. T.; Taguchi, S.; Abe, H.; Tsuge, T. Superior Thermal Stability and Fast Crystallization Behavior of a Novel, Biodegradable  $\alpha$ -Methylated Bacterial Polyester. *NPG Asia Materials* **2021**, *13*.
- (23) Lang, K.; Buehler, K.; Schmid, A. Multistep Synthesis of (s)-3-Hydroxyisobutyric Acid from Glucose Using *Pseudomonas Taiwanensis* VLB120 B83 T7 Catalytic Biofilms. *Advanced Synthesis and Catalysis* **2015**, *357*, 1919–1927.
- (24) Gao, R.; Li, Z. Biosynthesis of 3-Hydroxy-3-Methylbutyrate from L-leucine by Whole-Cell Catalysis. *Journal of Agricultural and Food Chemistry* **2021**, *69*, 3712–3719.
- (25) Yuzawa, S.; Deng, K.; Wang, G.; Baidoo, E. E. K.; Northen, T. R.; Adams, P. D.; Katz, L.; Keasling, J. D. Comprehensive in Vitro Analysis of Acyltransferase Domain Exchanges in Modular Polyketide Synthases and Its Application for Short-Chain Ketone Production. *ACS Synthetic Biology* **2017**, *6*, 139–147.
- (26) Yuzawa, S.; Katz, L.; Keasling, J. D. Producing 3-Hydroxycarboxylic Acid and Ketone Using Polyketide Synthase, 0345462 A1, 2019.
- (27) Lachaux, C.; Frazão, C. J.; Krauber, F.; Morin, N.; Walther, T.; François, J. M. A New Synthetic Pathway for the Bioproduction of Glycolic Acid from Lignocellulosic Sugars Aimed as Maximal Carbon Conservation. *Frontiers in Bioengineering and Biotechnology* **2019**, *7*, DOI: [10.3389/fbioe.2019.00359](https://doi.org/10.3389/fbioe.2019.00359).
- (28) Mizuno, S.; Enda, Y.; Saika, A.; Hiroe, A.; Tsuge, T. Biosynthesis of Polyhydroxyalkanoates Containing 2-Hydroxy-4-Methylvalerate and 2-Hydroxy-3-Phenylpropionate Units from a Related or Unrelated Carbon Source. *Journal of Bioscience and Bioengineering* **2018**, *125*, 295–300.
- (29) Cheong, S.; Clomburg, J. M.; Gonzalez, R. A Synthetic Pathway for the Production of 2-Hydroxyisovaleric Acid in *Escherichia Coli*. *Journal of Industrial Microbiology and Biotechnology* **2018**, *45*, 579–588.
- (30) Chou, A.; Clomburg, J. M.; Qian, S.; Gonzalez, R. 2-Hydroxyacyl-CoA Lyase Catalyzes Acyloin Condensation for One-Carbon Bioconversion. *Nature Chemical Biology* **2019**, *15*, 900–906.



- (31) Kunioka, M.; Doi, Y. Thermal Degradation of Microbial Copolyesters: Poly(3-Hydroxybutyrate-Co-3-Hydroxyvalerate) and Poly(3-Hydroxybutyrate-Co-4-Hydroxybutyrate). *Macromolecules* **1990**, *23*, 1933–1936.
- (32) Utsunomia, C.; Ren, Q.; Zinn, M. Poly(4-Hydroxybutyrate): Current State and Perspectives. *Frontiers in Bioengineering and Biotechnology* **2020**, *8*, DOI: [10.3389/fbioe.2020.00257](https://doi.org/10.3389/fbioe.2020.00257).
- (33) Yim, H.; Haselbeck, R.; Niu, W.; Pujol-Baxley, C.; Burgard, A.; Boldt, J.; Khandurina, J.; Trawick, J. D.; Osterhout, R. E.; Stephen, R.; Estadilla, J.; Teisan, S.; Schreyer, H. B.; Andrae, S.; Yang, T. H.; Lee, S. Y.; Burk, M. J.; Van Dien, S. Metabolic Engineering of Escherichia Coli for Direct Production of 1,4-Butanediol. *Nature Chemical Biology* **2011**, *7*, 445–452.
- (34) Choi, S.; Kim, H. U.; Kim, T. Y.; Lee, S. Y. Systematic Engineering of TCA Cycle for Optimal Production of a Four-Carbon Platform Chemical 4-Hydroxybutyric Acid in Escherichia Coli. *Metabolic Engineering* **2016**, *38*, DOI: [10.1016/j.ymben.2016.09.004](https://doi.org/10.1016/j.ymben.2016.09.004).
- (35) Cen, X.; Liu, Y.; Chen, B.; Liu, D.; Chen, Z. Metabolic Engineering of Escherichia Coli for de Novo Production of 1,5-Pentanediol from Glucose. *ACS Synthetic Biology* **2021**, *10*, 192–203.
- (36) Sohn, Y. J.; Kang, M.; Baritugo, K.-A.; Son, J.; Kang, K. H.; Ryu, M.-h.; Lee, S.; Sohn, M.; Jung, Y. J.; Park, K.; Park, S. J.; Joo, J. C.; Kim, H. T. Fermentative High-Level Production of 5-Hydroxyvaleric Acid by Metabolically Engineered Corynebacterium Glutamicum. *ACS Sustainable Chemistry & Engineering* **2021**, *9*, 2523–2533.
- (37) Schäfer, L.; Bühler, K.; Karande, R.; Bühler, B. Rational Engineering of a Multi-Step Biocatalytic Cascade for the Conversion of Cyclohexane to Polycaprolactone Monomers in Pseudomonas Taiwanensis. *Biotechnology Journal* **2020**, *15*, DOI: [10.1002/biot.202000091](https://doi.org/10.1002/biot.202000091).
- (38) Bretschneider, L.; Heuschkel, I.; Wegner, M.; Lindmeyer, M.; Bühler, K.; Karande, R.; Bühler, B. Conversion of Cyclohexane to 6-Hydroxyhexanoic Acid Using Recombinant Pseudomonas Taiwanensis in a Stirred-Tank Bioreactor. *Frontiers in Catalysis* **2021**, *1*, DOI: [10.3389/fctls.2021.683248](https://doi.org/10.3389/fctls.2021.683248).
- (39) Salamanca, D.; Bühler, K.; Engesser, K.-H.; Schmid, A.; Karande, R. Whole-Cell Biocatalysis Using the Acidovorax Sp . CHX100 Δ6HX for the Production of ω -Hydroxycarboxylic Acids from Cycloalkanes. *New BIOTECHNOLOGY* **2021**, *60*, 200–206.
- (40) Cheong, S.; Clomburg, J. M.; Gonzalez, R. Energy-and Carbon-Efficient Synthesis of Functionalized Small Molecules in Bacteria Using Non-Decarboxylative Claisen Condensation Reactions. *Nature Biotechnology* **2016**, *34*, 556–561.
- (41) Clomburg, J. M.; Blankschien, M. D.; Vick, J. E.; Chou, A.; Kim, S.; Gonzalez, R. Integrated Engineering of β-Oxidation Reversal and ω-Oxidation Pathways for the Synthesis of Medium Chain ω-Functionalized Carboxylic Acids. *Metabolic Engineering* **2015**, DOI: [10.1016/j.ymben.2015.01.007](https://doi.org/10.1016/j.ymben.2015.01.007).
- (42) He, Q.; Bennett, G. N.; San, K.-y.; Wu, H. Biosynthesis of Medium-Chain ω-Hydroxy Fatty Acids by AlkBGT of Pseudomonas Putida GPo1 with Native fadL in Engineered Escherichia Coli. *Frontiers in Bioengineering and Biotechnology* **2019**, *7*, 1–10.
- (43) Wernig, F.; Boles, E.; Oreb, M. De Novo Biosynthesis of 8-Hydroxyoctanoic Acid via a Medium-Chain Length Specific Fatty Acid Synthase and Cytochrome P450 in Saccharomyces Cerevisiae. *Metabolic Engineering Communications* **2020**, *10*, DOI: [10.1016/j.mec.2019.e00111](https://doi.org/10.1016/j.mec.2019.e00111).
- (44) Yoo, H.-w.; Jung, H.; Sarak, S.; Kim, Y. C.; Park, B. G.; Kim, B.-g.; Patil, M. D.; Yun, H. Multi-Enzymatic Cascade Reactions with Escherichia Coli -Based Modules for Synthesizing Various Bioplastic Monomers from Fatty Acid. *Green Chemistry* **2022**, *24*, 2222–2231.

- (45) Ahsan, M. M.; Sung, S.; Jeon, H.; Patil, M. D.; Chung, T.; Yun, H. Biosynthesis of Medium-to-Long-Chain  $\alpha,\omega$ -Diols from Free Fatty Acids Using CYP153A Monooxygenase, Carboxylic Acid Reductase, and *e. Coli* Endogenous Aldehyde Reductases. *Catalysts* **2018**, *8*, DOI: [10.3390/catal8010004](https://doi.org/10.3390/catal8010004).
- (46) Wang, J.; Li, C.; Zou, Y.; Yan, Y. Bacterial Synthesis of C3-C5 Diols via Extending Amino Acid Catabolism. *Proceedings of the National Academy of Sciences of the United States of America* **2020**, *117*, 19159–19167.
- (47) Beilen, J. B. V.; Kingma, J.; Witholt, B. Substrate Specificity of the Alkane Hydroxylase System of *Pseudomonas Oleovorans* GPOL. **1994**, *16*, 904–911.
- (48) Dong, Y. L.; Chong, G. G.; Li, C. X.; Chen, Q.; Pan, J.; Li, A. T.; Xu, J. H. Carving the Active Site of CYP153A7 Monooxygenase for Improving Terminal Hydroxylation of Medium-Chain Fatty Acids. *ChemBioChem* **2022**, *23*, DOI: [10.1002/cbic.202200063](https://doi.org/10.1002/cbic.202200063).
- (49) Notonier, S.; Gricman, L.; Pleiss, J.; Hauer, B. Semirational Protein Engineering of CYP153AM.Aq-CPRBM3 for Efficient Terminal Hydroxylation of Short- to Long-Chain Fatty Acids. *ChemBioChem* **2016**, DOI: [10.1002/cbic.201600207](https://doi.org/10.1002/cbic.201600207).
- (50) Rapp, L. R.; Marques, S. M.; Zukic, E.; Rowlinson, B.; Sharma, M.; Grogan, G.; Damborsky, J.; Hauer, B. Substrate Anchoring and Flexibility Reduction in CYP153AM.aq Leads to Highly Improved Efficiency toward Octanoic Acid. *ACS Catalysis* **2021**, *11*, DOI: [10.1021/acscatal.0c05193](https://doi.org/10.1021/acscatal.0c05193).
- (51) Chae, T. U.; Ahn, J. H.; Ko, Y. S.; Kim, J. W.; Lee, J. A.; Lee, E. H.; Lee, S. Y. Metabolic Engineering for the Production of Dicarboxylic Acids and Diamines. *Metabolic Engineering* **2020**, *58*, DOI: [10.1016/j.ymben.2019.03.005](https://doi.org/10.1016/j.ymben.2019.03.005).
- (52) Lama, S.; Seol, E.; Park, S. Development of *Klebsiella Pneumoniae* J2B as Microbial Cell Factory for the Production of 1,3-Propanediol from Glucose. *Metabolic Engineering* **2020**, *62*, 116–125.
- (53) Frazão, C. J.; Trichez, D.; Serrano-Bataille, H.; Dagkesamanskaia, A.; Topham, C.; Walther, T.; François, J. M. Construction of a Synthetic Pathway for the Production of 1,3-Propanediol from Glucose. *Nature Research Scientific Reports* **2019**, *9*.
- (54) Zhong, W.; Zhang, Y.; Wu, W.; Liu, D.; Chen, Z. Metabolic Engineering of a Homoserine-Derived Non-Natural Pathway for the de Novo Production of 1,3-Propanediol from Glucose. *ACS Synthetic Biology* **2019**, *8*, 587–595.
- (55) Zhang, Y.; Ma, C.; Dischert, W.; Soucaille, P.; Zeng, A. P. Engineering of Phosphoserine Aminotransferase Increases the Conversion of L-Homoserine to 4-Hydroxy-2-ketobutyrate in a Glycerol-Independent Pathway of 1,3-Propanediol Production from Glucose. *Biotechnology Journal* **2019**, *14*, DOI: [10.1002/biot.201900003](https://doi.org/10.1002/biot.201900003).
- (56) Li, Z.; Wu, Z.; Cen, X.; Liu, Y.; Zhang, Y.; Liu, D.; Chen, Z. Efficient Production of 1,3-Propanediol from Diverse Carbohydrates via a Non-Natural Pathway Using 3-Hydroxypropionic Acid as an Intermediate. *ACS Synthetic Biology* **2021**, *10*, 478–486.
- (57) Liu, Y.; Wang, W.; Zeng, A.-p. Biosynthesizing Structurally Diverse Diols via a General Route Combining Oxidative and Reductive Formations of OH-groups. *Nature Communications* **2022**, *13*, DOI: [10.1038/s41467-022-29216-5](https://doi.org/10.1038/s41467-022-29216-5).
- (58) Meng, H.; Wang, C.; Yuan, Q.; Ren, J.; Zeng, A.-p. An Aldolase-Based New Pathway for Bioconversion of Formaldehyde and Ethanol into 1,3-Propanediol in *Escherichia Coli*. *ACS Chemical Biology* **2021**, *10*, 799–809.

- (59) Wang, C.; Ren, J.; Zhou, L.; Li, Z.; Chen, L.; Zeng, A.-p. An Aldolase-Catalyzed New Metabolic Pathway for the Assimilation of Formaldehyde and Methanol to Synthesize 2-Keto-4 Hydroxybutyrate and 1,3-Propanediol in Escherichia Coli. *ACS Synthetic Biology* **2019**, *8*, 2483–2493.
- (60) Gascoyne, J. L.; Bommareddy, R. R.; Heeb, S.; Malys, N. Engineering Cupriavidus Necator H16 for the Autotrophic Production of (R)-1,3-Butanediol. *Metabolic Engineering* **2021**, *67*, 262–276.
- (61) Liu, Y.; Cen, X.; Liu, D.; Chen, Z. Metabolic Engineering of Escherichia Coli for High-Yield Production of (r)-1,3-Butanediol. *ACS Synthetic Biology* **2021**, *10*, 1946–1955.
- (62) Kataoka, N.; Vangnai, A. S.; Pongtharangkul, T.; Yakushi, T.; Matsushita, K. Production of 1,3-Diols in Escherichia Coli. *Bioresource Technology* **2017**, *245*, 1538–1541.
- (63) Nemr, K.; Müller, J. E. N.; Chan, J.; Gawand, P.; Choudhary, R.; Mendonca, B.; Lu, S.; Yu, X.; Yakunin, A. F.; Mahadevan, R. Engineering a Short, Aldolase-Based Pathway for (r)-1,3-Butanediol Production in Escherichia Coli. *Metabolic Engineering* **2018**, *48*, 13–24.
- (64) Dai, L.; Tai, C.; Shen, Y.; Guo, Y.; Tao, F. Biosynthesis of 1,4-Butanediol from Erythritol Using Whole-Cell Catalysis. *Biocatalysis and Biotransformation* **2019**, *37*, 92–96.
- (65) Wang, J.; Jain, R.; Shen, X.; Sun, X.; Cheng, M.; Liao, J. C.; Yuan, Q.; Yan, Y. Rational Engineering of Diol Dehydratase Enables 1,4-Butanediol Biosynthesis from Xylose. *Metabolic Engineering* **2017**, *40*, 148–156.
- (66) Little, A.; Pellis, A.; Comerford, J. W.; Naranjo-Valles, E.; Hafezi, N.; Mascal, M.; Farmer, T. J. Effects of Methyl Branching on the Properties and Performance of Furandioate-Adipate Copolyesters of Bio-Based Secondary Diols. *ACS Sustainable Chemistry & Engineering* **2020**, *8*, 14471–14483.
- (67) Lu, C.; Leitner, N.; Wijffels, R. H.; Martins dos Santos, V. A. P.; Weusthuis, A. Microbial Production of Medium-Chain-Length Diols via Two-Stage Process under Mild Conditions. *Bioresource Technology* **2022**, *352*, DOI: [10.1016/j.biortech.2022.127111](https://doi.org/10.1016/j.biortech.2022.127111).
- (68) Prather, K. L. J.; Martin, C. H. De Novo Biosynthetic Pathways : Rational Design of Microbial Chemical Factories. **2008**, 468–474.
- (69) Sveshnikova, A.; MohammadiPeyhani, H.; Hatzimanikatis, V. Computational Tools and Resources for Designing New Pathways to Small Molecules. *Current Opinion in Biotechnology* **2022**, *76*, 102722.
- (70) Delépine, B.; Duigou, T.; Carbonell, P.; Faulon, J.-I. RetroPath2 . 0 : A Retrosynthesis Work Fl Ow for Metabolic Engineers. **2018**, *45*, 158–170.
- (71) Robinson, C. J.; Carbonell, P.; Jarvis, A. J.; Yan, C.; Hollywood, K. A.; Dunstan, M. S.; Currin, A.; Swainston, N.; Spiess, R.; Taylor, S.; Mulherin, P.; Parker, S.; Rowe, W.; Matthews, N. E.; Malone, K. J.; Le Feuvre, R.; Shapira, P.; Barran, P.; Turner, N. J.; Micklefield, J.; Breitling, R.; Takano, E.; Scrutton, N. S. Rapid Prototyping of Microbial Production Strains for the Biomanufacture of Potential Materials Monomers. *Metabolic Engineering* **2020**, *60*, 168–182.
- (72) Vila-Santa, A.; Islam, M. A.; Ferreira, F. C.; Prather, K. L.; Mira, N. P. Prospecting Biochemical Pathways to Implement Microbe-Based Production of the New-to-Nature Platform Chemical Levulinic Acid. *ACS Synthetic Biology* **2021**, *10*, 724–736.
- (73) Ragaert, K.; Delva, L.; Van Geem, K. Mechanical and Chemical Recycling of Solid Plastic Waste. *Waste Management* **2017**, *69*, DOI: [10.1016/j.wasman.2017.07.044](https://doi.org/10.1016/j.wasman.2017.07.044).
- (74) Watanabe, Y.; Ishizuka, K.; Furutate, S.; Abe, H.; Tsuge, T. Biosynthesis and Characterization of Novel Poly(3-Hydroxybutyrate-Co-3-Hydroxy-2-Methylbutyrate): Thermal Behavior Associated with  $\alpha$ -Carbon Methylation. *RSC Advances* **2015**, *5*, 58679–58685.

- (75) Zhou, L.; Zhang, Z.; Shi, C.; Scoti, M.; Barange, D. K.; Gowda, R. R.; Chen, E. Y. Chemically Circular, Mechanically Tough, and Melt-Processable Polyhydroxyalkanoates. *Science* **2023**, *380*, DOI: [10.1126/science.adg4520](https://doi.org/10.1126/science.adg4520).
- (76) Yan, X.; Liu, X.; Yu, L.-P.; Wu, F.; Jiang, X.-R.; Chen, G.-Q. Biosynthesis of Diverse  $\alpha,\omega$ -Diol-Derived Polyhydroxyalkanoates by Engineered Halomonas Bluephagenesis. *Metabolic Engineering* **2022**, *72*, 275–288.
- (77) KEGG Database <https://www.genome.jp/kegg/>.
- (78) MetaCyc Database <https://metacyc.org/>.
- (79) Dugar, D.; Stephanopoulos, G. Relative Potential of Biosynthetic Pathways for Biofuels and Bio-Based Products. **2011**, *29*, 1074–1078.
- (80) Lang, K.; Zierow, J.; Buehler, K.; Schmid, A. Metabolic Engineering of Pseudomonas Sp. Strain VLB120 as Platform Biocatalyst for the Production of Isobutyric Acid and Other Secondary Metabolites. *Microbial Cell Factories* **2014**, *13*, DOI: [10.1186/1475-2859-13-2](https://doi.org/10.1186/1475-2859-13-2).
- (81) Alonso, S.; Rendueles, M.; Díaz, M. Microbial Production of Specialty Organic Acids from Renewable and Waste Microbial Production of Specialty Organic Acids from Renewable and Waste Materials. **2014**, DOI: [10.3109/07388551.2014.904269](https://doi.org/10.3109/07388551.2014.904269).
- (82) Walther, T.; Topham, C. M.; Irague, R.; Auriol, C.; Baylac, A.; Cordier, H.; Dressaire, C.; Lozano-Huguet, L.; Tarrat, N.; Martineau, N.; Stodel, M.; Malbert, Y.; Maestracci, M.; Huet, R.; André, I.; Remaud-Siméon, M.; François, J. M. Construction of a Synthetic Metabolic Pathway for Biosynthesis of the Non-Natural Methionine Precursor 2,4-Dihydroxybutyric Acid. *Nature Communications* **2017**, *8*, DOI: [10.1038/ncomms15828](https://doi.org/10.1038/ncomms15828).
- (83) Srinivasamurthy, V. S.; Böttcher, D.; Bornscheuer, U. T. A Multi-Enzyme Cascade Reaction for the Production of 6-Hydroxyhexanoic Acid. *Zeitschrift für Naturforschung - Section C Journal of Biosciences* **2019**, *74*, 71–76.
- (84) Choi, S. Y.; Park, S. J.; Kim, W. J.; Yang, J. E.; Lee, H.; Shin, J.; Lee, S. Y. One-Step Fermentative Production of Poly(Lactate-Co-Glycolate) from Carbohydrates in Escherichia Coli. *Nature Biotechnology* **2016**, *34*, 435–440.
- (85) Girhard, M.; Schuster, S.; Dietrich, M.; Dürre, P.; Urlacher, V. B. Cytochrome P450 Monooxygenase from Clostridium Acetobutylicum: A New  $\alpha$ -Fatty Acid Hydroxylase. *Biochemical and Biophysical Research Communications* **2007**, *362*, 114–119.
- (86) Miltenberger, K., Hydroxycarboxylic Acids, Aliphatic In *Ullmann's Encyclopedia of Industrial Chemistry*, 2000.
- (87) Pyo, S. H.; Dishisha, T.; Dayankac, S.; Gerelsaikhan, J.; Lundmark, S.; Rehnberg, N.; Hatti-Kaul, R. A New Route for the Synthesis of Methacrylic Acid from 2-Methyl-1,3- Propanediol by Integrating Biotransformation and Catalytic Dehydration. *Green Chemistry* **2012**, *14*, DOI: [10.1039/c2gc35214a](https://doi.org/10.1039/c2gc35214a).
- (88) O'Malley, M.; Solomon, K.; Mizunashi, W.; Yu, F. Biological Production of Methyl Methacrylate, US10676766B2, 2020.
- (89) Haas, T.; Schaffer, S.; Poetter, M.; Wessel, M.; Pfeffer, J. C.; Gehring, C.; Kirchner, N.; Wittmann, E. M. Biotechnological preparation of 3-hydroxyisobutyric acid, US 20150218600A1, 2015.
- (90) Česnik, M.; Sudar, M.; Roldan, R.; Hernandez, K.; Parella, T.; Clapés, P.; Charnock, S.; Vasić-Rački, Đ.; Findrik Blažević, Z. Model-Based Optimization of the Enzymatic Aldol Addition of Propanal to Formaldehyde: A First Step towards Enzymatic Synthesis of 3-Hydroxybutyric Acid. *Chemical Engineering Research and Design* **2019**, *150*, 140–152.

- (91) Seo, Y.; Lee, K.; Park, J.; Park, J.; Park, W.; Lee, J.; Lee, H.; Kang, K. Mutant Microorganism Comprising a Gene Encoding Methylmalonyl-CoA Reductase and Its Use, DE 10 2016 212 497 A1, 2017.
- (92) Junker, S.; Roldan, R.; Joosten, H. J.; Clapés, P.; Fessner, W. D. Complete Switch of Reaction Specificity of an Aldolase by Directed Evolution In Vitro: Synthesis of Generic Aliphatic Aldol Products. *Angewandte Chemie - International Edition* **2018**, *57*, DOI: [10.1002/anie.201804831](https://doi.org/10.1002/anie.201804831).
- (93) Froese, D. S.; Dobson, C. M.; White, A. P.; Wu, X.; Padovani, D.; Banerjee, R.; Haller, T.; Gerlt, J. A.; Surette, M. G.; Gravel, R. A. Sleeping Beauty Mutase (Sbm) Is Expressed and Interacts with Ygfd in Escherichia Coli. *Microbiological Research* **2009**, *164*, DOI: [10.1016/j.micres.2008.08.006](https://doi.org/10.1016/j.micres.2008.08.006).
- (94) Zhang, Z.; Chu, R.; Wei, W.; Song, W.; Ye, C.; Chen, X.; Wu, J.; Liu, L.; Gao, C. Systems Engineering of Escherichia Coli for High-Level Glutarate Production from Glucose. *Nature Communications* **2024**, *15*, DOI: [10.1038/s41467-024-45448-z](https://doi.org/10.1038/s41467-024-45448-z).
- (95) Sheppard, M. J.; Kunjapur, A. M.; Wenck, S. J.; Prather, K. L. Retro-Biosynthetic Screening of a Modular Pathway Design Achieves Selective Route for Microbial Synthesis of 4-Methyl-Pentanol. *Nature Communications* **2014**, *5*, DOI: [10.1038/ncomms6031](https://doi.org/10.1038/ncomms6031).
- (96) Salis, H. M.; Mirsky, E. A.; Voigt, C. A. Automated Design of Synthetic Ribosome Binding Sites to Control Protein Expression. *Nature Biotechnology* **2009**, *27*, 946–950.
- (97) Datsenko, K. A.; Wanner, B. L. One-Step Inactivation of Chromosomal Genes in Escherichia Coli K-12 Using PCR Products. *Proceedings of the National Academy of Sciences of the United States of America* **2000**, *97*, 6640–6645.
- (98) Bradford, M. M. A Rapid and Sensitive Method for the Quantitation of Microgram Quantities of Protein Utilizing the Principle of Protein-Dye Binding. *Analytical Biochemistry* **1976**, *72*, DOI: [10.1016/0003-2697\(76\)90527-3](https://doi.org/10.1016/0003-2697(76)90527-3).
- (99) Trott, O.; Olson, A. J. AutoDock Vina: Improving the Speed and Accuracy of Docking with a New Scoring Function, Efficient Optimization, and Multithreading. *Journal of Computational Chemistry* **2010**, *31*, DOI: [10.1002/jcc.21334](https://doi.org/10.1002/jcc.21334).
- (100) Hanwell, M. D.; Curtis, D. E.; Lonie, D. C.; Vandermeersch, T.; Zurek, E.; Hutchison, G. R. Avogadro: An Advanced Semantic Chemical Editor, Visualization, and Analysis Platform | Journal of Cheminformatics | Full Text. *Journal of Cheminformatics* **2018**, *4*.
- (101) Tseng, H. C.; Harwell, C. L.; Martin, C. H.; Prather, K. L. Biosynthesis of Chiral 3-Hydroxyvalerate from Single Propionate-Unrelated Carbon Sources in Metabolically Engineered E. Coli. *Microbial Cell Factories* **2010**, *9*, 96.
- (102) Kawashima, Y.; Cheng, W.; Mifune, J.; Orita, I.; Nakamura, S.; Fukui, T. Characterization and Functional Analyses of R-specific Enoyl Coenzyme a Hydratases in Polyhydroxyalkanoate-Producing Ralstonia Eutropha. *Applied and Environmental Microbiology* **2012**, *78*, 493–502.
- (103) McMahon, M. D.; Prather, L. J. Functional Screening and In Vitro Analysis Reveal Thioesterases with Enhanced Substrate Specificity Profiles That Improve Short-Chain Fatty Acid Production in Escherichia Coli. *Applied and Environmental Microbiology* **2014**, *80*, 1042–1050.
- (104) Kim, J.-j. P.; Miura, R. Acyl-CoA Dehydrogenases and Acyl-CoA Oxidases. *European Journal of Biochemistry* **2004**, *493*, 483–493.
- (105) McMahon, B.; Gallagher, M. E.; Mayhew, S. G. The Protein Coded by the PP2216 Gene of Pseudomonas Putida KT2440 Is an Acyl-CoA Dehydrogenase That Oxidises Only Short-Chain Aliphatic Substrates. *FEMS Microbiology Letters* **2005**, *250*, 121–127.

- (106) Zhang, Y.-x.; Denoya, C. D.; Skinner, D. D.; Fedechko, R. W.; McArthur, H. A. I.; Morgenstern, M. R.; Davies, R. A.; Lobo, S.; Reynolds, K. A.; Hutchinson, C. R. Genes Encoding Acyl-CoA Dehydrogenase ( AcdH ) Homologues from Streptomyces Coelicolor and Streptomyces Avermitilis Provide Insights into the Metabolism of Small Branched-Chain Fatty Acids and Macrolide Antibiotic Production. **1999**, 2323–2334.
- (107) Campbell, J. W.; Cronan Jr., J. E. The Enigmatic Escherichia Coli fadE Gene Is yafH. *Journal of Bacteriology* **2002**, *184*, 3759–3764.
- (108) Vögeli, B.; Geyer, K.; Gerlinger, P. D.; Benkstein, S.; Cortina, N. S.; Erb, T. J. Combining Promiscuous Acyl-CoA Oxidase and Enoyl-CoA Carboxylase/Reductases for Atypical Polyketide Extender Unit Biosynthesis. *Cell Chemical Biology* **2018**, *25*, 833–839.
- (109) Kim, S.; Kim, K. J. Crystal Structure of Acyl-CoA Oxidase 3 from Yarrowia Lipolytica with Specificity for Short-Chain Acyl-CoA. *Journal of Microbiology and Biotechnology* **2018**, *28*, 597–605.
- (110) Seaver, L. C.; Imlay, J. A. Alkyl Hydroperoxide Reductase Is the Primary Scavenger of Endogenous Hydrogen Peroxide in Escherichia Coli. *Journal of Bacteriology* **2001**, *183*, DOI: [10.1128/JB.183.24.7173-7181.2001](https://doi.org/10.1128/JB.183.24.7173-7181.2001).
- (111) Gollop, N.; Damri, B.; Chipman, D. M.; Barak, Z. Physiological Implications of the Substrate Specificities of Acetohydroxy Acid Synthases from Varied Organisms. *Journal of Bacteriology* **1990**, *172*, 3444–3449.
- (112) Dhande, Y. K.; Xiong, M.; Zhang, K. Production of C 5 Carboxylic Acids in Engineered Escherichia Coli. *Process Biochemistry* **2012**, *47*, 1965–1971.
- (113) Crosby, H. A.; Pelletier, D. A.; Hurst, G. B.; Escalante-Semerena, J. C. System-Wide Studies of N-lysine Acetylation in Rhodopseudomonas Palustris Reveal Substrate Specificity of Protein Acetyltransferases. *Journal of Biological Chemistry* **2012**, *287*, DOI: [10.1074/jbc.M112.352104](https://doi.org/10.1074/jbc.M112.352104).
- (114) Meng, Y.; Ingram-Smith, C.; Cooper, L. L.; Smith, K. S. Characterization of an Archaeal Medium-Chain Acyl Coenzyme A Synthetase from Methanosarcina Acetivorans. *Journal of Bacteriology* **2010**, *192*, DOI: [10.1128/JB.00600-10](https://doi.org/10.1128/JB.00600-10).
- (115) Cann, A. F.; Liao, J. C. Production of 2-Methyl-1-Butanol in Engineered Escherichia Coli. **2008**, 89–98.
- (116) Jost, M.; Cracan, V.; Hubbard, P. A.; Banerjee, R.; Drennan, C. L. Visualization of a Radical B12 Enzyme with Its G-protein Chaperone. *Proceedings of the National Academy of Sciences of the United States of America* **2015**, *112*, DOI: [10.1073/pnas.1419582112](https://doi.org/10.1073/pnas.1419582112).
- (117) Cracan, V.; Padovani, D.; Banerjee, R. IcmF Is a Fusion between the Radical B12 Enzyme Isobutyryl-CoA Mutase and Its G-protein Chaperone. *Journal of Biological Chemistry* **2010**, *285*, DOI: [10.1074/jbc.M109.062182](https://doi.org/10.1074/jbc.M109.062182).
- (118) Cracan, V.; Banerjee, R. Novel Coenzyme B 12-Dependent Interconversion of Isovaleryl-CoA and Pivalyl-CoA. *Journal of Biological Chemistry* **2012**, *287*, DOI: [10.1074/jbc.M111.320051](https://doi.org/10.1074/jbc.M111.320051).
- (119) Pavoncello, V.; Barras, F.; Bouveret, E. Degradation of Exogenous Fatty Acids in Escherichia Coli. *Biomolecules* **2022**, *12*, DOI: [10.3390/biom12081019](https://doi.org/10.3390/biom12081019).
- (120) Tsuge, T.; Hisano, T.; Taguchi, S.; Doi, Y. Alteration of Chain Length Substrate Specificity of Aeromonas Caviae R-enantiomer-specific Enoyl-Coenzyme A Hydratase through Site-Directed Mutagenesis. *Applied and Environmental Microbiology* **2003**, *69*, DOI: [10.1128/AEM.69.8.4830-4836.2003](https://doi.org/10.1128/AEM.69.8.4830-4836.2003).

- (121) Hisano, T.; Tsuge, T.; Fukui, T.; Iwata, T.; Miki, K.; Doi, Y. Crystal Structure of the (R)-Specific Enoyl-CoA Hydratase from *Aeromonas Caviae* Involved in Polyhydroxyalkanoate Biosynthesis. *Journal of Biological Chemistry* **2003**, *278*, DOI: [10.1074/jbc.M205484200](https://doi.org/10.1074/jbc.M205484200).
- (122) Yang, Y.; Min, J.; Xue, T.; Jiang, P.; Liu, X.; Peng, R.; Huang, J. W.; Qu, Y.; Li, X.; Ma, N.; Tsai, F. C.; Dai, L.; Zhang, Q.; Liu, Y.; Chen, C. C.; Guo, R. T. Complete Bio-Degradation of Poly(Butylene Adipate-Co-Terephthalate) via Engineered Cutinases. *Nature Communications* **2023**, *14*, DOI: [10.1038/s41467-023-37374-3](https://doi.org/10.1038/s41467-023-37374-3).
- (123) Hino, K.; Yada, K.; Saeki, K. Method for Producing 3-Methyl-1,5-Pentanediol, (United States of America), 2009.
- (124) Xiong, M.; Schneiderman, D. K.; Bates, F. S.; Hillmyer, M. A.; Zhang, K. Scalable Production of Mechanically Tunable Block Polymers from Sugar. *Proceedings of the National Academy of Sciences of the United States of America* **2014**, *111*, 8357–8362.
- (125) Spanjers, C. S.; Schneiderman, D. K.; Wang, J. Z.; Wang, J.; Hillmyer, M. A.; Zhang, K.; Dauenhauer, P. J. Branched Diol Monomers from the Sequential Hydrogenation of Renewable Carboxylic Acids. *ChemCatChem* **2016**, *8*, DOI: [10.1002/cctc.201600710](https://doi.org/10.1002/cctc.201600710).
- (126) Schrewe, M.; Magnusson, A. O.; Willrodt, C.; Bühler, B.; Schmid, A. Kinetic Analysis of Terminal and Unactivated C-H Bond Oxyfunctionalization in Fatty Acid Methyl Esters by Monooxygenase-Based Whole-Cell Biocatalysis. *Advanced Synthesis and Catalysis* **2011**, *353*, DOI: [10.1002/adsc.201100440](https://doi.org/10.1002/adsc.201100440).
- (127) Hattori, M.; Tanaka, N.; Kanehisa, M.; Goto, S. SIMCOMP/SUBCOMP: Chemical Structure Search Servers for Network Analyses. *Nucleic Acids Research* **2010**, *38*, 652–656.
- (128) Martin, V. J. J.; Pitera, D. J.; Withers, S. T.; Newman, J. D.; Keasling, J. D. Engineering a Mevalonate Pathway in *Escherichia Coli* for PProduction of Terpenoids. *Nature Biotechnology* **2003**, *21*, 796–802.
- (129) Meng, D. C.; Shen, R.; Yao, H.; Chen, J. C.; Wu, Q.; Chen, G. Q. Engineering the Diversity of Polyesters. *Current Opinion in Biotechnology* **2014**, *29*, 24–33.
- (130) Jambunathan, P.; Zhang, K. Novel Pathways and Products from 2-Keto Acids. *Current Opinion in Biotechnology* **2014**, *29*, 1–7.
- (131) Zhang, K.; Sawaya, M. R.; Eisenberg, D. S.; Liao, J. C. Expanding Metabolism for Biosynthesis of Nonnatural Alcohols. *Proceedings of the National Academy of Sciences of the United States of America* **2008**, *105*, 20653–20658.
- (132) Ji, Y.; Mao, G.; Wang, Y.; Bartlam, M. Structural Insights into Diversity and N-Alkane Biodegradation Mechanisms of Alkane Hydroxylases. *Frontiers in Microbiology* **2013**, *4*, DOI: [10.3389/fmicb.2013.00058](https://doi.org/10.3389/fmicb.2013.00058).
- (133) Bond-Watts, B. B.; Weeks, A. M.; Chang, M. C. Biochemical and Structural Characterization of the Trans-Enoyl-Coa Reductase from *Treponema Denticola*. *Biochemistry* **2012**, *51*, 6827–6837.
- (134) Pierre, F. S.; Cui, L.; Priest, D. G.; Endy, D.; Dodd, I. B.; Shearwin, K. E. One-Step Cloning and Chromosomal Integration of DNA. *ACS Synthetic Biology* **2013**, *2*, 537–541.
- (135) Tyo, K. E.; Ajikumar, P. K.; Stephanopoulos, G. Stabilized Gene Duplication Enables Long-Term Selection-Free Heterologous Pathway Expression. *Nature Biotechnology* **2009**, *27*, DOI: [10.1038/nbt.1555](https://doi.org/10.1038/nbt.1555).
- (136) Matelska, D.; Shabalin, I. G.; Jab, J.; Domagalski, M. J.; Kutner, J.; Ginalski, K.; Minor, W. Classification, Substrate Specificity and Structural Features of D-2-hydroxyacid Dehydrogenases : 2HADH Knowledgebase. **2018**, *8*, 1–23.

- (137) Yi, Y.; Li, Z. Evolving P450<sub>pyr</sub> Monooxygenase for Regio- and Stereoselective Hydroxylations. *Chimia* **2015**, *69*, DOI: [10.2533/chimia.2015.136](https://doi.org/10.2533/chimia.2015.136).
- (138) Yang, Y.; Chi, Y. T.; Toh, H. H.; Li, Z. Evolving P450<sub>pyr</sub> Monooxygenase for Highly Regioselective Terminal Hydroxylation of N-Butanol to 1,4-Butanediol. *Chemical Communications* **2015**, *51*, DOI: [10.1039/c4cc08479a](https://doi.org/10.1039/c4cc08479a).
- (139) Koch, D. J.; Chen, M. M.; Van Beilen, J. B.; Arnold, F. H. In Vivo Evolution of Butane Oxidation by Terminal Alkane Hydroxylases AlkB and CYP153A6. *Applied and Environmental Microbiology* **2009**, *75*, DOI: [10.1128/AEM.01758-08](https://doi.org/10.1128/AEM.01758-08).
- (140) Cooley, R. B.; Dubbels, B. L.; Sayavedra-Soto, L. A.; Bottomley, P. J.; Arp, D. J. Kinetic Characterization of the Soluble Butane Monooxygenase from *Thauera butanivorans*, Formerly 'Pseudomonas butanovora'. *Microbiology* **2009**, *155*, DOI: [10.1099/mic.0.028175-0](https://doi.org/10.1099/mic.0.028175-0).
- (141) Shah, K. U.; Gangadeen, I. Integrating Bioplastics into the US Plastics Supply Chain: Towards a Policy Research Agenda for the Bioplastic Transition. *Frontiers in Environmental Science* **2023**, *11*.